

SCHOOL OF CIVIL ENGINEERING



JOINT HIGHWAY  
RESEARCH PROJECT

JHRP-77-17

BRIDGE VIBRATION  
STUDIES

Ali Shahabadi



PURDUE UNIVERSITY  
INDIANA STATE HIGHWAY COMMISSION



Interim Report

BRIDGE VIBRATION STUDIES

TO: J. F. McLaughlin, Director  
Joint Highway Research Project

FROM: H. L. Michael, Associate Director  
Joint Highway Research Project

September 7, 1977

Project: C-36-56S

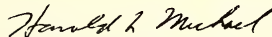
File: 7-4-19

The attached Interim Report "Bridge Vibration Studies" is submitted on the HPR-1(15) Part II Research Study of the same title. The Report has been authored by Mr. Ali Shahabadi, Graduate Instructor on our staff, under the direction of Professors J. T. Gaunt and R. H. Lee.

One result of this study is the finding that for the low range of frequencies maximum jerk is the main cause of disturbance to the human body while for the medium range of frequencies maximum acceleration is the primary cause. Additional study showed that surface roughness had the most effect on jerk and acceleration while girder flexibility had little effect on jerk. Transverse vehicle position was also found to be of importance to the dynamic response of the bridge and that dynamic response could be reasonably determined by using analytical programs.

The Report is forwarded to the Board for acceptance as partial fulfillment of the objectives of the research. This is the last Interim Report on this Study and will be followed at an early date by the summarizing Final Report. After acceptance of the attached by the Board it will be forwarded for ISHC and FHWA approval.

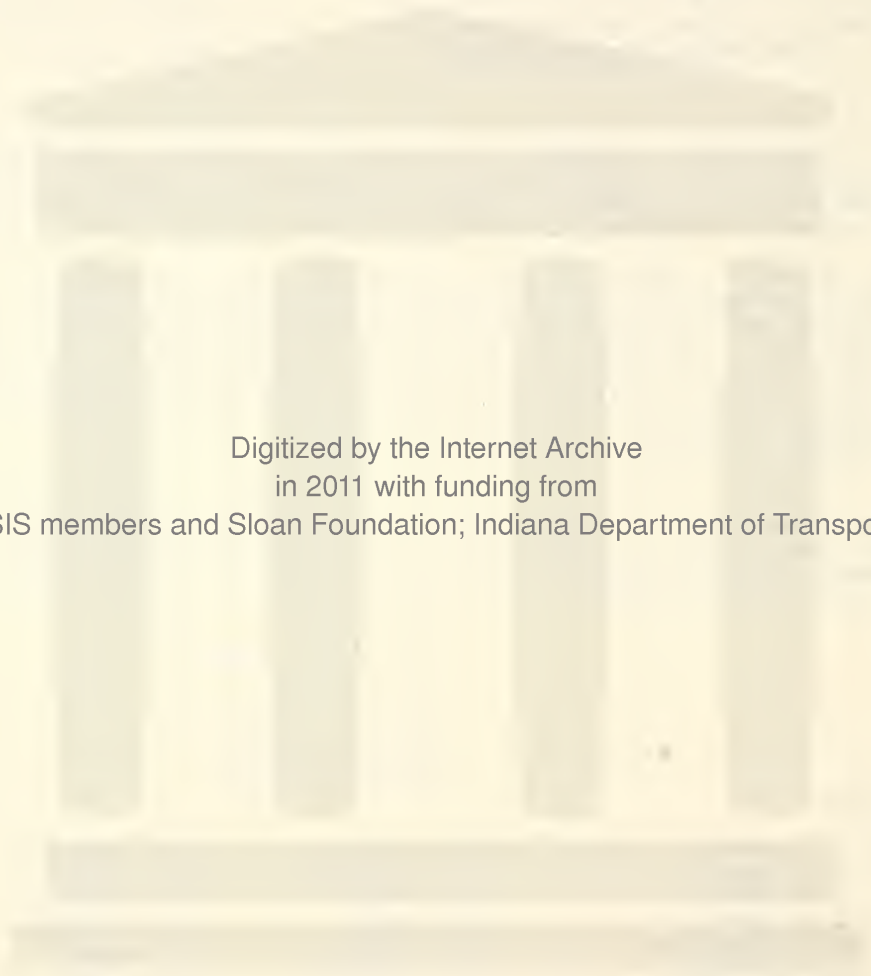
Respectfully submitted,



Harold L. Michael  
Associate Director

HLM:ms

cc: W. L. Dolch	K. R. Hoover	C. F. Scholer
R. L. Eskew	G. A. Leonards	M. B. Scott
G. D. Gibson	R. F. Marsh	K. C. Sinha
W. H. Goetz	R. D. Miles	C. A. Venable
M. J. Gutzwiller	P. L. Owens	L. E. Wood
G. K. Hallock	G. T. Satterly	E. J. Yoder
D. E. Hancher		S. R. Yoder



Digitized by the Internet Archive  
in 2011 with funding from  
LYRASIS members and Sloan Foundation; Indiana Department of Transportation

<http://www.archive.org/details/bridgevibrations00shah>

1. Report No. JHRP-77-17	2. Government Accession No.	3. Recipient's Catalog No.	
4. Title and Subtitle BRIDGE VIBRATION STUDIES		5. Report Date September 7, 1977	6. Performing Organization Code
		8. Performing Organization Report No. JHRP-77-17	
7. Author(s) Ali Shahabadi		10. Work Unit No.	11. Contract or Grant No. HPR-1(15) Part II
9. Performing Organization Name and Address Joint Highway Research Project Civil Engineering Building Purdue University West Lafayette, Indiana 47907		13. Type of Report and Period Covered Interim Report	
		14. Sponsoring Agency Code	
12. Sponsoring Agency Name and Address Indiana State Highway Commission State Office Building 100 North Senate Avenue Indianapolis, Indiana 46204		15. Supplementary Notes Prepared in cooperation with the U.S. Dept. of Transportation, Federal Highway Administration, on HPR Part I Research Study titled "Bridge Vibration Studies"	
16. Abstract The objective of this investigation was to study the vibration of highway bridges due to moving vehicles and the effect of vibrations on bridge users. In order to establish a criterion for human response to vibration, the available literature on human response to vibration was reviewed. As a result of this study it was found that for the low range of frequencies, maximum jerk and for the medium range of frequencies, maximum acceleration are the main causes of the disturbance to the human body. Maximum values of jerk and acceleration for user comfort were suggested. An extensive parametric study was done on jerk and acceleration, which showed that surface roughness had the most effect and that girder flexibility had very little effect.  As a result of the comparison between the analytical results and the field results, it was concluded that the dynamic response of a bridge to a vehicle could be determined, with a reasonable degree of accuracy, by using the analytical programs. A simplified method was also suggested that could be used to determine the maximum dynamic responses, such as acceleration and jerk, of a bridge due to a given vehicle.			
17. Key Words Bridge Vibration; Bridge Design; Bridge Accelerations; Human Response to Bridge Vibration		18. Distribution Statement No restrictions. This document is available to the public through the National Technical Information Service, Springfield, VA 22161.	
19. Security Classif. (of this report) Unclassified	20. Security Classif. (of this page) Unclassified	21. No. of Pages 154	22. Price



Interim Report  
BRIDGE VIBRATION STUDIES

by

Ali Shahabadi  
Graduate Instructor in Research

Joint Highway Research Project

Project No.: C-36-56S

File No.: 7-4-19

Prepared as Part of an Investigation

Conducted by

Joint Highway Research Project  
Engineering Experiment Station  
Purdue University

in cooperation with the  
Indiana State Highway Commission  
and the

U.S. Department of Transportation  
Federal Highway Administration

The contents of this report reflect the views of the author who is responsible for the facts and the accuracy of the data presented herein. The contents do not necessarily reflect the official views or policies of the Federal Highway Administration. This report does not constitute a standard, specification, or regulation.

Purdue University  
West Lafayette, Indiana  
September 7, 1977





## ACKNOWLEDGMENTS

This study was conducted under the general guidance of Professor John T. Gaunt and Professor Robert H. Lee. Their help and recommendations throughout this investigation are gratefully acknowledged.

The author wishes to extend his thanks to Professor C. D. Sutton, Professor M. J. Gutzwiller and Professor E. C. Zachmanoglou for their guidance and helpful suggestions.

The author further appreciates the financial support received from the Joint Highway Research Project.



## TABLE OF CONTENTS

	<u>Page</u>
LIST OF TABLES . . . . .	vii
LIST OF FIGURES. . . . .	ix
LIST OF SYMBOLS. . . . .	xvii
HIGHLIGHT SUMMARY. . . . .	xix
INTRODUCTION . . . . .	1
CHAPTER I: HUMAN RESPONSE TO VIBRATION. . . . .	3
1.1. General . . . . .	3
1.2. Methods and Procedures. . . . .	4
1.3. Transmissibility of Vibration in the Human Body . . . . .	5
1.4. Human Sensitivity Curves. . . . .	9
1.5. Factors Affecting Human Comfort . . . . .	10
1.5.1. Amplitudes. . . . .	10
1.5.2. Velocity. . . . .	11
1.5.3. Acceleration. . . . .	11
1.5.4. Jerk. . . . .	11
1.6. Human Response to Vibration Curves. . . . .	12
1.6.1. Boeing Airplane Company Tests . . . . .	12
1.6.2. Human Response to Damped Vibrations . . . . .	17
1.6.3. Human Response to Non-Sinusoidal Vibration. . . . .	22
1.7. Scales and Parameters . . . . .	22
1.8. Conclusions . . . . .	25
CHAPTER II: FUNDAMENTAL FREQUENCIES . . . . .	29
2.1. General . . . . .	29
2.2. Special Tests and Observations. . . . .	30
2.3. Effect of Girder Flexibility on Fundamental Frequencies. . . . .	49
2.4. Effect of Slab Thickness on Fundamental Frequencies . . . . .	49
CHAPTER III: ROAD ROUGHNESS . . . . .	53
3.1. General . . . . .	53
3.2. Analysis of the Bridge Profiles . . . . .	54
3.3. Simulation of the Road Roughness. . . . .	63
3.4. Theoretical Comparison of Actual and Simulated Bridge Profiles . . . . .	63



## TABLE OF CONTENTS (Continued)

	<u>Page</u>
CHAPTER IV: LOAD DISTRIBUTION ON HIGHWAY BRIDGES. . . . .	82
4.1. General . . . . .	82
4.2. Effect of Transverse Position of the Vehicle on Load Distribution . . . . .	83
4.3. Effect of Speed on Dynamic Deflection of the Beams. . . . .	89
4.4. Effect of the Weight of the Vehicle on Dynamic Deflection. . . . .	89
4.5. Effect of Slab Thickness on Dynamic Deflection. . . . .	89
4.6. Effect of Girder Flexibility on Dynamic Deflection. . . . .	97
4.7. Comparison of Measured and Theoretical Values of Dynamic Deflections . . . . .	97
CHAPTER V: JERK STUDY . . . . .	104
5.1. General . . . . .	104
5.2. Effect of Transverse Position of Load on Jerk . . . . .	105
5.3. Effect of Slab Stiffness on Jerk. . . . .	105
5.4. Effect of Reduction in Moment of Inertia of Girders on Jerk . . . . .	112
5.5. Effect of Road Roughness on Acceleration and Jerk of Highway Bridges. . . . .	112
CHAPTER VI: COMPARISON OF ACTUAL AND THEORETICAL DYNAMIC RESPONSES . . . . .	122
6.1. General . . . . .	122
6.2. Comparison of Dynamic Deflections . . . . .	125
6.3. Comparison of Measured and Theoretical Accelerations. . . . .	127
CHAPTER VII: SIMPLIFIED METHOD OF DETERMINING MAXIMUM DYNAMIC RESPONSES OF HIGHWAY BRIDGES. . . . .	133
7.1. General . . . . .	133
7.2. Description and Usage of the Simplified Method. . . . .	133
7.3. Procedure for Estimating Dynamic Deflection and Fundamental Frequencies . . . . .	135
CHAPTER VIII: CONCLUSIONS AND RECOMMENDATIONS . . . . .	140
8.1. Conclusions . . . . .	140
8.1.1. Human Response to Vibration . . . . .	140
8.1.2. Torsional Frequency . . . . .	140
8.1.3. Dynamic Load Distribution . . . . .	141
8.1.4. Jerk. . . . .	141
8.2. Recommendations . . . . .	141
8.2.1. Analytical Computer Programs. . . . .	141
8.2.2. Simplified Method . . . . .	142



## TABLE OF CONTENTS (Continued)

	<u>Page</u>
BIBLIOGRAPHY . . . . .	143
APPENDICES . . . . .	146
APPENDIX A - Human Response to Vibration Curves . . . . .	146
APPENDIX B - Simplified Methods for Determining Fundamental Frequencies. . . . .	154
APPENDIX C - Road Roughness Analysis Curves . . . . .	177
APPENDIX D - Description of the Single Span Bridge (SB-C-1) .	214
APPENDIX E - Time Derivative of Discrete Functions. . . . .	215
APPENDIX F - Fundamental Bending Frequency of Three Span Bridges . . . . .	229





## LIST OF TABLES

<u>Table</u>	<u>Page</u>
2.1 Theoretical and Measured Fundamental Frequencies. . . . .	33
2.2 Effect of Reduction of Moment of Inertia on Fundamental Frequencies. . . . .	50
2.3 Effect of Slab Thickness on Fundamental Frequencies . . .	50
4.1 Effect of Load Position on Dynamic Deflection . . . . .	85
4.2 Effect of Load Position on Percentage of Load on Each Beam . . . . .	86
4.3 Effect of Speed on Dynamic Deflection . . . . .	90
4.4 Effect of Speed of Vehicle on Percentage Load on Each Beam. . . . .	91
4.5 Effect of Vehicle Weight on Dynamic Deflection. . . . .	92
4.6 Effect of Vehicle Weight on Percentage Load on Each Beam. . . . .	93
4.7 Effect of Slab Thickness on Dynamic Deflection of Each Beam . . . . .	94
4.8 Effect of Slab Thickness on Percentage of Load on Each Beam. . . . .	95
4.9 Effect of Reduction of Moment of Inertia of Beams on Dynamic Deflection . . . . .	98
4.10 Effect of Reduction of Moment of Inertia on Percentage of Load on Each Beam . . . . .	99
4.11 Maximum Measured Dynamic Deflections of single Span Bridge (SB-C-1) for Various Speeds and Transverse Vehicle Positions . . . . .	100



## LIST OF TABLES (Continued)

<u>Table</u>		<u>Page</u>
4.12	Maximum Measured Dynamic Deflections of two span Bridge (KCSG-A-1) for Various Speeds and Transverse Vehicle Positions . . . . .	101
4.13	Maximum Measured Dynamic Deflections of Three Span Bridge (CSB-C-1) for Various Speeds and Transverse Vehicle Positions . . . . .	102
5.1	Effect of Load Position on Maximum Jerk in Each Beam. . .	106
5.2	Effect of Load Position on Jerk in Each Beam at the Instant that Maximum Jerk Value Occurs. . . . .	107
5.3	Effect of Slab Thickness on Maximum Jerk in Each Beam. . .	113
5.4	Effect of Reduction in Moment of Inertia on Maximum Jerk in Each Beam . . . . .	115
5.5	Effect of Maximum Amplitude of Simulated Road Roughness on Acceleration . . . . .	118
5.6	Effect of Maximum Amplitude of Road Roughness on Jerk . .	119
6.1	Comparison of Measured and Calculated Dynamic Responses of the Single Span Bridge (SB-C-1). . . . .	130
6.2	Comparison of Measured and Calculated Dynamic Responses of the Two Span Bridge (KCSG-A-1) . . . . .	131
6.3	Comparison of Measured and Calculated Dynamic Responses for the Three Span Bridge (CSB-C-1) . . . . .	132
7.1	Measured Fundamental Frequencies and Maximum Measured Accelerations and Deflections for the Bridges in the Study . . . . .	137
7.2	Comparison of the Maximum Measured Accelerations with the Accelerations Obtained from the Simplified Method . .	138
Appendix		
Table		
B.1	Finite Difference Coefficients. . . . .	158
B.2	Torsional Properties of Rolled Sections . . . . .	161



## LIST OF FIGURES

<u>Figure</u>	<u>Page</u>
1.1 Simplified Mechanical System Representing the Human Body Standing on a Vertically Vibrating Platform. . . . .	7
1.2 Mechanical Impedance of Standing and Sitting Human Subject Vibrating in the Direction of his Longitudinal Axis as a Function of Frequency . . . . .	7
1.3 Transmissibility of Longitudinal Vertical Vibration from Table to Various Part of Body of Seated Human Subject as a Function of Frequency. . . . .	8
1.4 Transmissibility of Vertical Vibration from Table to Various Parts of the Body of a Standing Human Subject as a Function of Frequency. . . . .	8
1.5 Domains of Various Strengths of Sensations for Standing Person Subject to Vertical Vibration . . . . .	13
1.6 Domains of Various Strength of Sensations for Standing Person Subject to Vertical Vibration . . . . .	14
1.7 Results of Early Test on Vibrating Platform . . . . .	15
1.8 Amplitude-Frequency Results with Vertical Motion for Group 1 . . . . .	16
1.9 Summary of Four Vibration Levels for Group A, Illustrating Overlap Between Levels Resulting from Individual Differences. . . . .	18
1.10 Summary of Four Vibration Levels for Group B, Illustrating Overlap Between Levels Resulting from Individual Differences. . . . .	19
1.11 A Summary of Data for Judgment Levels 1, 2, 3, and 4. This Coordinates System Presents the Major Physical Descriptions of Vibration, Including an Indication of the Relation that Jerk has to the System . . . . .	20



## LIST OF FIGURES (Continued)

<u>Figure</u>		<u>Page</u>
1.12	Comfortable Limits Recommended by Various Investigators for Vertical Vibration or Axis Unspecified. . . . .	21
1.13	Barely Perceptible Rating . . . . .	23
1.14	Strongly Perceptible Rating . . . . .	23
1.15	Distinctly Perceptible Rating . . . . .	23
1.16	Comparison of the Effects of Sinusoidal and Random Vibration on Human Tolerance. . . . .	24
1.17	Vertical Vibration Limits for Automobile Passenger Comfort, After Janeway. . . . .	26
1.18	Vibration Strength in Vibrars, After Koch and Steffens. . . . .	27
2.1	Deflected Shape for Fundamental Bending Mode of Single Span Bridge. . . . .	31
2.2	Deflected Shape for Fundamental Bending Mode of Two Span Bridge . . . . .	31
2.3	Deflected Shape for Fundamental Torsion Mode of Single Span Bridge. . . . .	32
2.4	Deflected Shape for Fundamental Torsion Mode of Two Span Bridge . . . . .	32
2.5	Accelerometer Locations for Special Tests . . . . .	35
2.6	Acceleration Records from Two Accelerometers in the First Span. Accelerometers Have the Same Transverse Location but are on Opposite Sides of the Bridge. . . . .	36
2.7	Acceleration Records from Two Accelerometers in the First Span. Accelerometers Have the Same Transverse Location but are on Opposite Sides of the Bridge. . . . .	38
2.8	Fourier Spectrum of the Free Vibration of Acceleration, Transverse Vehicle Position - Bridge Center Line. . . . .	39
2.9	Fourier Spectrum of the Free Vibration of Acceleration, Transverse Vehicle Position - Travel Lane . . . . .	40
2.10	Fourier Spectrum of the Free Vibration of Acceleration, Transverse Vehicle Position - Curb Lane . . . . .	41





## LIST OF FIGURES (Continued)

<u>Figure</u>		<u>Page</u>
2.11	Fourier Spectrum of the Free Vibration of Acceleration, Transverse Vehicle Position - Bridge Center Line. . . . .	43
2.12	Fourier Spectrum of the Free Vibration of Acceleration, Transverse Vehicle Position - Travel Lane . . . . .	44
2.13	Fourier Spectrum of the Free Vibration of Acceleration, Transverse Vehicle Position - Curb Lane . . . . .	45
2.14	Fourier Spectrum of the Free Vibration of Acceleration, Transverse Vehicle Position - Bridge Center Line. . . . .	46
2.15	Fourier Spectrum of the Free Vibration of Acceleration, Transverse Vehicle Position - Travel Lane . . . . .	47
2.16	Fourier Spectrum of the Free Vibration of Acceleration, Transverse Vehicle Position - Curb Lane . . . . .	48
2.17	Effect of Reduction of Moment of Inertia on Fundamental Frequencies . . . . .	51
2.18	Effect of Slab Thickness on Fundamental Frequencies . . . . .	52
3.1	Bridge Roughness Profile. . . . .	58
3.2	Power Spectrum. . . . .	59
3.3	Phase Angle . . . . .	60
3.4	$\ln(-\ln(R))$ , $\ln(n)$ Relationship. . . . .	61
3.5	Suggested $\ln(-\ln(R))$ , $\ln(n)$ Relationship. . . . .	62
3.6	Simulated Road Roughness. . . . .	64
3.7	Bridge Roughness Profile. . . . .	65
3.8	Power Spectrum. . . . .	66
3.9	Phase Angle . . . . .	67
3.10	$\ln(-\ln(R))$ , $\ln(n)$ Relationship. . . . .	68
3.11	Deflection Record . . . . .	69
3.12	Velocity Record . . . . .	70



## LIST OF FIGURES (Continued)

<u>Figure</u>	<u>Page</u>
3.13 Acceleration Records . . . . .	71
3.14 Jerk Records . . . . .	72
3.15 Deflection Record . . . . .	74
3.16 Velocity Record . . . . .	75
3.17 Acceleration Records . . . . .	76
3.18 Jerk Records . . . . .	77
3.19 Deflection Record . . . . .	78
3.20 Velocity Record . . . . .	79
3.21 Acceleration Records . . . . .	80
3.22 Jerk Records . . . . .	81
4.1 Transverse Position of Vehicle on Bridge . . . . .	84
4.2 Effect of Load Position on Percentage of Load on Each Beam . . . . .	87
4.3 Effect of Slab Thickness on Percentage of Load on Each Beam . . . . .	96
5.1 Effect of Load Position on Maximum Jerk in Each Beam . . . . .	108
5.2 Effect of Load Position on Jerk in Each Beam at the Instant that the Maximum Jerk Value Occurs . . . . .	110
5.3 Effect of Slab Thickness on Maximum Jerk in Each Beam . . . . .	114
5.4 Effect of Reduction in Moment of Inertia on Maximum Jerk in Each Beam . . . . .	116
5.5 Effect of Maximum Amplitude of Simulated Road Roughness on Acceleration . . . . .	120
5.6 Effect of Maximum Amplitude of Simulated Road Roughness on Jerk . . . . .	121
6.1 Vehicle Models for Single Span Bridge . . . . .	123
6.2 Bridge Model for Two and Three Span Bridges . . . . .	124



## LIST OF FIGURES (Continued)

<u>Figure</u>	<u>Page</u>	
6.3	Vehicle Models for Two and Three Span Bridge. . . . .	126
6.4	Deflection Record, Research and Training Center Bus, Deflection Gauge Located at .5L in First Span. . . .	128
7.1	Comparison of the Maximum Measured Accelerations with the Accelerations Obtained from the Simplified Method . .	139
 Appendix		
Figure		
A.1	Human Response to Vibration as Reported by Bolt, Beranek and Newman. . . . .	147
A.2	Dieckman's Scale of Strain for Vertical Vibrations. . . .	148
A.3	Ride Indices for Vertical Accelerations as Reported by Balchelor. . . . .	149
A.4	Subjective Responses of the Human Body to Vibratory Motion, After Goldman . . . . .	150
A.5	Subjective Responses of the Human Body to Vibratory Motion, After Goldman . . . . .	151
A.6	Contours of Equal Sensitivity to Vibration. . . . .	152
A.7	Riding' Comfort Indices for Vertical Vibration, After Matsubara . . . . .	153
B.1	Assumed Deflected Shape for Fundamental Torsion . . . .	156
B.2	Assumed Deflected Shape Along the Y Axis. . . . .	156
B.3	Slab Division Used in the Finite Difference Analysis. . .	157
B.4	Torsional Function Coefficient, $\gamma$ . . . . .	160
B.5	Forces and Moments Acting Along the Y Axis. . . . .	163
B.6	Fourier Spectrum of the Free Vibration Portion of Accelerometer No. 1 . . . . .	165
B.7	Fourier Spectrum of the Free Vibration Portion of Accelerometer No. 1 . . . . .	166



## LIST OF FIGURES (Continued)

<u>Figure</u>		<u>Page</u>
B.8	Fourier Spectrum of the Free Vibration Portion of the Deflection Record . . . . .	167
B.9	Fourier Spectrum of the Free Vibration Portion of Accelerometer No. 1 . . . . .	168
B.10	Fourier Spectrum of the Free Vibration Portion of Accelerometer No. 2 . . . . .	169
B.11	Fourier Spectrum of the Free Vibration Portion of Accelerometer No. 1 . . . . .	170
B.12	Fourier Spectrum of the Free Vibration Portion of Accelerometer No. 1 . . . . .	171
B.13	Fourier Spectrum of the Free Vibration Portion of Accelerometer No. 2 . . . . .	172
B.14	Fourier Spectrum of the Free Vibration Portion of Accelerometer No. 2 . . . . .	173
B.15	Fourier Spectrum of the Free Vibration Portion of Accelerometer No. 2 . . . . .	174
B.16	Fourier Spectrum of the Free Vibration Portion of Accelerometer No. 1 . . . . .	175
B.17	Fourier Spectrum of the Free Vibration Portion of Accelerometer No. 1 . . . . .	176
C.1	Bridge Roughness Profile. . . . .	178
C.2	Power Spectrum. . . . .	179
C.3	Phase Angle . . . . .	180
C.4	$\ln(-\ln(R))$ , $\ln(n)$ Relationship. . . . .	181
C.5	Bridge Roughness Profile. . . . .	182
C.6	Power Spectrum. . . . .	183
C.7	Phase Angle . . . . .	184
C.8	$\ln(-\ln(R))$ , $\ln(n)$ Relationship. . . . .	185





## LIST OF FIGURES (Continued)

<u>Figure</u>		<u>Page</u>
C.9	Bridge Roughness Profile. . . . .	186
C.10	Power Spectrum. . . . .	187
C.11	Phase Angle . . . . .	188
C.12	Ln(-Ln(R)), Ln(n) Relationship. . . . .	189
C.13	Bridge Roughness Profile. . . . .	190
C.14	Power Spectrum. . . . .	191
C.15	Phase Angle . . . . .	192
C.16	Ln(-Ln(R)), Ln(n) Relationship. . . . .	193
C.17	Bridge Roughness Profile. . . . .	194
C.18	Power Spectrum. . . . .	195
C.19	Phase Angle . . . . .	196
C.20	Ln(-Ln(R)), Ln(n) Relationship. . . . .	197
C.21	Bridge Roughness Profile. . . . .	198
C.22	Power Spectrum. . . . .	199
C.23	Phase Angle . . . . .	200
C.24	Ln(-Ln(R)), Ln(n) Relationship. . . . .	201
C.25	Bridge Roughness Profile. . . . .	202
C.26	Power Spectrum. . . . .	203
C.27	Phase Angle . . . . .	204
C.28	Ln(-Ln(R)), Ln(n) Relationship. . . . .	205
C.29	Bridge Roughness Profile. . . . .	206
C.30	Power Spectrum. . . . .	207
C.31	Phase Angle . . . . .	208
C.32	Ln(-Ln(R)), Ln(n) Relationship. . . . .	209



## LIST OF FIGURES (Continued)

<u>Figure</u>		<u>Page</u>
C.33	Bridge Roughness Profile. . . . .	210
C.34	Power Spectrum. . . . .	211
C.35	Phase Angle . . . . .	212
C.36	$\ln(-\ln(R))$ , $\ln(n)$ Relationship. . . . .	213
E.1	Simulated Acceleration Function . . . . .	217
E.2	Comparison of Exact and Approximate Derivatives . . . . .	218
E.3	Comparison of Exact and Approximate Derivatives . . . . .	219
E.4	Comparison of Exact and Approximate Derivatives . . . . .	220
E.5	Comparison of Exact and Approximate Derivatives . . . . .	221
E.6	Comparison of Exact and Approximate Derivatives . . . . .	222
E.7	Comparison of Exact and Approximate Derivatives . . . . .	223
E.8	Comparison of Exact and Approximate Derivatives . . . . .	224
E.9	Comparison of Exact and Approximate Derivatives . . . . .	225
E.10	Comparison of Exact and Approximate Derivatives . . . . .	226
E.11	Comparison of Exact and Approximate Derivatives . . . . .	227
E.12	Comparison of Exact and Approximate Derivatives . . . . .	228
F.1	Frequency Coefficient for Three Span Bridges. . . . .	230



## LIST OF SYMBOLS

A	amplitude of vibration
$A_n$	nth cosine amplitude in Fourier expansion
$B_n$	nth sine amplitude in Fourier expansion
D	maximum displacement
$DB_i$	deflection at the center of the ith beam
$DS_i$	slab deflection at ith point along the width of the bridge
e	base of natural logarithm
E	modulus of elasticity of steel ( $PS_i$ )
f	frequency (cycles/sec)
$F(x)$	profile function along the length of the bridge
$F_p$	equivalent concentrated forces at each division point
g	acceleration of gravity ( $386 \text{ in/sec}^2$ )
G	shear modulus of elasticity
h	distance between the adjacent points of slab division used in the finite difference analysis
I	total cross-sectional moment of inertia
J	polar mass moment of inertia
L	length of single span bridge or each span of two span bridge
M	number of division points along the width of the bridge
$MB_i$	moment at ith point of the beam
MN	net resultant moment
n	frequency (cycles/bridge length)



$N$	number of division points along the length of the bridge used in the finite difference analysis
$NB$	maximum number of beams
$NH$	maximum number of harmonics
$NR$	maximum number of measured ordinates for each bridge profile
$PB_i$	concentrated force at the center of the $i$ th beam
$PS_i$	$i$ th concentrated slab force along the width of the bridge
$R_i$	$i$ th amplitude in cosine expansion of Fourier series
$R_B(t)$	bending dynamic response function
$R_T(t)$	torsion dynamic response function
$t$	time
$u$	Poisson's ratio
$x$	displacement
$x$	velocity
$x$	acceleration
$x$	jerk
$w$	vertical deflection
$W$	total mass of the bridge
$\beta$	Weibull parameter
$\gamma$	torsional function coefficient
$\kappa$	total torsional stiffness of the bridge
$\phi$	phase angle
$\mu$	Weibull parameter
$\omega$	angular frequency
$\theta_i$	rotation at the center of the $i$ th beam





## HIGHLIGHT SUMMARY

The objective of this investigation was to study the vibration of highway bridges due to moving vehicles and the effect of vibrations on bridge users. In order to establish a criterion for human response to vibration, available literature on human response to vibration was reviewed. Since the primary vibration of girder bridges is in the vertical direction, the effect of vertical vibration (foot to head direction) on the human body was studied. As a result of this study it was found that for the low range of frequencies, maximum jerk and for the medium range of frequencies, maximum acceleration are the main causes of the disturbance to the human body. Based on these findings a parametric study was done on jerk and acceleration. Parametric study showed that surface roughness had the most effect on jerk and acceleration and the girder flexibility had very little effect on jerk. Reduction of the girder stiffness by 30% did not increase jerk by more than 11%.

In the analytical study of the vibration of the bridges it was found that the contribution of the torsional mode to the dynamic response was significant. The transverse vehicle position was found to be greatly related to the contribution of the torsional mode to the dynamic response of the bridge. The closer the vehicle was to the curb the more the contribution of the torsional modes.



Distribution of the vehicle load to the beams was not uniform and was found to be highly dependent on the transverse vehicle position. Beams closer to the wheels carried a greater portion of the vehicle load. For cases where the vehicle was close to the curb, the edge beam carried the largest portion of the vehicle load.

As a result of the comparison between the analytical results and the field results, it was concluded that the dynamic response of a bridge to a vehicle could be determined, with a reasonable degree of accuracy, by using the analytical programs. A simplified method was also suggested that could be used to determine the maximum dynamic responses, such as acceleration and jerk, of a bridge due to a given vehicle.



## INTRODUCTION

Determination of the dynamic response of structures, especially bridges, has been the topic of numerous studies in recent years; however the related question of user comfort on these vibrating bridges has received relatively little attention. Although humans are subjected to the vibrations of many structures, there is seldom any direct provision in design codes to ensure user comfort. The current bridge codes impose restrictions upon girder depth-span ratios and static deflection-span ratios in the hope that these limits will provide satisfactory dynamic performance. The human body, however, is primarily sensitive to dynamic effects such as acceleration and change of acceleration rather than to displacements.

The general objectives of this research program have been to obtain a better understanding of the dynamic performance of highway bridges and of the vibrations sensed by bridge users in order to develop a dynamic-based design criterion which would more effectively ensure the comfort of the users. Specific tasks have included:

- 1) identification through analytical studies of the parameters of the bridge-vehicle system which are most significant in their effect upon the dynamic response of the bridge,
- 2) measurement and analysis of the dynamic performance of bridges under actual traffic in the field,



- 3) comparison of field measurements with analytical predictions,
- 4) identification of reasonable quantitative dynamic criteria for user sensitivity to vibrations, and
- 5) development of a simple dynamic-based design criterion for controlling bridge vibrations.

The first phase of the research, reported by Aramraks [31]\*, consisted primarily of analytical studies of the effects of varying some of the parameters of the structure-vehicle system. Somewhat surprisingly, the most significant effect was found to be the roughness of roadway. Other important parameters included girder stiffness, span length and vehicle speed.

As stated in the original proposal and by mutual agreement of the researchers and sponsors, existing computer programs were to be used whenever possible for the analytical studies. Two alternatives were strongly considered: (1) a finite element program which had recently been developed by investigators at the University of Illinois and (2) two somewhat less sophisticated special purpose programs for simply supported and continuous beam bridges developed somewhat earlier at the University of Illinois. Their cooperation in supplying these programs is gratefully acknowledged.

In view of the numerous parametric studies planned, the costs of using the sophisticated but time-consuming finite element program would have been prohibitive. Thus it was decided to make use of a simple span analysis and program developed by Oran [35] and a multi-span bridge beam program developed by Veletsos and Huang [36]. The validity of

---

\*Numbers in brackets are reference numbers.





their analyses had been verified by comparisons with the results of laboratory studies on simply supported beams, as well as with the results of the AASHO Road Test bridges. The analytical models, the methods of analysis, and the programs are summarized in detail by Aramraks [31].

The second phase of the research, reported by Kropp [33], consisted of an extensive field study of the dynamic responses of 62 beam-type bridges located throughout the state of Indiana. The bridges were instrumented with accelerometers mounted on the curbs of the bridge decks at midspan and by a taut-wire cantilever beam deflection transducer attached at the location of the accelerometer on the traffic side of the bridge. The accelerations and dynamic deflections produced by a control vehicle and by actual vehicular traffic were recorded in analog form on magnetic tape. The records were later digitized for plotting and analysis. The analysis included determining the maximum displacement, velocity, acceleration, jerk, and damping ratio for each of the 900 digitized vehicle crossings. One of the significant findings of this investigation was that there were only five vehicle crossings which produced a maximum acceleration greater than  $100 \text{ in/sec}^2$  - a level not thought to be excessive for short term accelerations. The frequency content was also determined for selected crossings for comparison with the predicted natural frequencies of the bridges. Excellent correlation was obtained between deflection and corresponding accelerometer measurements.

The first section of this report presents a literature survey aimed at selecting reasonable criteria for human sensitivity to bridge



vibrations. The importance of jerk claimed by some investigators prompted parametric studies focused on this variable to supplement Aramraks' acceleration studies. With the availability of extensive field data, it became possible to look critically at roadway roughness effects. Whereas Aramraks considered only uniform sinusoidal roughness, this report contains analytical studies using actual roadway profiles as well as random simulated profiles.

Kropp's extensive field measurements have also been compared with analytical predictions. Certain limitations of the analytical models are discussed and evaluated, and a simple dynamic-based design criterion is proposed.



## CHAPTER I

### HUMAN RESPONSE TO VIBRATION

#### 1.1. General

Human sensitivity to vibration poses serious technical problems for engineers in various fields. In the field of transportation there is concern for comfort in automobiles [1], civil aircraft [2], and in design of military aircraft for maximum efficiency [3]. There is concern for the residents of houses that are subjected to vibration due to railway traffic [4] and industrial machinery. One of the recent concerns of civil engineers has been the objectionable level of vibration on urban bridges used by pedestrians and vehicles. The nature of the problem is easy to grasp. It is readily apparent that there are both physiological and psychological reactions when humans are subjected to vibration. In cases where humans are disturbed by vibration of low frequency and large amplitudes, human reactions are basically physiological (low frequency and large amplitude vibrations are associated with sea sickness). On the other hand, in cases where a person is subjected to unexpected vibration, for instance, when a pedestrian on a bridge experiences whole body vibration due to traffic crossing the bridge, his reaction may be totally psychological. In such a case, a pedestrian may associate unexpected motion of the bridge with its poor design and possibly its failure, not knowing that this type of vibration is quite normal for the bridge.



In order to find out which bridges have excessive vibration as far as bridge users are concerned, it was necessary to do a literature review on human susceptibility to vibration. In the course of this literature review it was found that because of the complexity of human nature, one can not define clear cut boundaries of human sensitivity to vibration. But rather, depending upon the frequency of the vibration, there are regions of comfort and discomfort. In this literature review, only human response to vertical vibration is studied because the primary vibration of the bridge types considered is in the vertical direction.

The materials and related figures in this section of the report are taken from various sources. Since most of the reports from which these materials were taken were not the original reports, whenever possible the original references are given. Reference [39] is a summary paper which includes an extensive bibliography.

## 1.2. Methods and Procedures

The earliest measurements done in the field of Human Response to Vibrations (HRV) was by Mallock in 1902 [4]. He obtained his results when investigating some complaints of unpleasant vibration caused by passing traffic to certain houses near Hyde Park. These vibrations, when measured, rarely exceeded .001 inch in amplitude and consisted of frequencies ranging from 10 CPS to 15 CPS. From his results he deduced that it was acceleration which caused the discomfort, and that a vibration which gives an acceleration of 1 percent of gravity,  $3.8 \text{ in/sec}^2$  ( $.098 \text{ m/sec}^2$ ) is noticeable. Since Mallock's investigation, numerous experiments have been done in the field of HRV. These





experiments have been performed on different people having different age, sex and backgrounds. The environmental conditions under which these experiments were done vary from one experiment to another. Basically there are two groups of experiments: first, experiments in which humans were subjected to actual field test conditions, and second, experiments in which humans were subjected to simulated test conditions (shaking tables). Most of the available literature on HRV is based on the results of tests that used shaking tables. In shaking table experiments, tables were excited in a so-called "simple harmonic motion". In this type of excitation, amplitude and frequency of the excitation could easily be varied. Except for one experiment by Parmelee and Wiss [5] in which damping was considered, all the other experiments were done on the basis of no damping. Among the available literature on HRV only one experiment by Pradko, Orr and Lee [6] was found to have studied the effect of random excitation mixed frequencies on humans. Results of these tests are mostly available in the form of "sensitivity curves". Each of these curves is supposed to represent a certain level of comfort.

Before studying various results of human sensitivity to vibration, it is felt that it would be beneficial, for better understanding and explaining behavior of the results, to study how vibration is transmitted in the human body.

### 1.3. Transmissibility of Vibration in the Human Body

The combination of soft tissue and bone in the structure of the body together with the body's geometric dimension results in a system which exhibits different types of response to vibratory energy



depending on the frequency range [7]. At low frequencies, below approximately 100 CPS, the body can be described for most practical purposes as a lumped parameter system for which resonance occurs due to interaction of tissue masses with purely elastic structure. At higher frequencies, through the audio frequency range and up, the body behaves more as a complex distributed system. Simple mechanical systems, such as the one shown in Figure (1.1), for a standing man, are usually sufficient to describe the important features of the response of the human body to low frequency vibration. It is rather difficult to assign numerical values to the elements of the circuit, since they depend on the body type of the subject, body position and muscle tone.

Mechanical impedance of a man standing or sitting on a vertically vibrating platform is shown in Figure (1.2). Below approximately 2 CPS, the body acts as a unit mass. For a sitting man the first resonance is between 4-6 CPS, and that of a standing man is about 5 CPS. When the human body is subjected to vertical vibration, different parts of the body do not experience the same amplitude of vibration. Examples of the relative amplitudes for different parts of the body when it is subjected to vibration are shown in Figure (1.3) for a standing subject and in Figure (1.4) for a sitting subject. The curves show an amplification of motion in the region of resonance and a decrease at higher frequencies. The impedance and transmissibility factors are changed considerably by individual differences, body posture and the type of support. Transmissibility values as high as 4 for a sitting man and as high as 2 for a standing man have been observed by Dieckmann [8]. Dieckmann's results show, above approximately 10 CPS



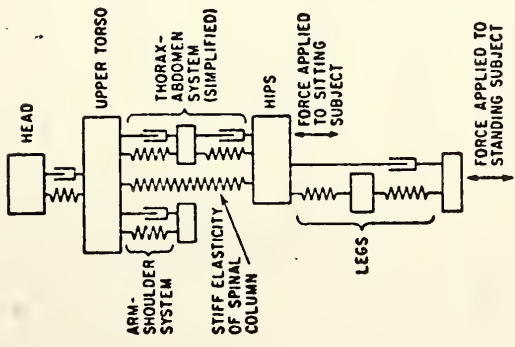


Figure 1.1. Simplified Mechanical System Representing the Human Body-- Standing on a Vertically Vibrating Platform at Low Frequencies[7].

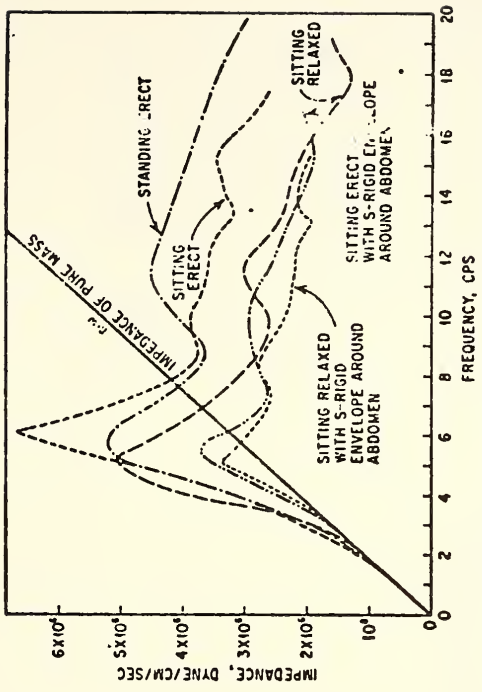


Figure 1.2. Mechanical Impedance of Standing and Sitting Human Subject Vibrating in the Direction of His Longitudinal Axis as a Function of Frequency [7].



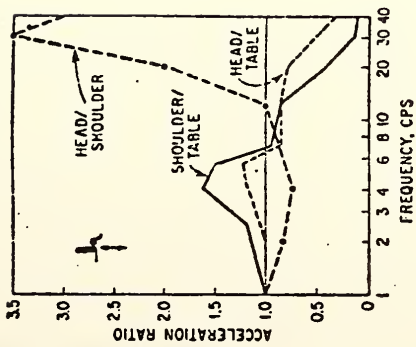


Figure 1.3. Transmissibility of Longitudinal Vertical Vibration from Table to Various Parts of Body of Seated Human Subject as a Function of Frequency [7].

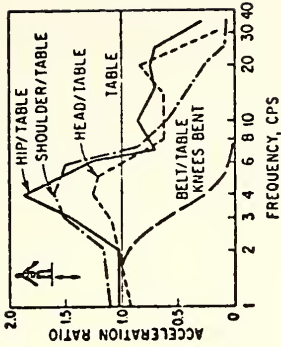


Figure 1.4. Transmissibility of Vertical Vibration from Table to Various Parts of the Body of a Standing Human Subject as a Function of Frequency [7].





vibration displacement amplitudes of the body are smaller than the exciting table and they decrease continuously with increasing frequency.

#### 1.4. Human Sensitivity Curves

Every vibratory motion has associated with it certain frequencies and amplitudes. In the case of sinusoidal motion without damping, the displacement function takes the form

$$x = A \sin \omega t$$

where  $A$  = amplitude of vibration

$\omega$  = angular velocity

$t$  = time

Velocity, acceleration, and jerk (rate of change of acceleration) are given by the following formulas.

$$\dot{x} = A\omega \cos \omega t$$

$$\ddot{x} = -A\omega^2 \sin \omega t$$

$$\dddot{x} = -A\omega^3 \cos \omega t$$

The maximum values of  $x$ ,  $\dot{x}$ ,  $\ddot{x}$ ,  $\dddot{x}$  are given by  $A$ ,  $A\omega$ ,  $A\omega^2$ ,  $A\omega^3$ , respectively. Since  $\omega = 2\pi f$ , where  $f$  = frequency, the maximum values for  $x$ ,  $\dot{x}$ ,  $\ddot{x}$ ,  $\dddot{x}$ , may be expressed in terms of frequency and amplitude only.

The maximums are  $A$ ,  $2\pi fA$ ,  $4\pi^2 f^2 A$ ,  $8\pi^3 f^3 A$ , respectively. The results of HRV curves are usually shown in the form of a series of curves. These curves are usually plotted on frequency-acceleration or frequency-displacement coordinates. Each of these curves is supposed to represent a certain level of comfort. Since a systematic scale for measuring



human comfort has not yet been developed, each investigator in this field has adopted his own levels of comfort. For example, Goldman [9] used three different levels: 1, perceptible; 2, unpleasant; 3, intolerable. Gorill and Snyder [10] used five levels: 1, threshold of perception; 2, definitely or easily perceptible; 3, irritating or annoying; 4, maximum tolerable for continuous operation; 5, highest intensity endured. Though it is not possible to exactly determine how various comfort levels of two different investigators in this field compare to each other, it is possible to get a range in which one could classify a vibration as being comfortable or not.

#### 1.5. Factors Affecting Human Comfort

Factors that affect human comfort may be classified in two groups. The first group includes human factors, such as weight, height, and degree of exposure to vibration. (People who are exposed to vertical vibration in their work tend to rate a given vibration less than people who are not exposed to vibration in their everyday lives.)

The second group includes factors that are related to the vibration, such as duration of exposure, amplitude, velocity, acceleration and jerk. Experiments show duration of the vibration to be strongly related to HRV. The longer the duration of exposure the higher the uncomfortable rating.

##### 1.5.1 Amplitudes

Some investigators have stated that above a certain frequency, only amplitude of the vibration affects discomfort.



### 1.5.2. Velocity

Hirschfield [14] noted that "Human beings are not directly sensitive to velocity. They are sometimes indirectly sensitive, as when high velocity produces high wind pressure upon part of the body. If a person is carried in a completely closed box at a constant speed he could not tell whether the box was standing or being moved at high speed. The reason for this is simple, once we are in a motion at a constant speed, no force is needed to operate on us to keep us in such motion". However, Janeway [11] stated that at 20 Hz to 60, the thresholds are a function of velocity.

### 1.5.3. Acceleration

According to Hirschfield, "Conditions are quite different when velocity is being changed, and acceleration occurs. To produce acceleration a force must act upon us." Many investigators reported that linear acceleration is detected by the otolith, a part of the inner ear. The threshold of these sensors to linear acceleration of long duration (greater than a few seconds) is about  $.32 \text{ ft/sec}^2$  ( $.0981 \text{ m/sec}^2$ ).

### 1.5.4. Jerk

Once an adjustment is made by the human body for acceleration, the body will adapt to the constant force acting on it. However, with changing acceleration, a continuously changing bodily adjustment is required. This rate of change of acceleration, called "jerk" is also a critical component of motion comfort. Janeway concluded that at frequencies of from 1-6 Hz the rate of change of acceleration rather than the acceleration itself is the cause for human discomfort. The



results that were obtained by Boeing Airplane Co. verify Janeway's results for low frequency regions.

#### 1.6. Human Response to Vibration Curves

One of the earliest studies done on human response to vibration was by Reiher and Meister [12]. They subjected some 15 people, aged 25 to 40 years, to vertical sinusoidal vibration without damping for about 5 minutes. The results have been plotted on frequency-displacement and frequency-peak displacement coordinates. It should be noted that the product of peak amplitude and frequency is proportional to peak velocity in the case of sinusoidal vibration. Figures (1.5) and (1.6) show these results. In 1933, Jacklin and Liddle [13] conducted a series of experiments on HRV at the Purdue University Experiment Station. For their early test on a vibratory platform, they used 31 subjects, both sexes, and a rigid wooden chair with no cushions as a seat. The motion produced was in the vertical direction and it was described as "a very close approximation of simple harmonic motion". In their later tests they used approximately 100 young men, aged from 17-27 years. The results of early tests and later tests for vertical motion are shown in Figures (1.7) and (1.8).

#### 1.6.1 Boeing Airplane Company Tests

Parks and Snyder [10] conducted a series of experiments using Boeing human vibration facilities. They subjected 16 employees to low frequency sinusoidal vibration. The 16 subjects were divided into two groups, Group A and Group B. Group A was tested at frequencies, 1, 1-1/2, 2, 4, 6, 10, 14, 18 and 23 Hz; Group B at frequencies 1-1/2, 3, 5, 8, 12, 16, 18, 20 and 27 Hz. Vibration levels were established in





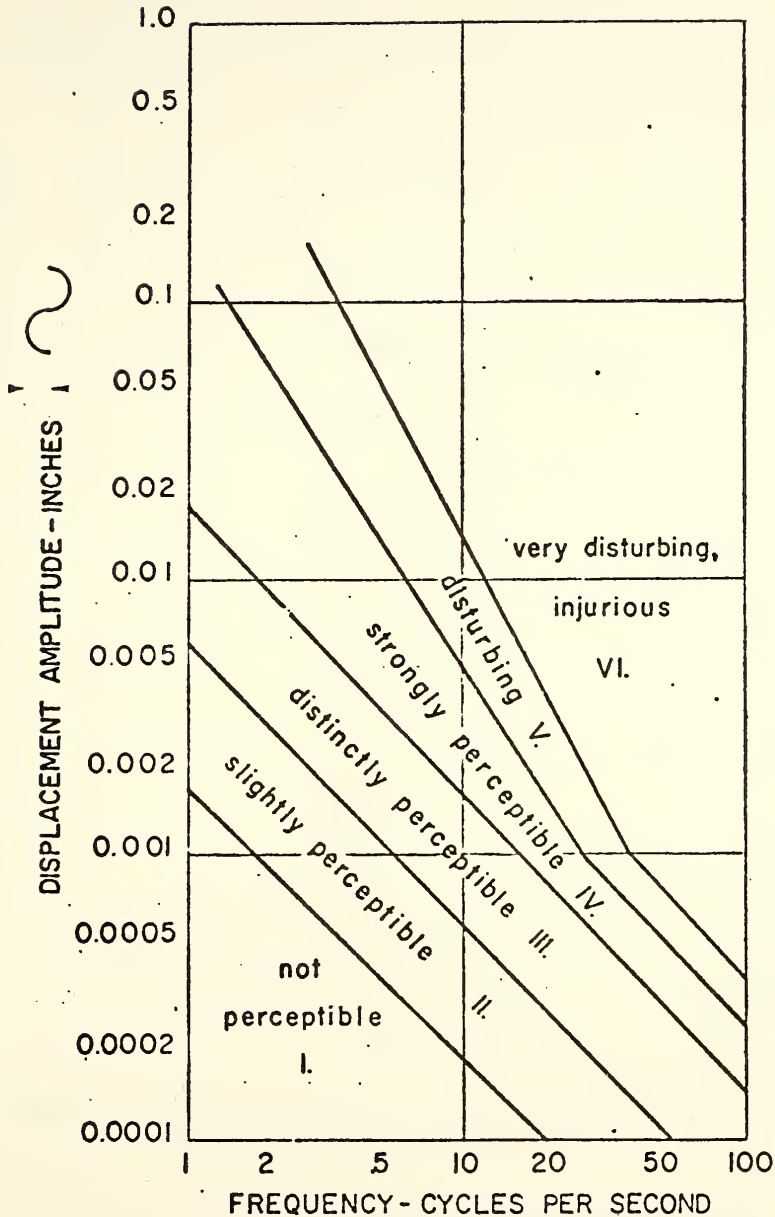


Figure 1.5. Domains of Various Strengths of Sensations for Standing Persons Subject to Vertical Vibration.



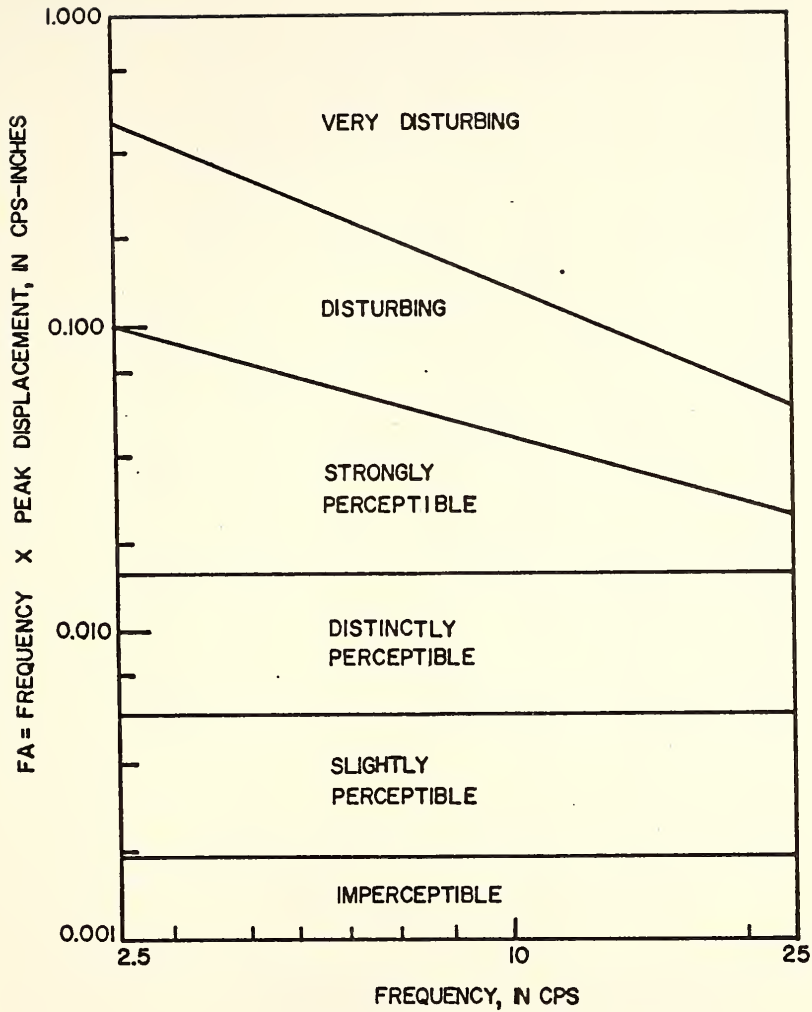
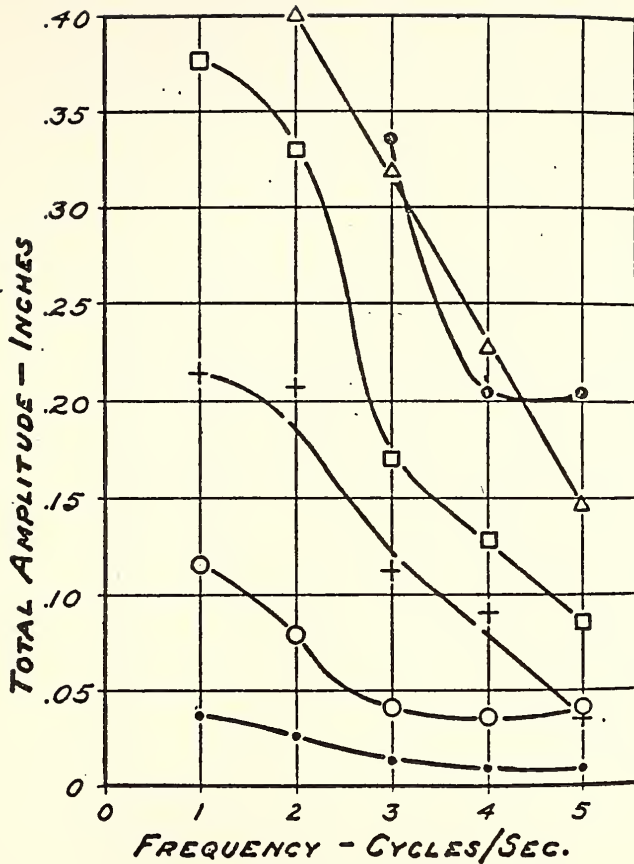


Figure 1.6. Domains of Various Strength of Sensations for Standing Person Subject to Vertical Vibration





LEGEND:

- |               |                 |
|---------------|-----------------|
| ● PERCEPTIBLE | □ UNCOMFORTABLE |
| ○ PLEASING    | △ DISAGREEABLE  |
| + BEARABLE    | ⊙ UNBEARABLE    |

Figure 1.7. Results of Early Tests on Vibrating Platform.



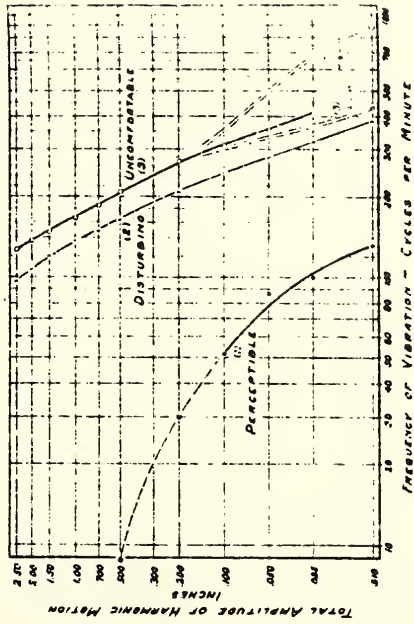


Figure 1.8. Amplitude-Frequency Results with Vertical Motion for Group 1.





terms of four levels defined as: 1, definitely perceptible; 2, mildly annoying; 3, extremely annoying; 4, alarming. A summary of the data for 4 vibration levels of Groups A and B is presented in Figures (1.9) and (1.10). Combined results of Groups A and B are shown in Figure (1.11). Figure (1.12) shows results of 15 different investigators. Each of these curves is supposed to represent comfort limits of the human body to vertical vibration. As it can be seen, there is not a good agreement among these results for the lowest comfort limit. However, most of them seem to agree that for low frequency range of 1 to 5 CPS, human comfort limits for different frequencies may be approximated by constant jerk levels. More information on these curves is contained in Appendix A.

#### 1.6.2 Human Response to Damped Vibrations

Although numerous investigations have been conducted on HRV, only a few have considered the effect of damping. Parmelee and Wiss [5] investigated the effect of damping on human response to sinusoidal vibration. The Wiss and Parmelee project consisted of subjecting individuals in a standing position to vertical displacements having various combinations of frequency, peak amplitude, and damping and having the persons rate each vibration according to the following classification: 1, imperceptible; 2, barely perceptible; 3, distinctly perceptible; 4, strongly perceptible; 5, severe. The ranges of frequencies, peak displacements, and damping used were as follows:

- 1) frequencies - 2.5, 4, 6, 9, 14, 25 CPS
- 2) peak displacements - .0001, .0003, .001, .003, .01, .03,  
.1 inches



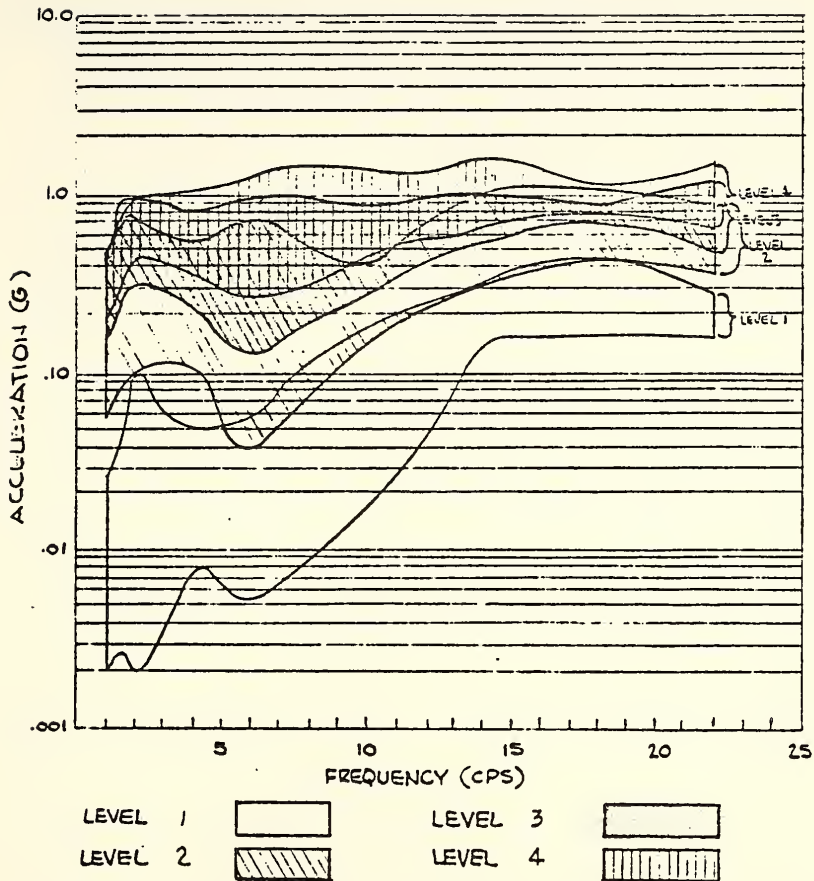


Figure 1.9. Summary of Four Vibration Levels for Group A, Illustrating Overlap Between Levels Resulting from Individual Differences.



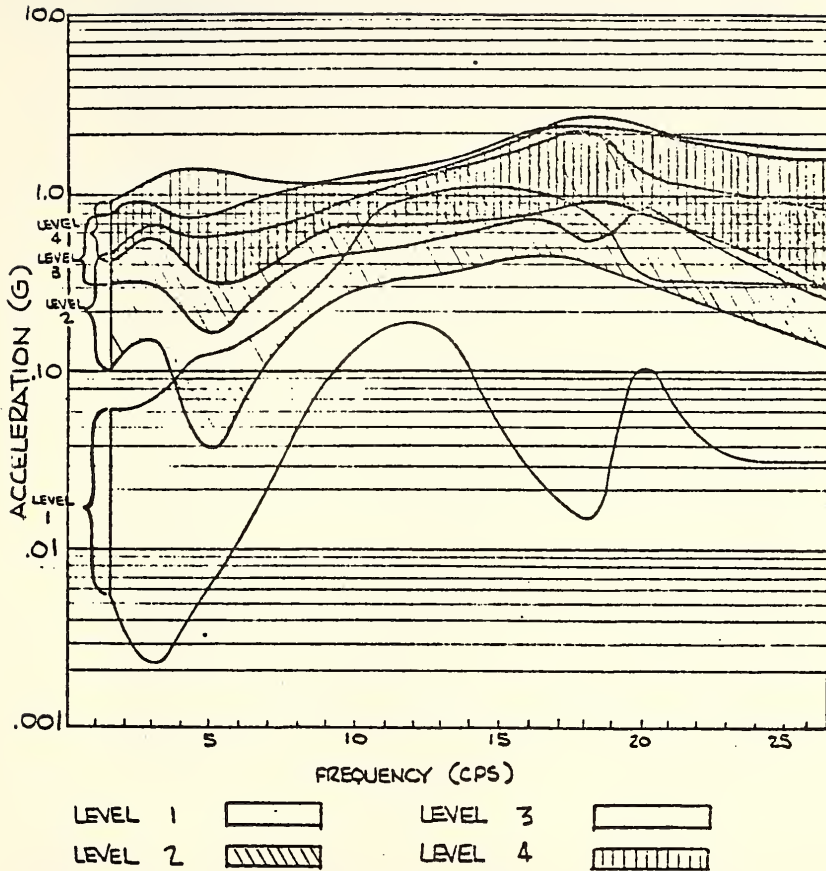


Figure 1.10. Summary of Four Vibration Levels for Group B, Illustrating Overlap Between Levels Resulting from Individual Differences.



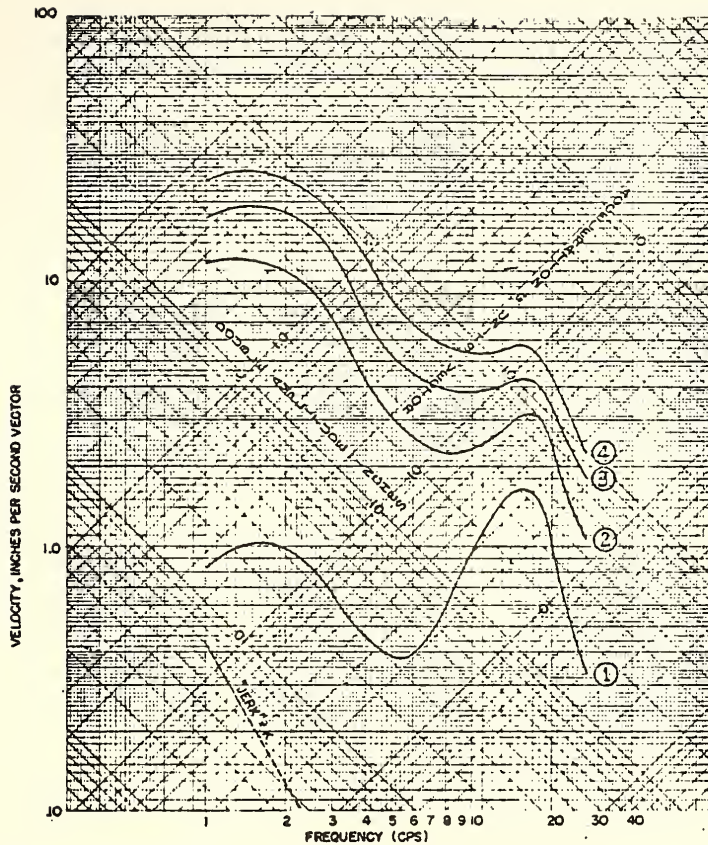


Figure 1.11. A Summary of Data for Judgment Levels 1, 2, 3 and 4. This Coordinate System Presents the Major Physical Descriptions of Vibration, Including an Indication of the Relation that Jerk has to the System.





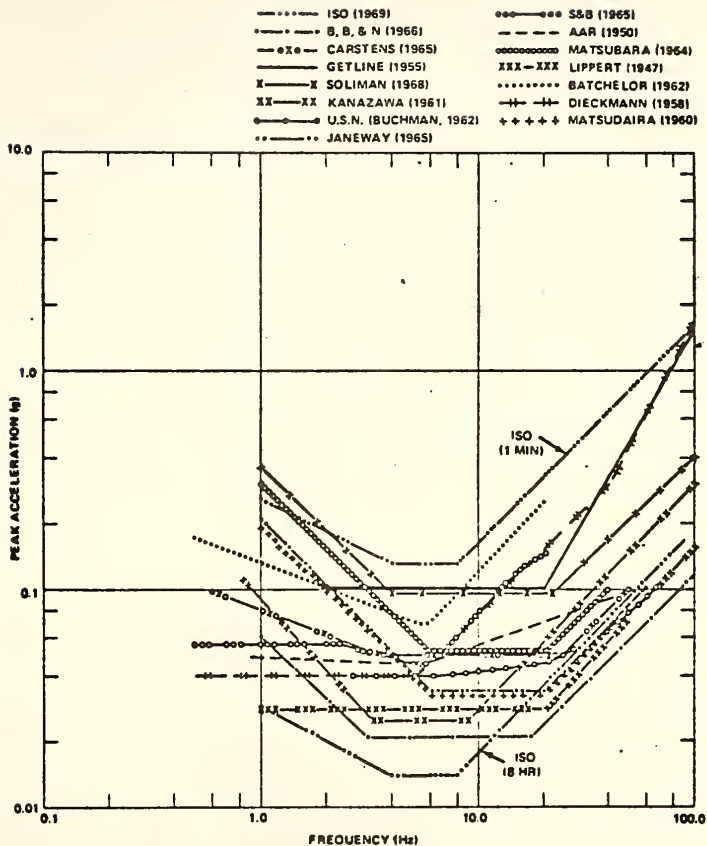


Figure 1.12. Comfort Limits Recommended by Various Investigators for Vertical Vibration or Axis Unspecified [38].



3) damping - .01, .02, .04, .08, .16 of critical damping

The results for barely perceptible, distinctly perceptible and strongly perceptible ratings are shown in Figures (1.13), (1.14), and (1.15). The vertical bars at each circle show one standard deviation above and below mean value of response.

### 1.6.3. Human Response to Non-Sinusoidal Vibration

Only one study was found to have been concerned with a comparison between sinusoidal and random vibration. Pradko, Orr and Lee [6] studied the effects of vertical sinusoidal vibration for the frequency range from 1 to 30 Hz and of vertical random (white noise) vibration through both a 2 Hz and a 10 Hz bandwidth. The center frequencies were in the same range as that used for sinusoidal vibration. The results are shown in Figure (1.16). These curves represent tolerance limits of the subjects.

## 1.7. Scales and Parameters

Most of the investigators in the field of HRV have proposed certain parameters and equations that fit their own results rather well. However, no scale or parameter has yet been suggested that can be used in general cases. In studies of the effects of vibration due to subway trains, Mallock [4] suggested that " $an^3$ " should be a constant. Digby and Sanky [15] proposed that setting " $an$ " equal to a constant would yield best results. Reiher and Meister did not suggest any parameters in describing the nature of their work but another German investigator, Zeller [16], introduced the unit PAL. the PAL is defined as equal to  $10 \log 2x$  where  $x$  is equal to  $a^2/n$  ( $a$  = max amplitude,  $n$  = frequency).



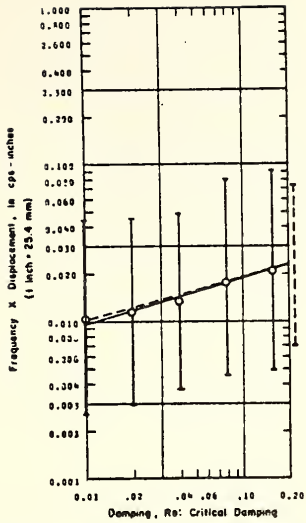


Figure 1.13. Barely Perceptible Rating.

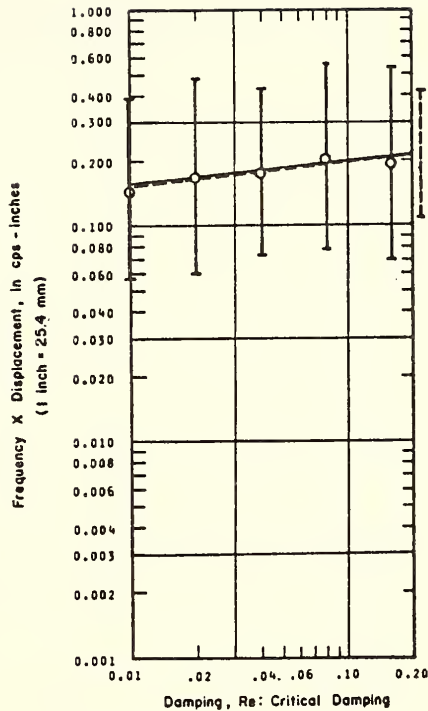


Figure 1.14. Strongly Perceptible Rating.

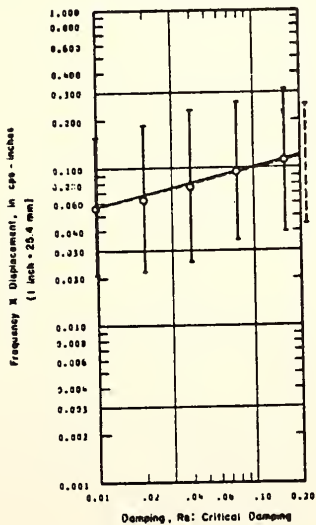


Figure 1.15. Distinctly Perceptible Rating.



NOTE: UPPER AND LOWER CURVES FOR EACH CONDITION BRACKET THE TRUE VALUES OF THE MEAN WITH 90% CONFIDENCE.

SUBJECTS JUDGED TOLERANCE AS A CONDITION IN WHICH PAIN, LOSS OF PHYSICAL STABILITY OR ADVANCED STAGES OF BLURRED VISION WERE CONSIDERED UNACCEPTABLE.

AT LEAST SOME DIFFERENT SUBJECTS USED FOR THE DIFFERENT CONDITIONS.

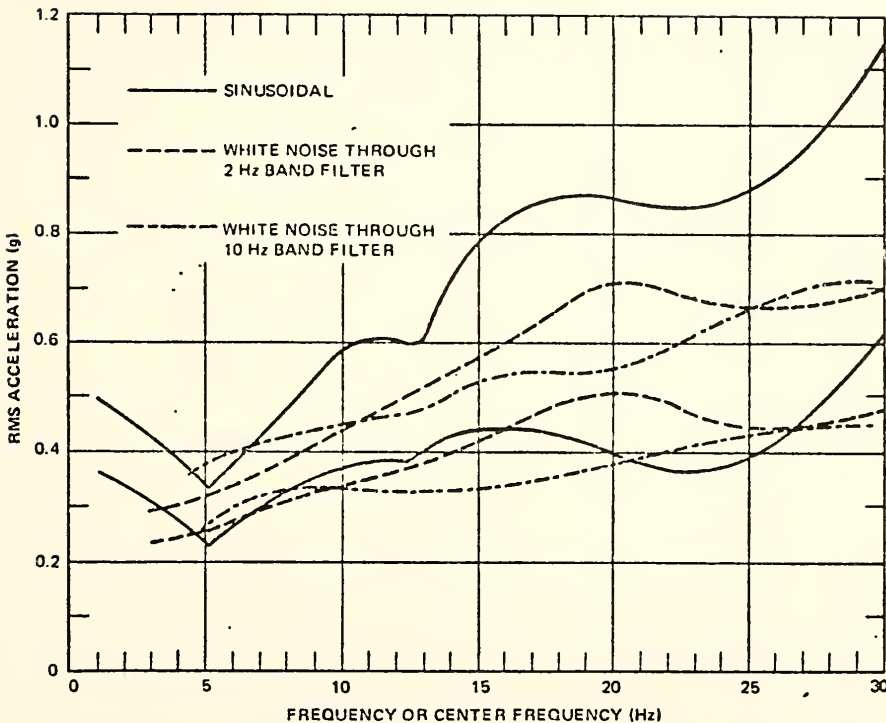


Figure 1.16. Comparison of the Effects of Sinusoidal and Random Vibration on Human Tolerance.





Janeway [11] described levels of equal sensations in terms of a series of parameters as shown in Figure (1.17). For 1-6 CPS, he suggested that equal sensations are given by constant jerk, from 6-20 CPS constant acceleration, and from 20 to 60 CPS constant velocity. Koch [17] introduced a scale of VIBRARS similar to Zeller's PAL. Koch's scale of VIBRAR is shown in Figure (1.18).

### 1.8. Conclusions

Based on this literature review one may conclude that because of the complexity of the human body and individual differences, there are no clear cut boundaries of human sensitivity to vibration but rather there are zones of sensitivity. These zones appear to have contours which depend on frequency and may be defined by constant levels of jerk, acceleration and velocity. Since this literature review is done in connection with a bridge vibration study and the dominant frequencies of most highway bridges are less than 20 CPS, levels of jerk and acceleration are of main concern. Various jerk and acceleration levels for perceptible up to uncomfortable can easily be calculated for simple harmonic excitations from HRV curves.

For the low frequency range (1 to 6 CPS) the limit, which applies to jerk, is about  $1200 \text{ in/sec}^3$ , and for the medium frequency range (6-20 CPS) the limit, which applies to acceleration, is  $40 \text{ in/sec}^2$ . It should be mentioned that pedestrians on a bridge are subjected to vibrations for a relatively short duration of time ( $\approx 15 \text{ sec}$ ) and that they are subjected to transient vibrations. The comfort limits stated here are based on HRV curves that used sustained vibrations for, usually, not less than several minutes. Experiments have shown that



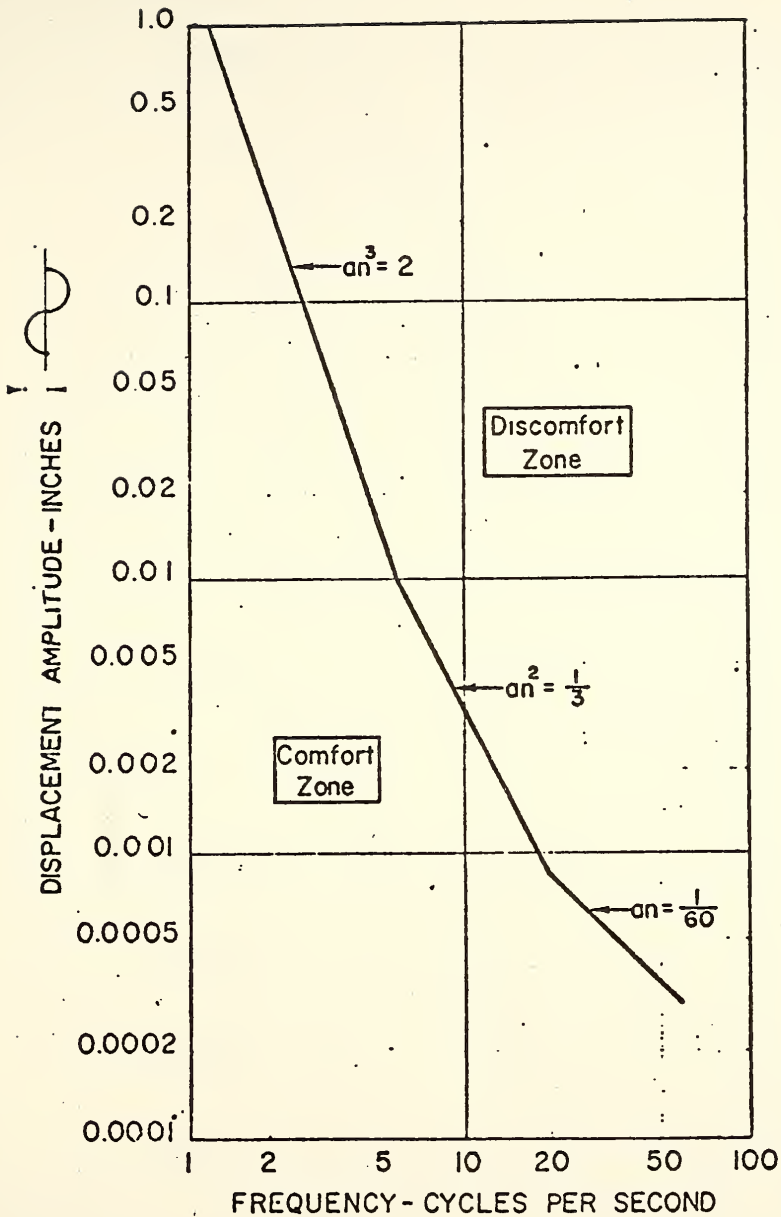


Figure 1.17. Vertical Vibration Limits for Automobile Passenger Comfort. After Janeway.



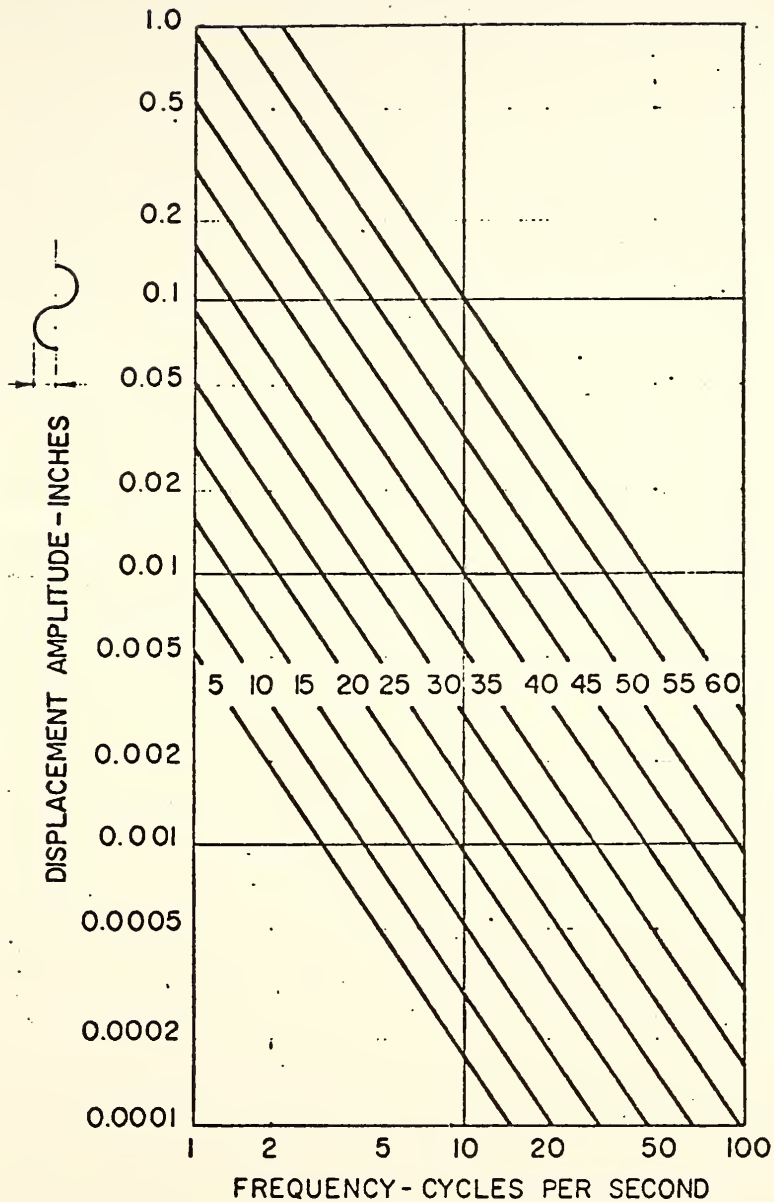


Figure 1.18. Vibration Strength in Vibrars, after Koch and Steffens.



the tolerance of the human body for transient vibration is several times that of sustained vibration. Lenzen [18] suggested that tolerance limits be multiplied by a factor of the order of 10 if the vibration decays to less than 10 percent of its initial magnitude in 5 to 12 cycles. Jacobsen and Ayre [19] showed that 3 percent critical damping is required to meet Lenzen's requirement. Based on the study done by Kropp [33], highway bridges were found to have up to 2.5% damping. Thus, comfort limits of  $1200 \text{ in/sec}^3$  and  $40 \text{ in/sec}^2$  on jerk and acceleration are very conservative. More reasonable limits would be at least three times the stated limits. As a criteria for human response to vertical transient vibration for a short duration of time, limits of  $3600 \text{ in/sec}^3$  on jerk and  $120 \text{ in/sec}^2$  on acceleration have been adopted in this bridge vibration study. It should be mentioned that perceptible limits are far less than these limits. The perceptible limit for acceleration is about  $4 \text{ in/sec}^2$  and that of jerk is about  $120 \text{ in/sec}^3$ . What these limits actually mean is that any low frequency vibration (1-6 CPS) with jerk in the range of 120 to  $3600 \text{ in/sec}^3$  and any medium frequency range vibration (6-20 CPS) with acceleration in the range of 4 to  $120 \text{ in/sec}^2$  can be felt by the human body but will not, in general, cause discomfort.





## CHAPTER II

### FUNDAMENTAL FREQUENCIES

#### 2.1. General

In the studies [27,28,29] done on dynamic response of two and three span highway beam bridges under moving loads, the assumption has usually been made that bridges vibrate only in their bending mode. In this study, the bending mode of vibration refers to the case in which dynamic deflections of the bridge are symmetric with respect to the longitudinal center line of the bridge, and the torsional mode refers to the case in which dynamic deflections of the bridge are anti-symmetric with respect to the longitudinal center line. The bending mode assumption has been justified on the grounds that either there is no torsion in the dynamic response of highway bridges or that the torsion response is of such a magnitude that it can be neglected.

In the course of Kropp's field study [33] it became apparent that the torsional mode of vibration is significant and should not be neglected. The available program for the analysis of simple span bridges does take into account, to a certain extent, the torsional effect of bridge vibration. The programs for two and three span highway bridges, however, analyze the bridge as a single continuous beam thereby neglecting torsional behavior. In order to make use of these programs, it is necessary to have some idea about the percent contribution of the torsional mode to the dynamic response of bridges.



## 2.2. Special Tests and Observations

The fundamental bending frequency of a simple span or two span bridge with two equal spans can easily be determined by treating the bridge as a single beam with the same cross sectional moment of inertia and total mass as that of the bridge. A two span bridge which is symmetric about its center support has the same fundamental frequency as each of its spans. Figures (2.1) and (2.2) show the deflected shapes, which correspond to the fundamental bending frequency of simple span and two span bridges.

Figures (2.3) and (2.4) show the deflected shapes which correspond to the first torsional mode of vibration of single span and two span bridges. Fundamental bending and torsional frequencies of the single span and two span bridges in the study have been calculated by the simplified methods which are explained in Appendix B. Actual fundamental frequencies were obtained from frequency spectra (see Appendix B, Figures B.6 through B.17). These theoretical and measured frequencies are tabulated in Table (2.1). Results in Table (2.1) show that calculated bending frequencies are very close to the measured values but calculated frequencies for fundamental torsion are consistently less than measured values. The reason for this discrepancy is due to the neglect of the additional torsional stiffness caused by channels or cross bracing of the girders of the bridge. Measured fundamental torsional frequencies are between 7% to 30% higher than measured bending frequencies.

Since the bending frequencies using the non-composite moment of inertia were found to be too low, it has been concluded that there is



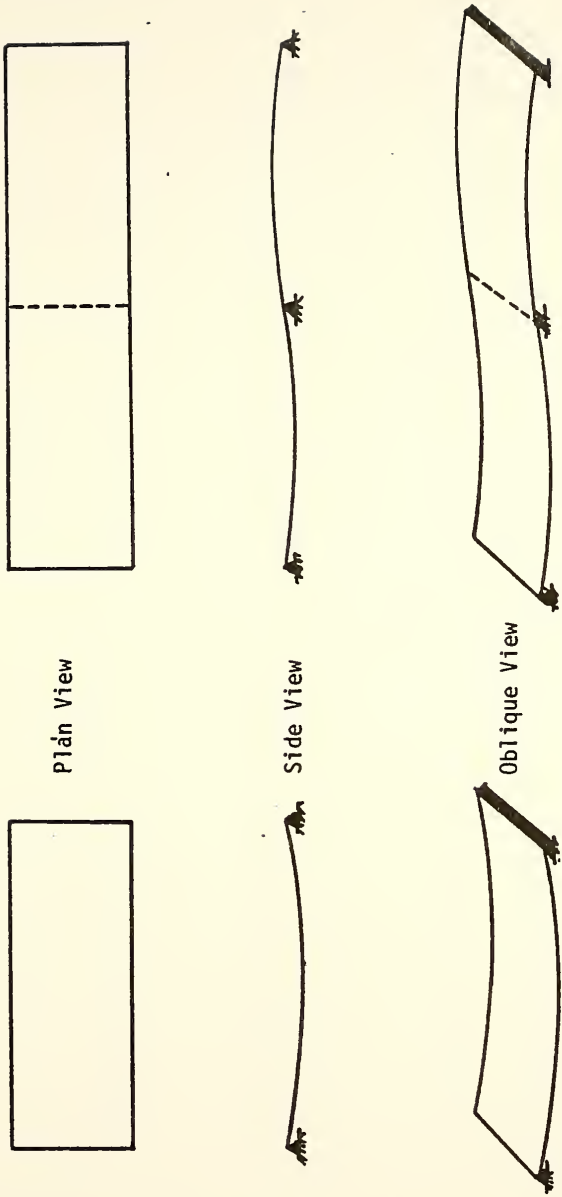


Figure 2.1. Deflected Shape for Fundamental Bending Mode of Single Span Bridge

Figure 2.2. Deflected Shape for Fundamental Bending Mode of Two Span Bridge



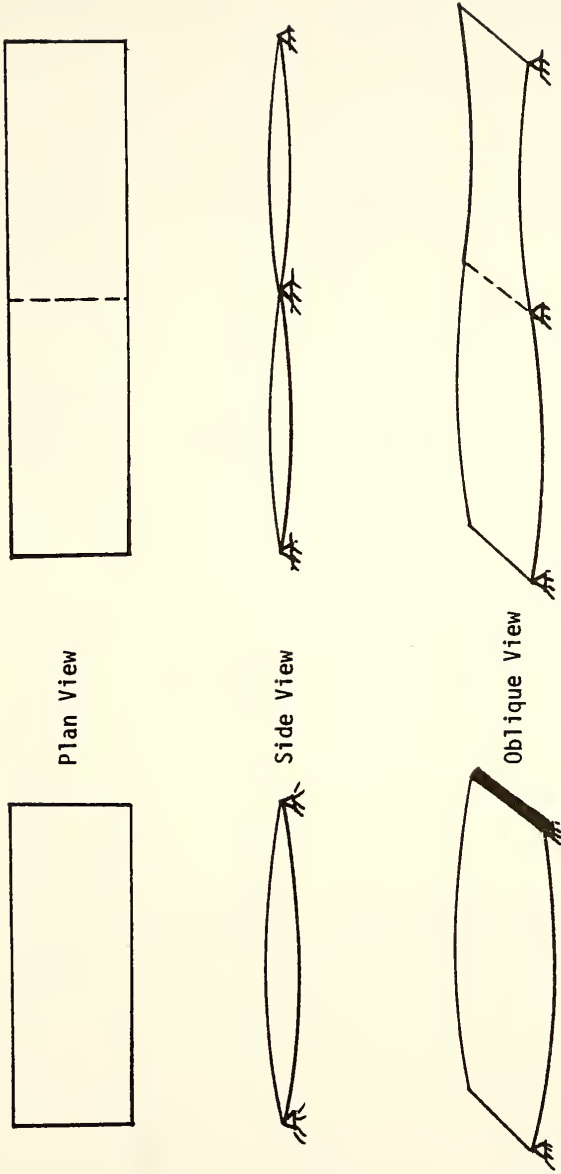


Figure 2.3. Deflected Shape for Fundamental Torsion of Single Span Bridge

Figure 2.4. Deflected Shape for Fundamental Torsion Mode of Two Span Bridge





Table 2.1. Theoretical and Measured Fundamental Frequencies

Bridge Type	Bending Frequency (HZ)		Torsional Frequency (HZ)		*
	Calculated	Measured	Calculated	Measured	
<u>Single Span</u>					
SB-A-4	6.39	7.62	6.56	8.40	10.
SB-B-1	6.95	6.77	7.55	7.88	16.
SB-C-1	4.82	4.88	4.97	5.27	8.
<u>Two Span</u>					
KCSB-A-1	2.71	2.73	2.92	3.32	21.
KCSB-B-1	2.19	2.15	2.32	2.73	27.
KCSB-C-2	3.73	3.81	3.82	4.10	7.
KCSB-D-2	2.62	2.83	2.80	3.03	7.
KCSG-A-1	2.27	2.34	2.42	2.83	21.
KCSG-B-1	2.20	2.22	2.63	2.90	30.
KCPG-A-1	2.36	2.44	2.70	3.12	28.
KCPG-B-2	2.29	2.25	2.40	2.83	26.

$$*100 \left( \frac{\text{Measured Torsional Frequency} - \text{Measured Bending Frequency}}{\text{Measured Bending Frequency}} \right)$$



full composite action and the girders should be treated as such. Throughout this study the composite moment of inertia of girders has been used rather than the moment of inertia of the girder alone.

Field results from two accelerometers placed on either side and at the transverse center line, shown in Figure (2.5), of one of the single span bridges in the study are shown in Figure (2.6). The curves shown in Figure (2.6) correspond to the output from accelerometer number 1, which is on the traffic side, accelerometer number 2, which is on the opposite side, and the difference.

Theoretically, if the bridge were only vibrating in its fundamental bending and torsional modes, the dynamic response of the bridge at the locations of accelerometers 1 and 2 could be expressed as:

$$\text{Dynamic Response 1} = R_B(t) + R_T(t)$$

$$\text{Dynamic Response 2} = R_B(t) - R_T(t)$$

where  $R_B(t)$  and  $R_T(t)$  are dynamic response functions corresponding to bending and torsion respectively. Taking the sum and the difference of these two responses one could obtain the effect of bending or torsion alone on the dynamic response of highway bridges. Unfortunately this is not the case, and taking the sum and the difference of the output of accelerometers 1 and 2 does not yield pure bending or pure torsional effects. This is primarily due to the fact that bridges do not vibrate at their fundamental modes only, but rather there is a combination of modes at which they vibrate. Since it is necessary to have some idea about the contribution of bending and torsion to dynamic response of a bridge, a series of special tests were made in



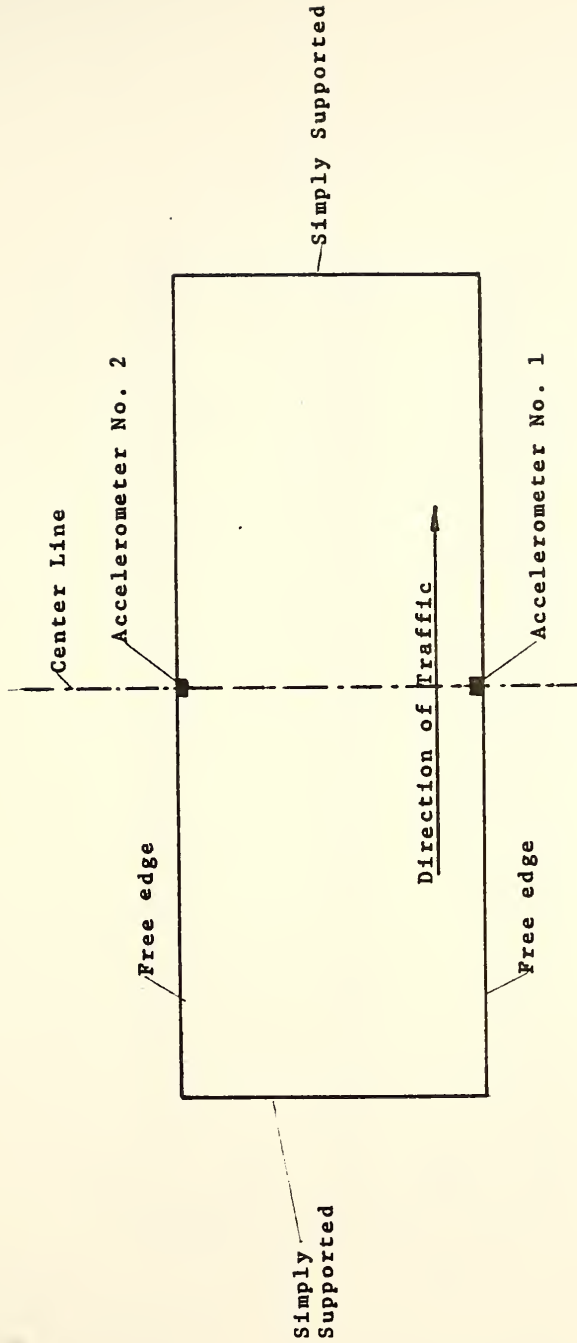


Figure 2.5 Accelerometer Locations for Special Tests



VEHICLE VELOCITY 40 MPH

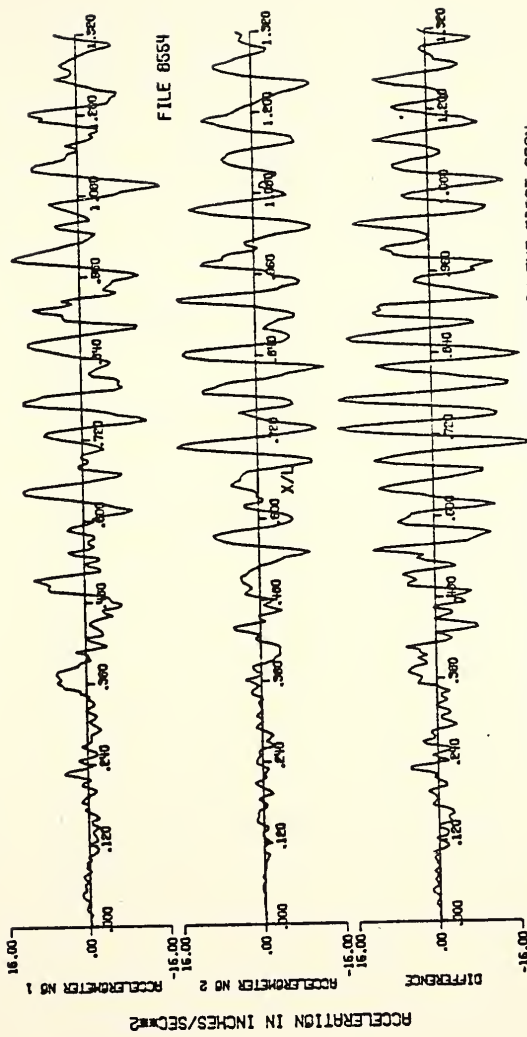


FIGURE 2.6 ACCELERATION RECORDS FROM TWO ACCELEROMETERS IN THE FIRST SPAN  
ACCELEROMETERS HAVE THE SAME TRANSVERSE LOCATION  
BUT ARE ON OPPOSITE SIDES OF THE BRIDGE

SINGLE SPAN STEEL BEAM BRIDGE  
SPAN LENGTH 72.0 FT  
MIDTH - 41.0 FT  
US 231 OVER HOME DITCH, JASPER COUNTY  
BRIDGE STUDY NUMBER 88-C-1





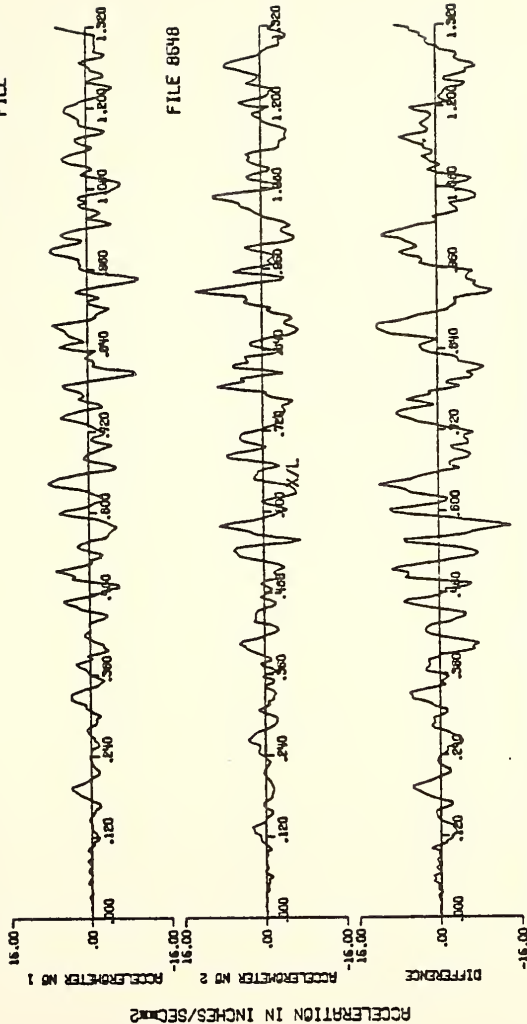
the hope that these tests would separate these effects. The special tests consisted of driving the vehicle down the center line of the bridge and getting the accelerometer 1 and 2 outputs. Theoretically, this should have eliminated any torsional (unsymmetrical) modes, and the output from the two accelerometers should have been identical. The outputs of accelerometers 1 and 2 are shown in Figure (2.7). The significant difference between accelerometers 1 and 2 shows the presence of torsion. Probable causes of the torsion are

- a) The vehicle was not exactly driven down the middle of the bridge,
- b) The bridge roughness under the two lines of wheels was not the same,
- c) The vehicle load was not evenly distributed on left and right line of wheels, and
- d) The vehicle initially had some rotation vibration about its longitudinal axis. This could have resulted from the uneven bumps on the road before the bridge.

One or a combination of these could have resulted in excitation of torsional modes. Running the vehicle down the center line of the bridge did not eliminate torsional modes, but it did cut torsional modes considerably. Figure (2.8) shows the frequency spectrum of the single span bridge under study (SB-C-1) for the case in which the vehicle was travelling close to the center line. Figures (2.9) and (2.10) show the frequency spectra for the same bridge with the vehicle in the travel lane and close to the curb. The first two peaks on the frequency spectrum charts correspond to fundamental bending and



VEHICLE VELOCITY 40 MPH  
FILE



FILE 8648

FIGURE 2.7 ACCELERATION RECORDS FROM TWO ACCELEROMETERS IN THE FIRST SPAN  
ACCELEROMETERS HAVE THE SAME TRANSVERSE LOCATION  
BUT ARE ON OPPOSITE SIDES OF THE BRIDGE

SINGLE SPAN STEEL BEAM BRIDGE  
SPAN LENGTH 75.0 FT  
HIGHLIGHT 41.0 FT  
US 231 OVER HOME DITCH, JASPER COUNTY  
BRIDGE STUDY NUMBER SB-C-1



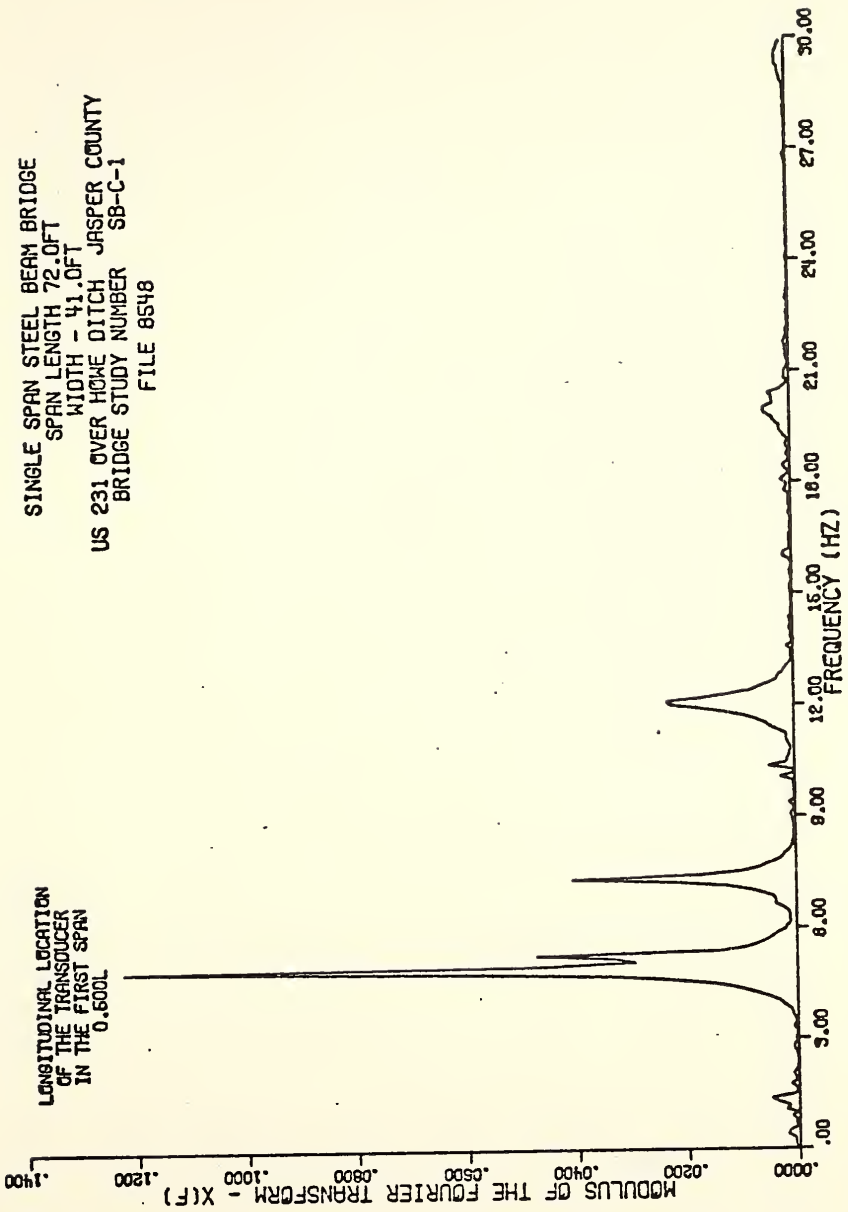


Figure 2.8. Fourier Spectrum of the Free Vibration of Acceleration, Transverse Vehicle Position-Bridge Centerline.



SINGLE SPAN STEEL BEAM BRIDGE  
 SPAN LENGTH 72.0 FT  
 WIDTH - 41.0 FT  
 US 231 OVER HOME DITCH JASPER COUNTY  
 BRIDGE STUDY NUMBER SB-C-1  
 FILE 8551

LONGITUDINAL LOCATION  
 OF THE TRANSDUCER  
 IN THE FIRST SPAN  
 0.500L

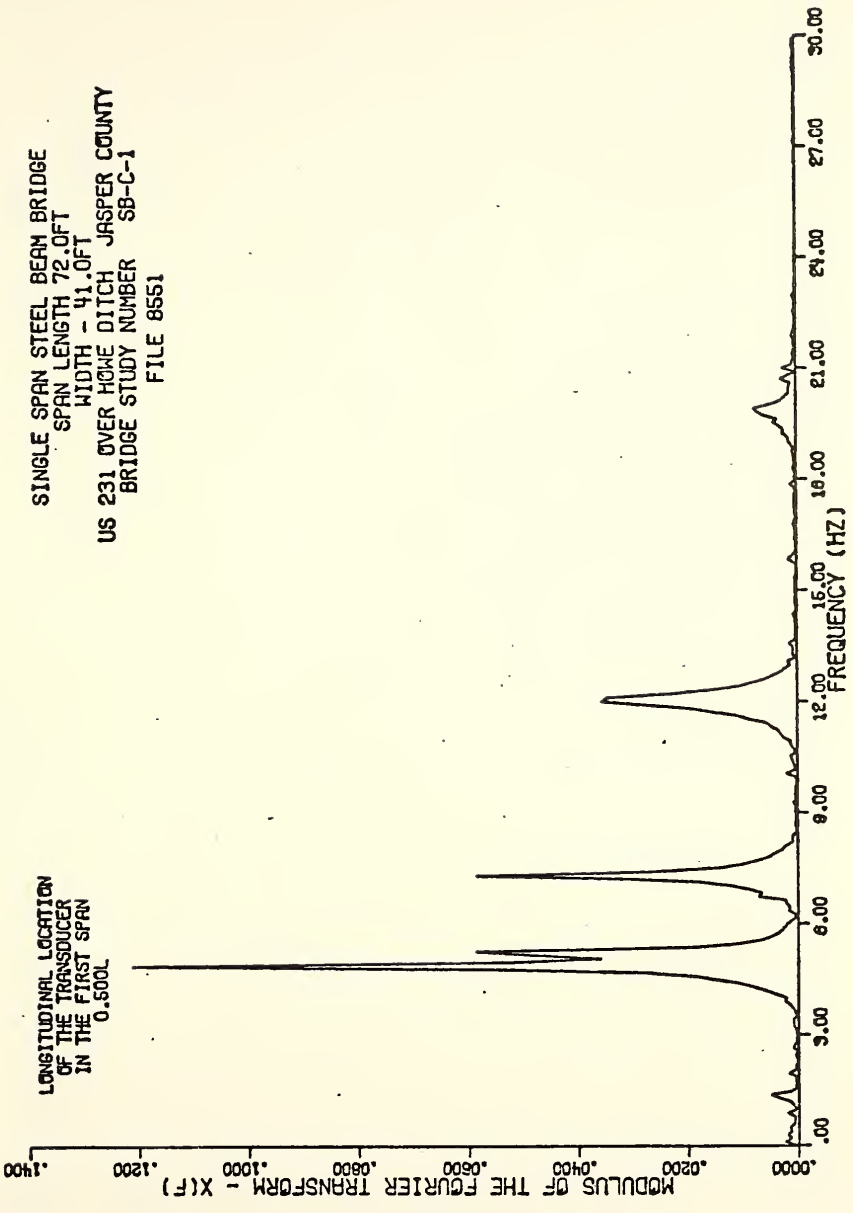


Figure 2.9. Fourier Spectrum of the Free Vibration of Acceleration, Transverse Vehicle Position-Travel Lane.





LONGITUDINAL LOCATION  
 OF THE TRANSDUCER  
 IN THE FIRST SPAN  
 0.600L

SINGLE SPAN STEEL BEAM BRIDGE  
 SPAN LENGTH 72.0FT  
 WIDTH - 41.0FT  
 US 231 OVER HOWE DITCH JASPER COUNTY  
 BRIDGE STUDY NUMBER SB-C-1  
 FILE 8554

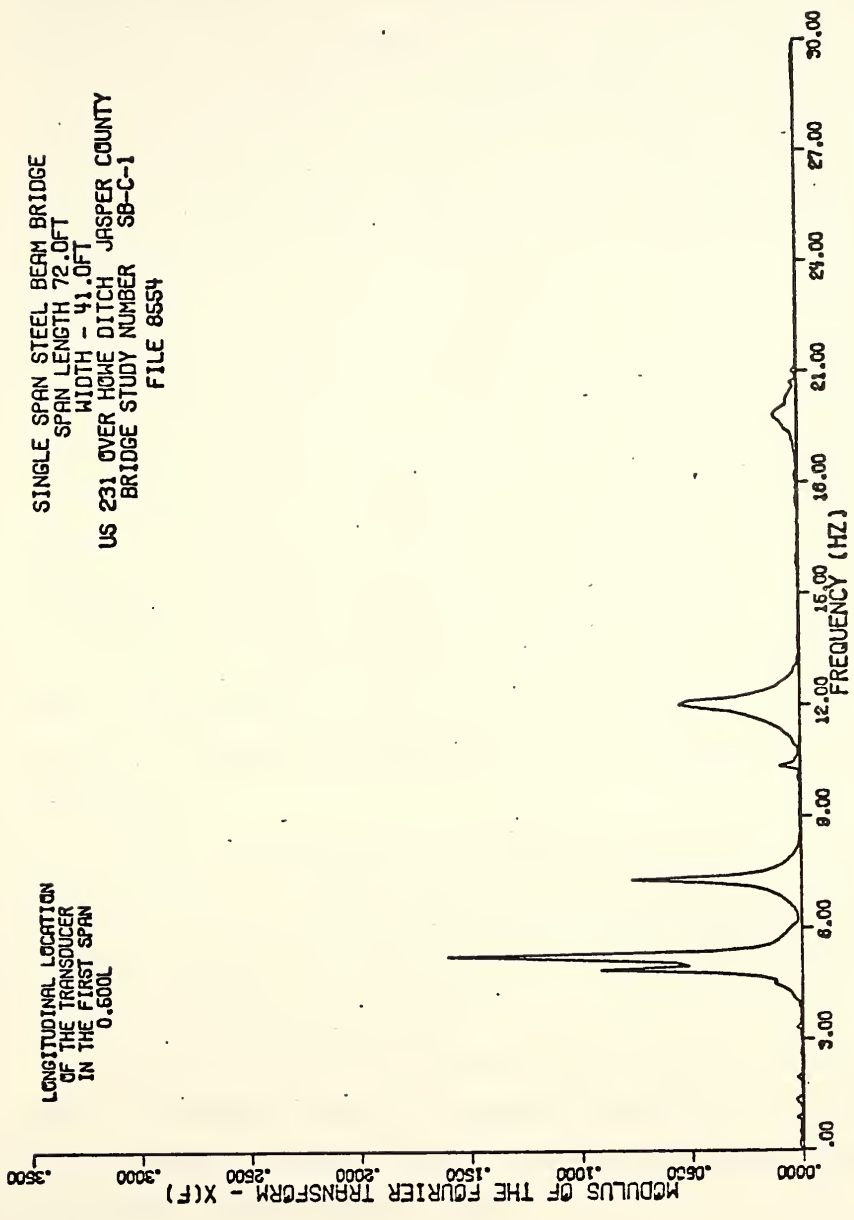


Figure 2.10. Fourier Spectrum of the Free Vibration of Acceleration, Transverse Vehicle Position-Curb Lane.



torsion respectively. The relative magnitudes of the peaks in the frequency spectrum charts indicate that when the vehicle was travelling close to the curb the fundamental torsional mode was excited more than the fundamental bending mode. The opposite happened when the vehicle was travelling close to the center line of the bridge. Similar results were obtained for the two span and the three span bridges in the study. Figures (2.11) through (2.16) show corresponding frequency spectrum charts.

Transverse position of the vehicle also has significant effects on the dynamic deflections and accelerations of the bridge. Dynamic deflection of the single span bridge at the location of accelerometer 1 was 10 times more for the case where the vehicle was close to the curb than for the case where the vehicle was on the center line. The corresponding increase for acceleration was about 70%.

For the two span bridge there was more than a 60% increase in dynamic deflection and a 40% increase for acceleration. Corresponding numbers for the three span bridge were 300% for deflection and 36% for acceleration.

Since it was not possible to totally eliminate torsional modes in the special tests, the theoretical contribution of the torsional mode to dynamic response was determined using the single span program. Results are discussed in later chapters.

Among the properties of the bridge which can be readily calculated are its fundamental bending and torsional frequencies. In following parts a parametric study is done in which factors affecting fundamental frequencies of the bridge are studied.



2-SPAN COMPOSITE CONTINUOUS PLATE GIRDER BRIDGE  
 SPAN LENGTHS 122.5FT.122.5FT  
 WIDTH - 32.0FT  
 WYANDOTTE ROAD OVER I-65 TIPPECANOE COUNTY  
 BRIDGE STUDY NUMBER KCSG-A-1  
 FILE 8497

LONGITUDINAL LOCATION  
 OF THE TRANSDUCER  
 IN THE FIRST SPAN  
 0.250L

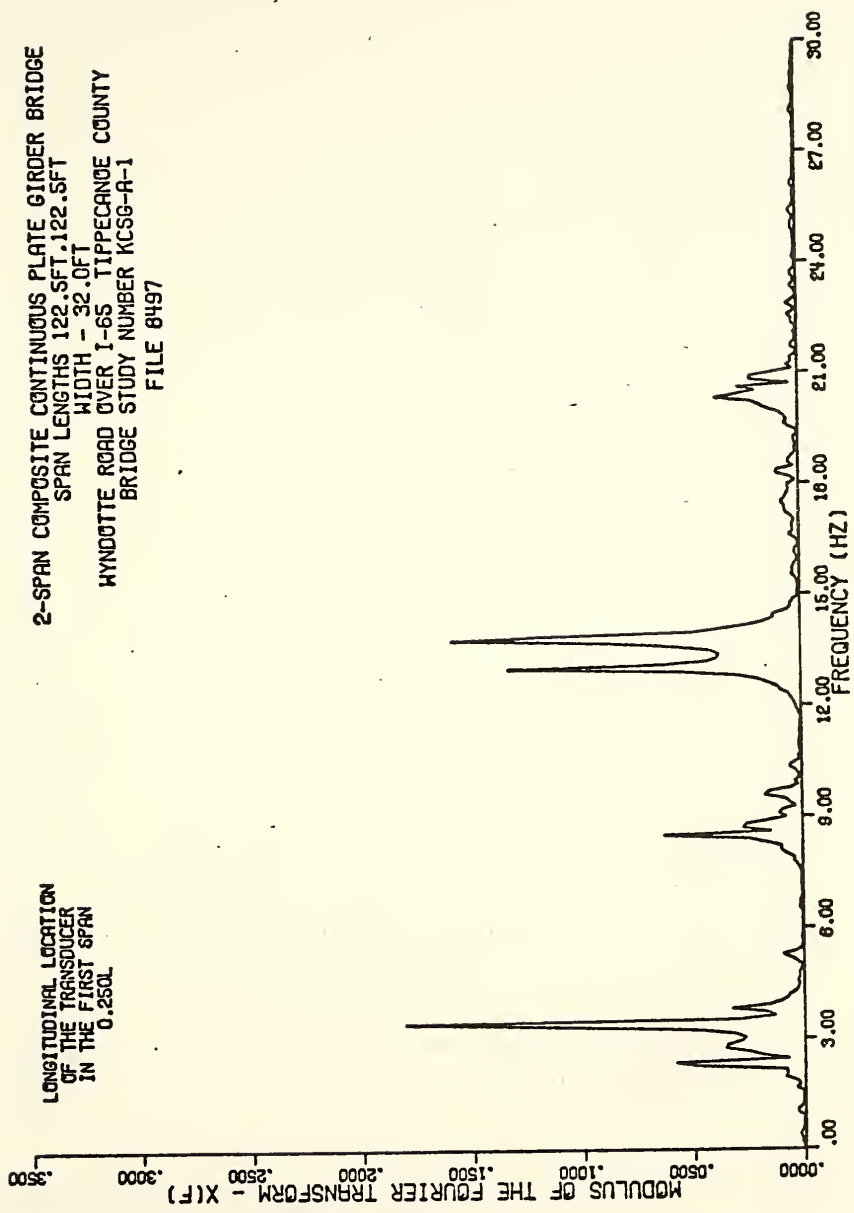


Figure 2.11. Fourier Spectrum of the Free Vibration of Acceleration, Transverse Vehicle Position-Bridge Centerline.



2-SPAN COMPOSITE CONTINUOUS PLATE GIRDER BRIDGE  
 SPAN LENGTHS 122.5FT, 122.5FT  
 WIDTH - 32.0FT  
 WYANDOTTE ROAD OVER I-65 TIPPECANOE COUNTY  
 BRIDGE STUDY NUMBER KCSG-A-1  
 FILE 8499

LONGITUDINAL LOCATION  
 OF THE TRANSDUCER  
 IN THE FIRST SPAN  
 0.250L

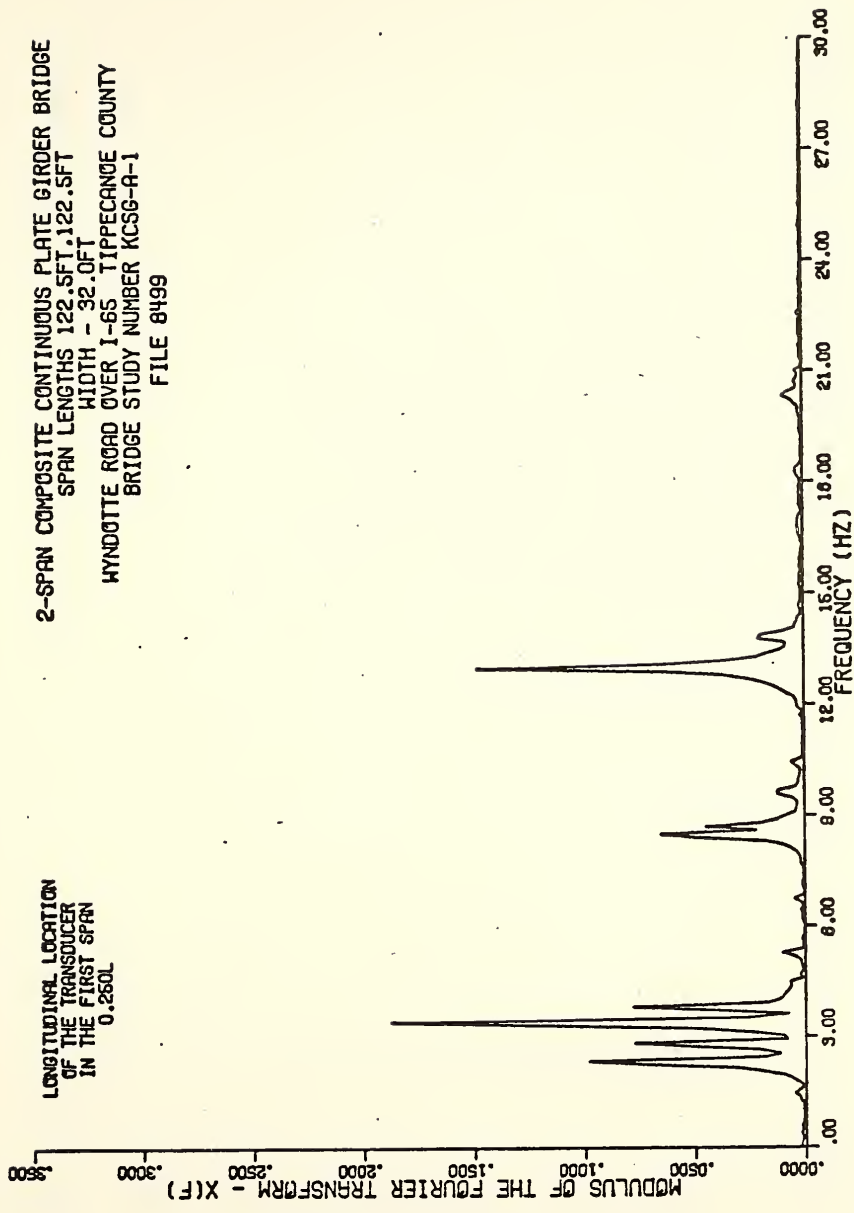


Figure 2.12. Fourier Spectrum of the Free Vibration of Acceleration, Transverse Vehicle Position-Travel Lane.





2-SPAN COMPOSITE CONTINUOUS PLATE GIRDER BRIDGE  
SPAN LENGTHS 122.5FT, 122.5FT  
WIDTH - 32.0FT  
HYNDOTTE ROAD OVER I-65, TIPPECANOE COUNTY  
BRIDGE STUDY NUMBER KCSG-A-1  
FILE 8501

LONGITUDINAL LOCATION  
OF THE TRANSDUCER  
IN THE FIRST SPAN  
0.250L

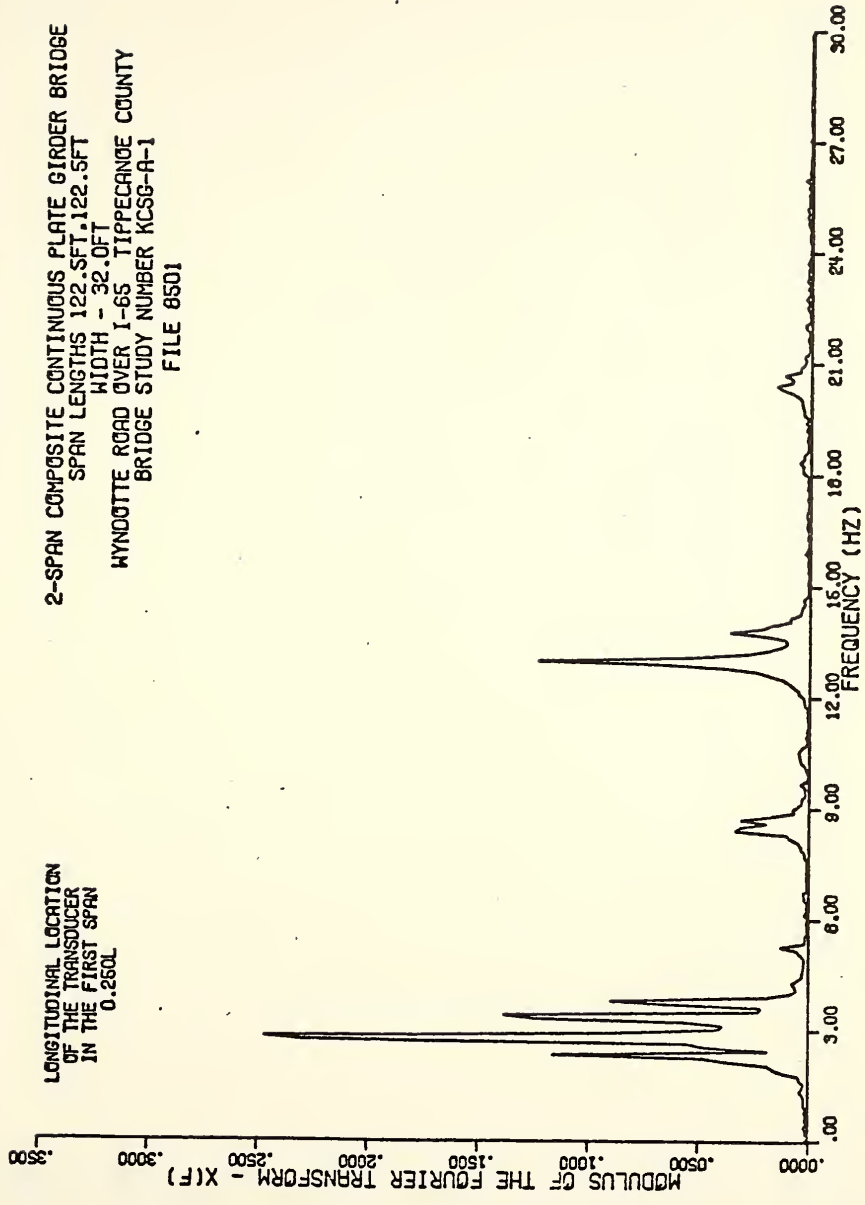


Figure 2.13. Fourier Spectrum of the Free Vibration of Acceleration, Transverse Vehicle Position-Curb Lane.



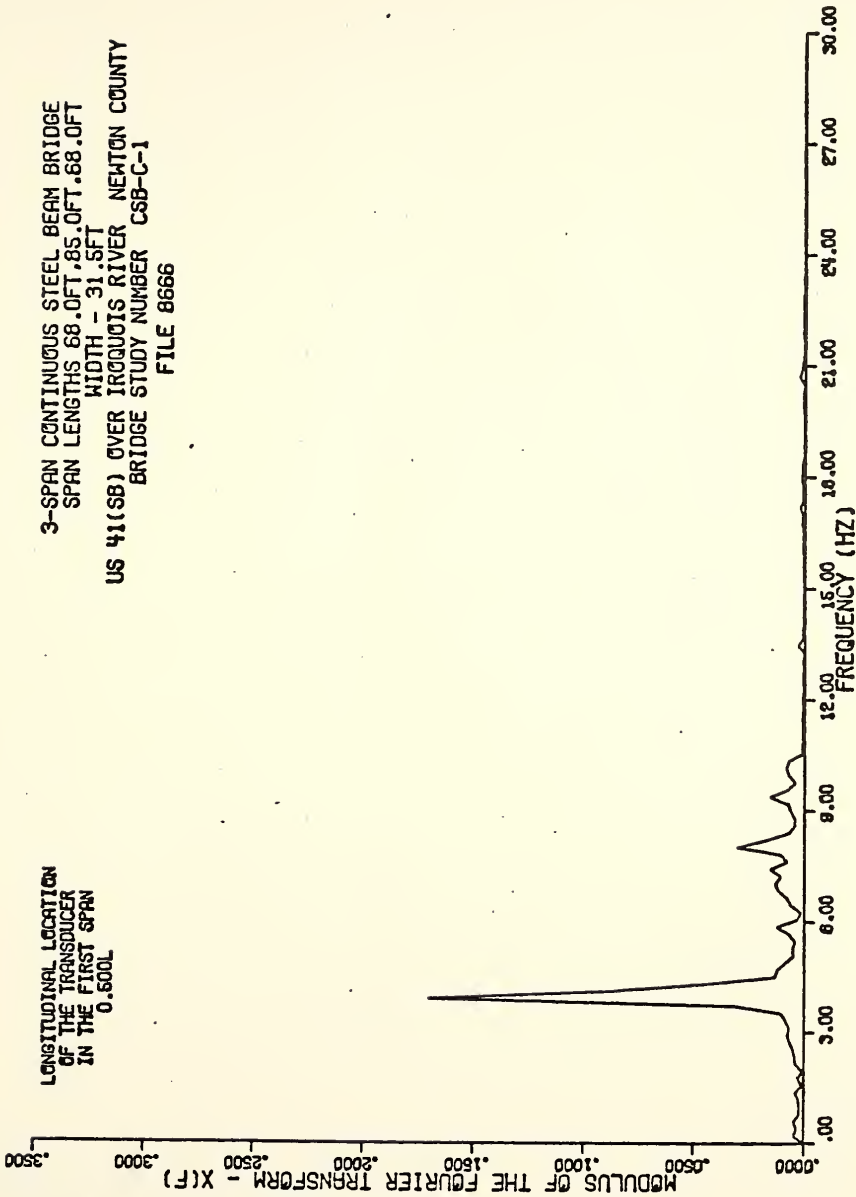


Figure 2.14. Fourier Spectrum of the Free Vibration of Deflection, Transverse Vehicle Position-Bridge Centerline.



3-SPAN CONTINUOUS STEEL BEAM BRIDGE  
SPAN LENGTHS 68.0FT, 65.0FT, 66.0FT  
WIDTH - 31.5FT  
US 41(SB) OVER ILLINOIS RIVER NEWTON COUNTY  
BRIDGE STUDY NUMBER CSB-C-1  
FILE 8689

LONGITUDINAL LOCATION  
OF THE TRANSDUCER  
IN THE FIRST SPAN  
0.600L

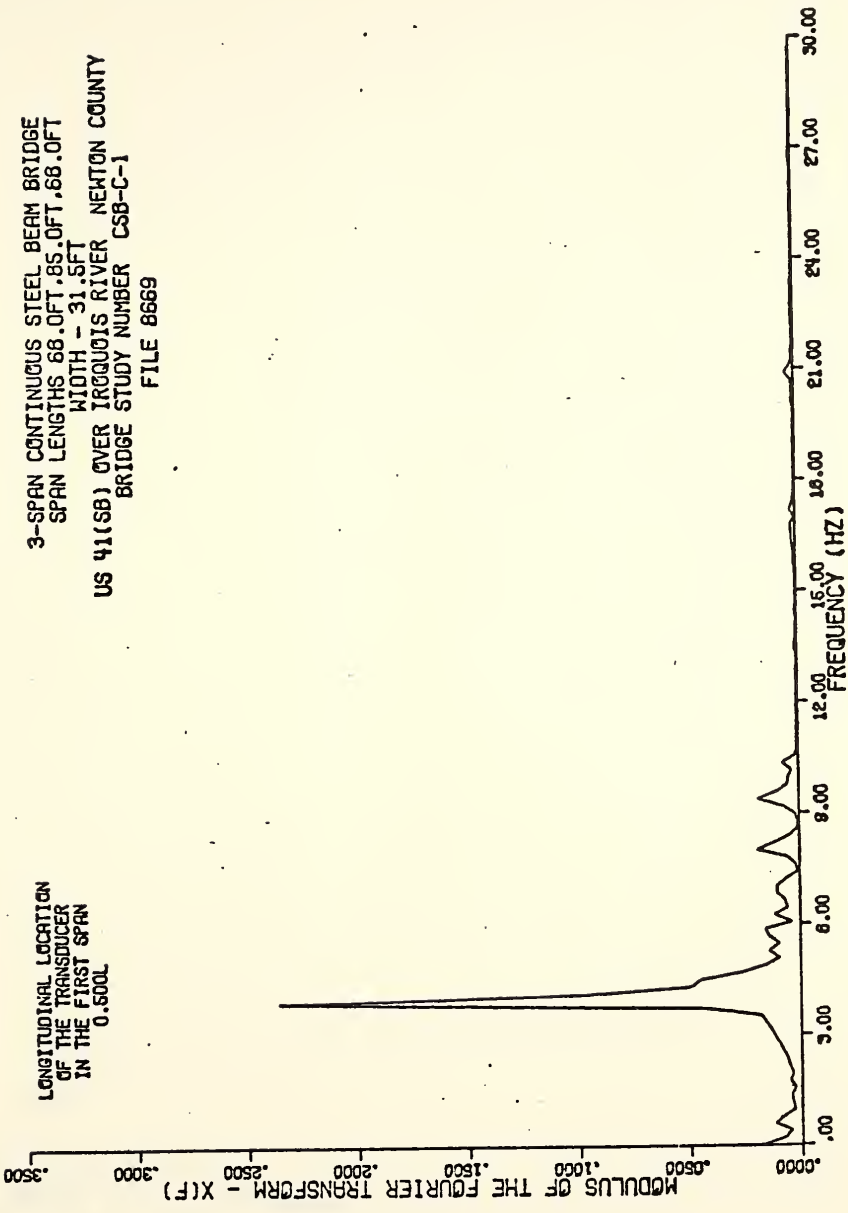


Figure 2.15. Fourier Spectrum of the Free Vibration of Deflection, Transverse Vehicle Position-Travel Lane.



3-SPAN CONTINUOUS STEEL BEAM BRIDGE  
 SPAN LENGTHS 68.0FT, 85.0FT, 68.0FT  
 WIDTH - 31.5FT  
 US 41(SB) OVER IROQUOIS RIVER NEWTON COUNTY  
 BRIDGE STUDY NUMBER CSB-C-1  
 FILE 8672

LONGITUDINAL LOCATION  
 OF THE TRANSDUCER  
 IN THE FIRST SPAN  
 0.600L

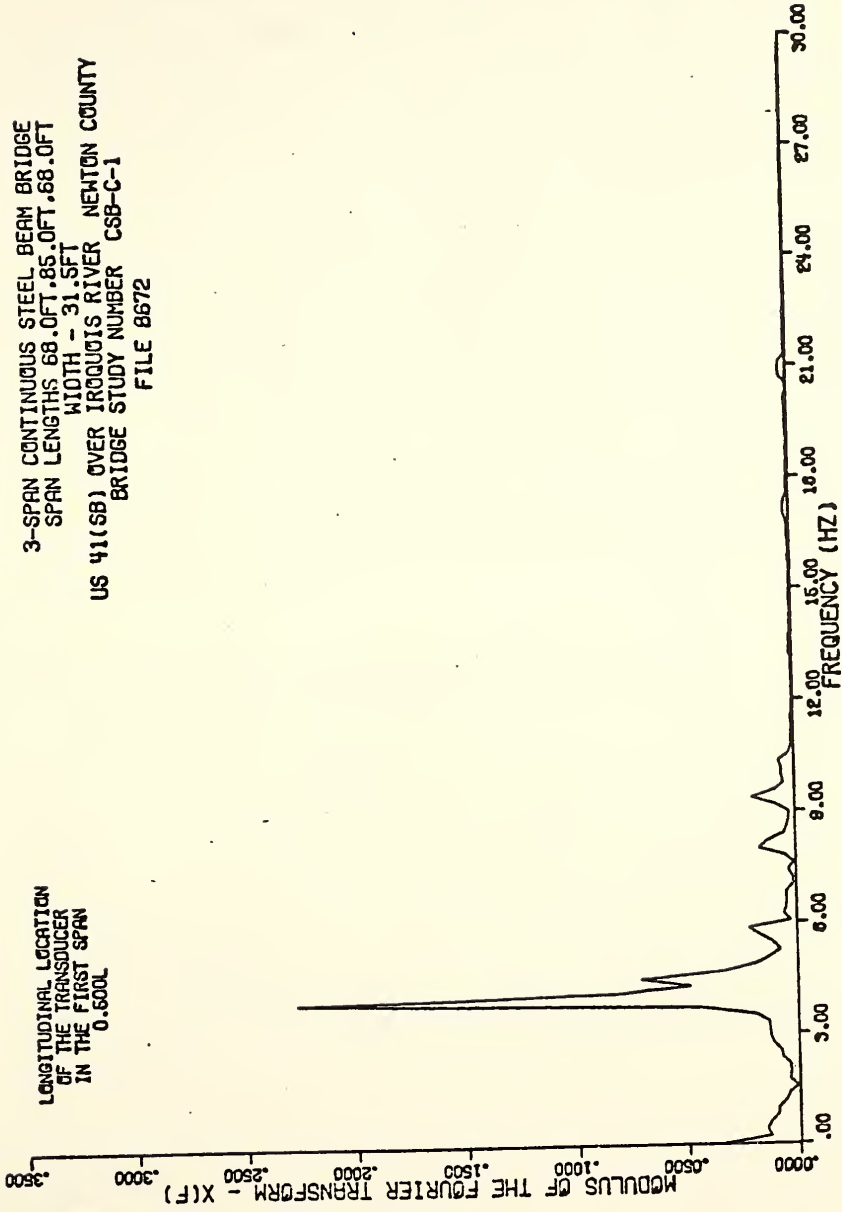


Figure 2.16. Fourier Spectrum of the Free Vibration of Deflection, Transverse Vehicle Position-Curb Lane.





### 2.3. Effect of Girder Flexibility on Fundamental Frequencies

At the design state, the structural engineer has the choice of using normal grade steel or high strength steel. Usage of high strength steel could reduce the cross sectional moment of inertia by up to 30% when compared to a comparable design using normal grade steel. In order to determine how the reduction of moment of inertia affects fundamental frequencies, fundamental frequencies of the single span bridge (SB-C-1) for the actual girder stiffness and for 10%, 20% and 30% reductions in stiffness are calculated and compared. Table (2.2) shows fundamental frequencies for various reductions in stiffness. The same results are shown graphically in Figure (2.17). Results indicate that a 30% reduction in girder stiffness reduces the fundamental bending frequency by 16.4% and the fundamental torsional frequency by 15.8%.

### 2.4. Effect of Slab Thickness on Fundamental Frequencies

The single span bridge (SB-C-1) has a 6" slab thickness. In order to account for transverse stiffness due to reinforcement, an effective slab thickness of 6.2" has been used. Fundamental frequencies of the bridge (SB-C-1) for 5", 6.2", 7" and 8" slab thicknesses are calculated and results are shown in Table (2.3). The same results are presented graphically in Figure (2.18). Results show that 30% increase in slab thickness reduces fundamental frequencies by not more than 8%.



Table 2.2. Effect of Reduction of Moment of Inertia on Fundamental Frequencies

Fundamental Mode	Frequency (HZ)			
	Percent Reduction			
	0	10	20	30
Bending	4.82	4.58	4.31	4.03
Torsion	4.97	4.72	4.46	4.17

Table 2.3. Effect of Slab Thickness on Fundamental Frequencies

Fundamental Mode	Frequency (HZ)			
	Slab Thickness (Inches) =			
	5.0	6.2	7.0	8.0
Bending	4.91	4.82	4.77	4.71
Torsion	5.28	4.97	4.78	4.61



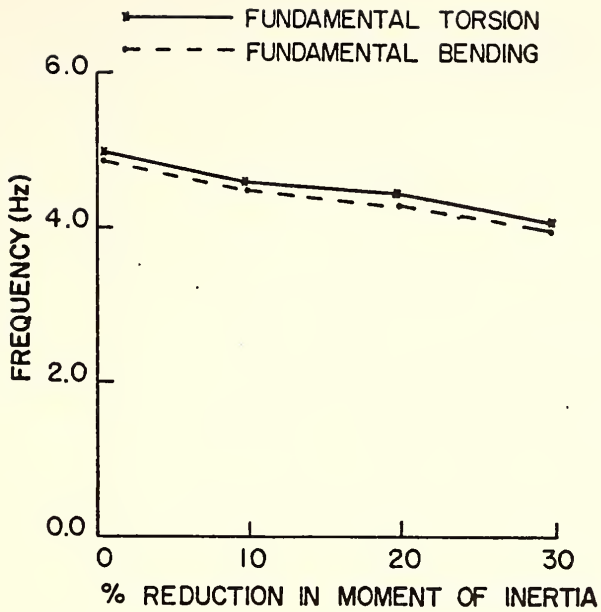


Figure 2.17. Effect of Reduction of Moment of Inertia on Fundamental Frequencies



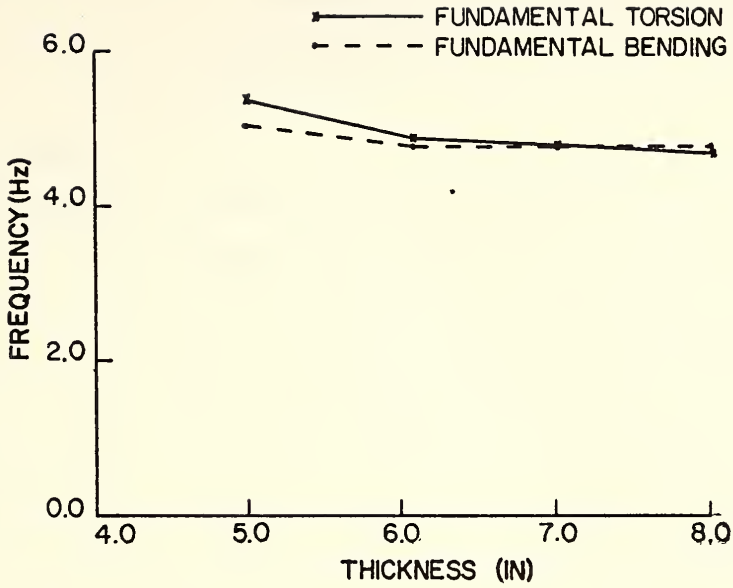


Figure 2.18. Effect of Slab Thickness on Fundamental Frequencies





## CHAPTER III

### ROAD ROUGHNESS

#### 3.1. General

Based on the theoretical study done by Aramraks [31], road roughness is one of the major factors affecting the dynamic behavior of highway bridges. In his theoretical study, Aramraks found that in some cases, when using sinusoidal type roughness, bridges exhibit as much as 20 times greater dynamic response (acceleration) than the same bridges without road roughness. This situation, amplification of the dynamic response by factor of 10 to 20, can exist, theoretically, if there is low damping in the system and the frequency of the exciting force is close to a natural frequency of the system. In the case of a bridge, the exciting force is due to the weight of the vehicle crossing it. The magnitude of the exciting force, which is the same as the interaction force between the bridge and the vehicle, depends on the weight and the suspension of the vehicle, the stiffness of the girders of the bridge and the road roughness.

Roadway roughness results from construction irregularities and from uneven surface wear. The sinusoidal variation of roughness used by Aramraks is convenient but not too realistic for an actual bridge. In order to arrive at a more reasonable representation of road roughness, six bridge profiles from three different bridges were studied.



Based on these six profiles a simulation method for road roughness is suggested that could be used as an "average" road roughness for bridge design. It should be mentioned that the profile of a given bridge does not remain the same but rather it changes with time. Because of nonuniform properties of the materials that are used for bridge surfaces, surface wear is not the same even across the width of the bridge. As a result, a given bridge shows completely different dynamic responses (especially acceleration and jerk) for different runs of the same vehicle across the bridge. Due to this fact, having an actual bridge profile does not guarantee that an exact dynamic response for acceleration or jerk can be calculated if the vehicle is not driven down the measured profile line.

### 3.2. Analysis of the Bridge Profiles

To simplify the analysis, it is assumed that the bridge profile is a function of the length of the bridge only. Let us call this function  $F(x)$ , where  $x$  is measured along the length of the bridge. For ease of the comparison, let the length of the bridge be 1. For mathematical purposes, it can be assumed that  $F(x)$  is periodic and has a period equal to the length of the bridge. With these assumptions,  $F(x)$  can be approximated by a series of sine and cosine waves.

$$F(x) \approx \sum_{n=0}^{NH} [A_n \cos(2n\pi x) + B_n \sin(2n\pi x)] \quad (3.1)$$

$$n = 0, 1, 2, \dots, NH$$

$$0 \leq x \leq 1$$

in which  $A_n$  and  $B_n$  are Fourier cosine and sine coefficients, respectively.



Let NR, which is an odd number, be the maximum number of measured ordinates. Furthermore, let NH, which is the maximum order of harmonics to be fitted, be given by  $\frac{NR-1}{2}$ . Theoretically, for continuous functions, n takes all the values from 0 to  $\infty$ . Since in this case there are only NR values for F(x), values of n > NH have no significant meaning.

The approximation of F(x), Eq. (3.1), may also be written in the form

$$F(x) \approx \sum_{n=0}^{NH} R_n \cos(2n\pi x - \phi_n) \quad (3.2)$$

$$n = 0, 1, 2, \dots, NH$$

$$0 \leq x \leq 1$$

where

$$\phi_n = \tan^{-1} \frac{B_n}{A_n} \quad (3.3)$$

and

$$R_n = \sqrt{A_n^2 + B_n^2} \quad (3.4)$$

The Computer Library of Purdue University is equipped with several routines which perform a Fourier analysis of a periodically tabulated function. Using one of these subroutines, such as "FORIT" [32], and performing a Fourier analysis on F(x), which has NR tabulated values, results in NH values of the A and of the B coefficients. Making use of Eqs. (3.3) and (3.4), NH values of the phase angle,  $\phi$ , and NH values of the amplitude, R, can be obtained for each bridge profile. With these values F(x) can be approximated by the sum of a series of



cosine waves, where the  $n$ th cosine wave has amplitude given by  $R_n$  and phase shift given by  $\phi_n$  and has  $n$  cycles per bridge length.

For ease of comparison,  $R$  values are normalized and then reduced by the factor 0.3. Since normalization and reduction by a factor are linear transformations, the profile obtained using new values of  $R$  and the same phase angles has the same shape but a different amplitude than the original  $F(x)$ .

Let us assume that the relationship between  $R$ 's and frequencies takes the form of the Weibull distribution function

$$R(n) = e^{-(n/\mu)^\beta} \quad (3.5)$$

where

- $R$  - amplitude in cosine expansion (also known as power spectrum)
- $e$  - base of natural logarithm
- $n$  - frequency cycles/bridge length
- $\mu, \beta$  - Weibull parameters.

Taking the natural log of both sides of Eq. (3.5) we have

$$\text{Ln}(R(n)) = -(n/\mu)^\beta$$

Multiplying both sides by  $-1$  and taking the natural log of both sides we have,

$$\begin{aligned} \text{Ln}(-\text{Ln}(R(n))) &= \beta \text{Ln}(n/\mu) \\ \text{Ln}(-\text{Ln}(R(n))) &= \beta \text{Ln}(n) - \beta \text{Ln}(\mu) \end{aligned} \quad (3.6)$$

Equations (3.6) indicate that plot of the left hand side versus  $\text{Ln}(n)$  is a linear relationship.





Figure (3.1) shows a profile for the Wyndotte Road bridge. The vertical axis labeled "Roughness Amplitude" is the total deviation of the bridge surface from a horizontal line drawn at the first support level. This total deviation is surface roughness plus vertical curve elevation. Figure (3.2) shows plot of calculated values of R, "power spectrum", versus n, cycles per bridge length.

The complements of the phase shift angles are plotted versus n, in Figure (3.3). Figure (3.4) shows a plot of  $\text{Ln}(-\text{Ln}(R))$  against  $\text{Ln}(n)$ . The corresponding figures for all the other bridge profiles are shown in Appendix C. Based on these figures, it has been concluded that the phase shift angle is random and has values that are uniformly distributed between  $+90^\circ$  and  $-90^\circ$  with  $0^\circ$  mean and that the  $\text{Ln}(-\text{Ln}(R))$  versus  $\text{Ln}(n)$  relationship may be approximated by two line segments as shown in Figure (3.5). The Weibull parameters for these two line segments are:

$$\beta = .76 \qquad \mu = .78 \qquad \text{first line segment}$$

$$\beta = .18 \qquad \mu = .0011 \qquad \text{second line segment}$$

Based on these parameter values R values are given by:

$$R = e^{-\left(\frac{n}{.78}\right)^{.76}} \qquad 1 \leq n \leq 6 \qquad (3.7)$$

$$R = e^{-\left(\frac{n}{.0011}\right)^{.18}} \qquad n \geq 6 \qquad (3.8)$$



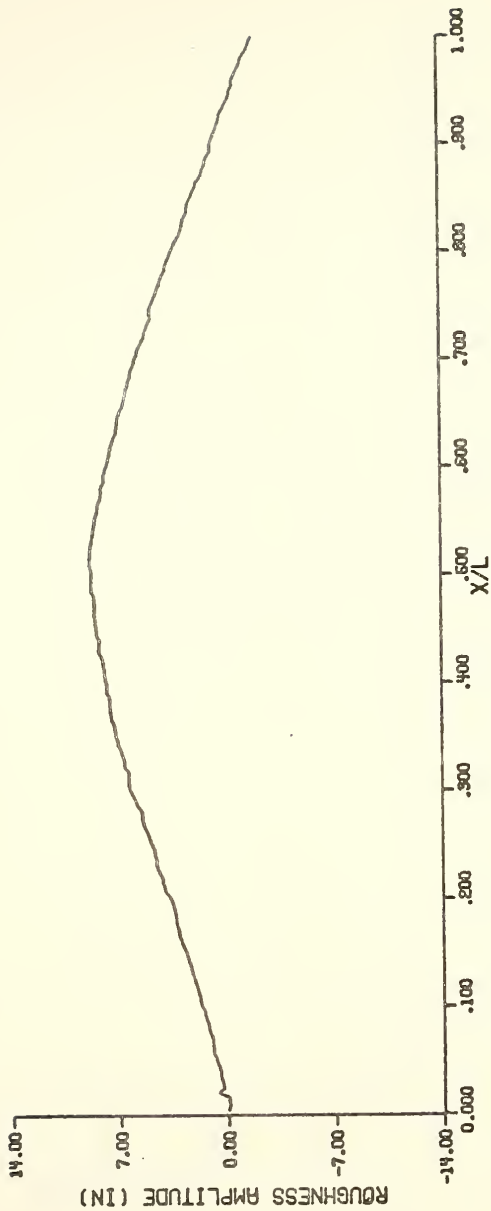


FIGURE 3.1 BRIDGE ROUGHNESS PROFILE

WYNDOTTE ROAD OVER I-66 IN TIPPECANOE CO.  
 122.6-122.6 FT. SPANS 35 FT. WIDTH  
 EAST BOUND LANE RIGHT WHEEL PATH



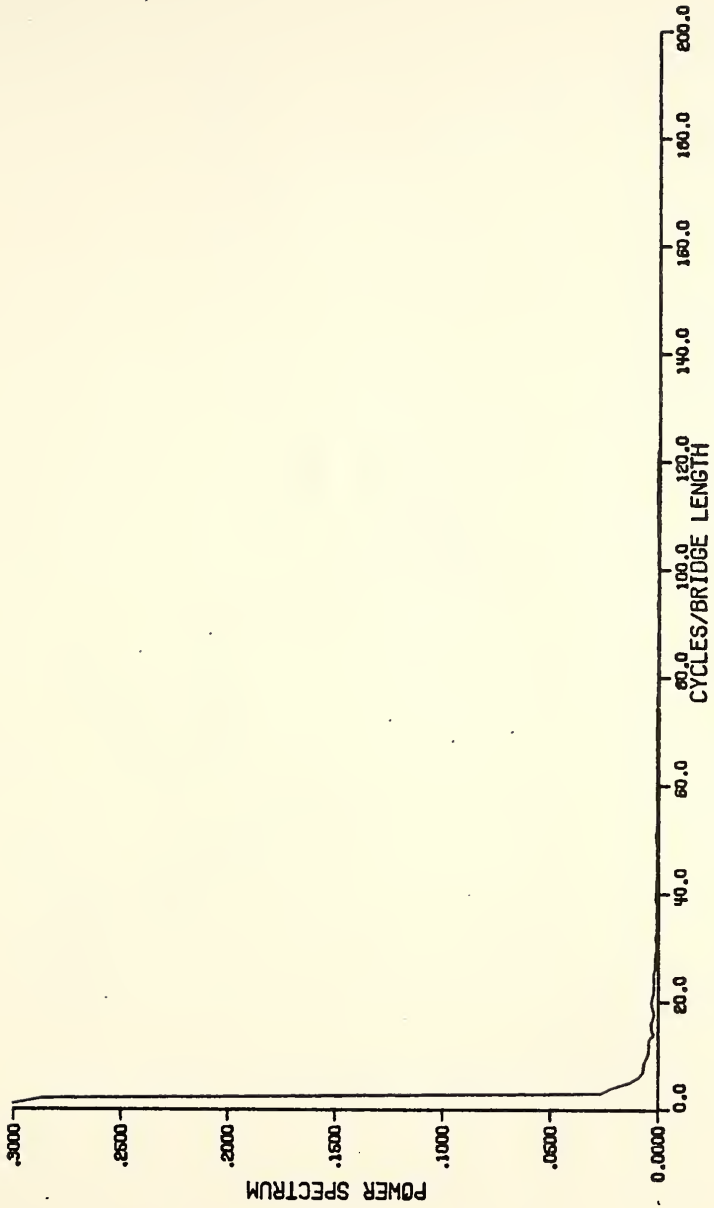


FIGURE 3.2 POWER SPECTRUM

WYDOTTE ROAD OVER I-65 IN TIPPECANOE CO.  
122.5-122.5 FT. SPANS 35 FT. WIDTH  
EAST BOUND LANE RIGHT WHEEL PATH



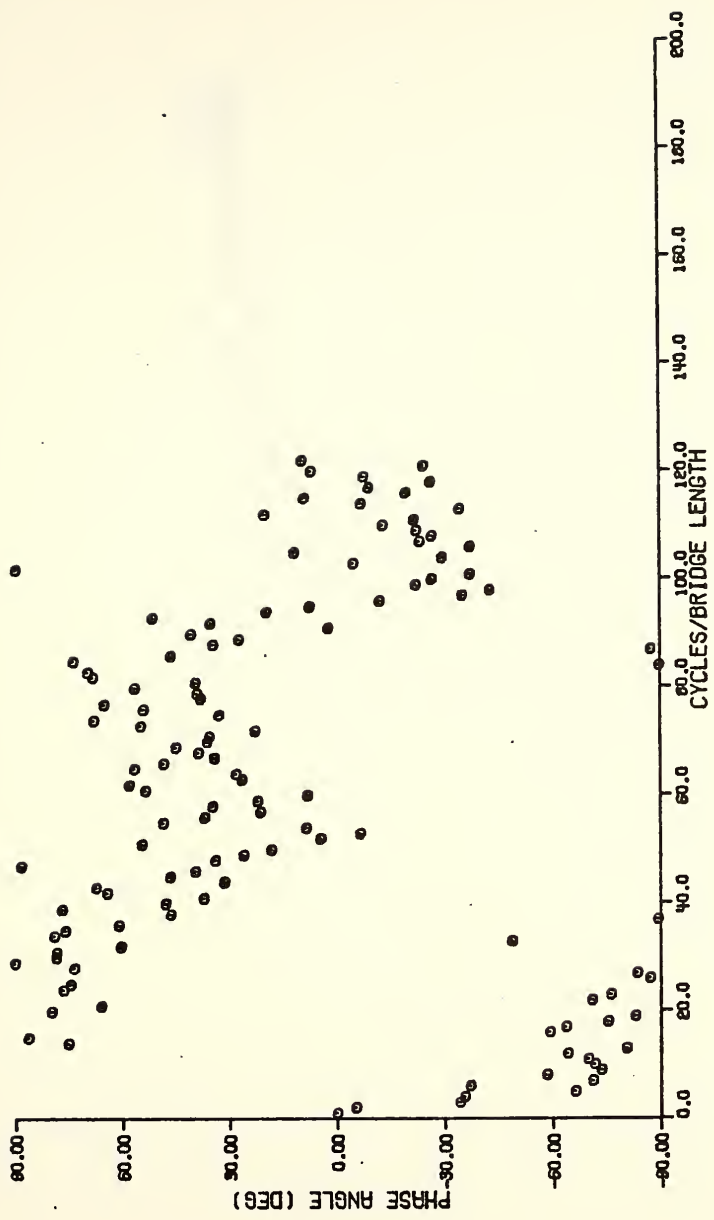


FIGURE 3.3 PHASE ANGLE

WYDOTTE ROAD OVER I-65 IN TIPPECANOE CO.  
122.6-122.6 FT. SPANS 35 FT. WIDTH  
EAST BOUND LANE RIGHT WHEEL PATH





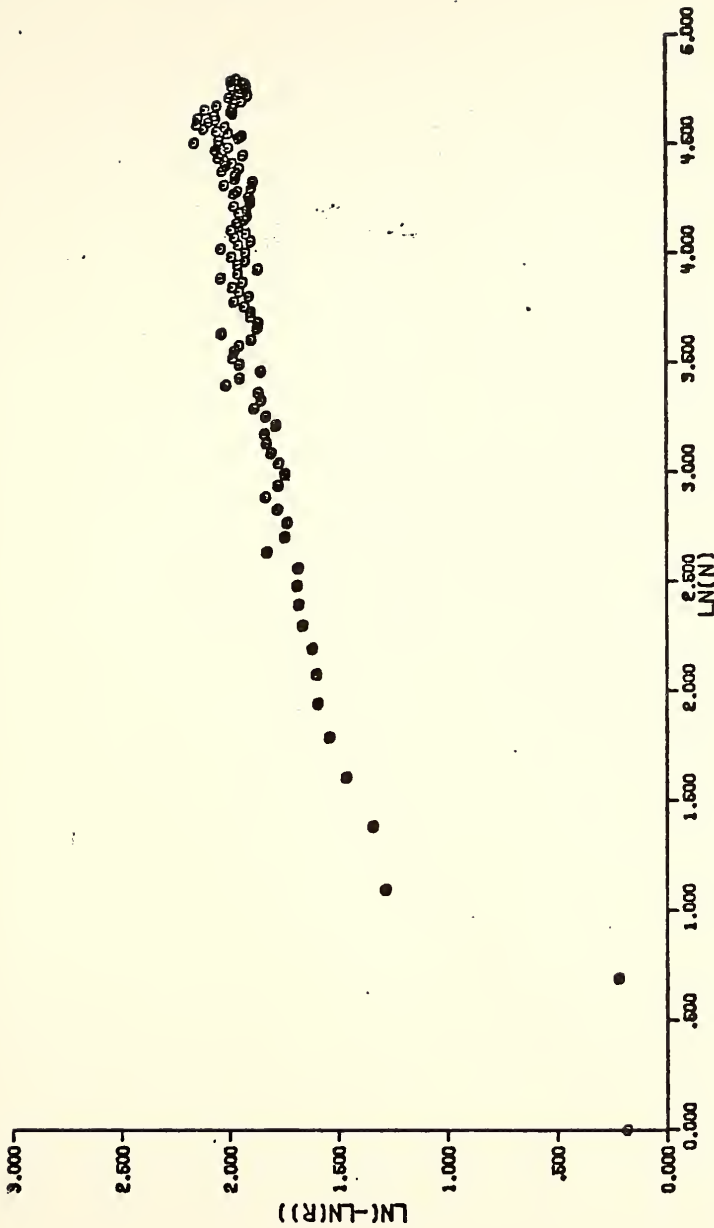
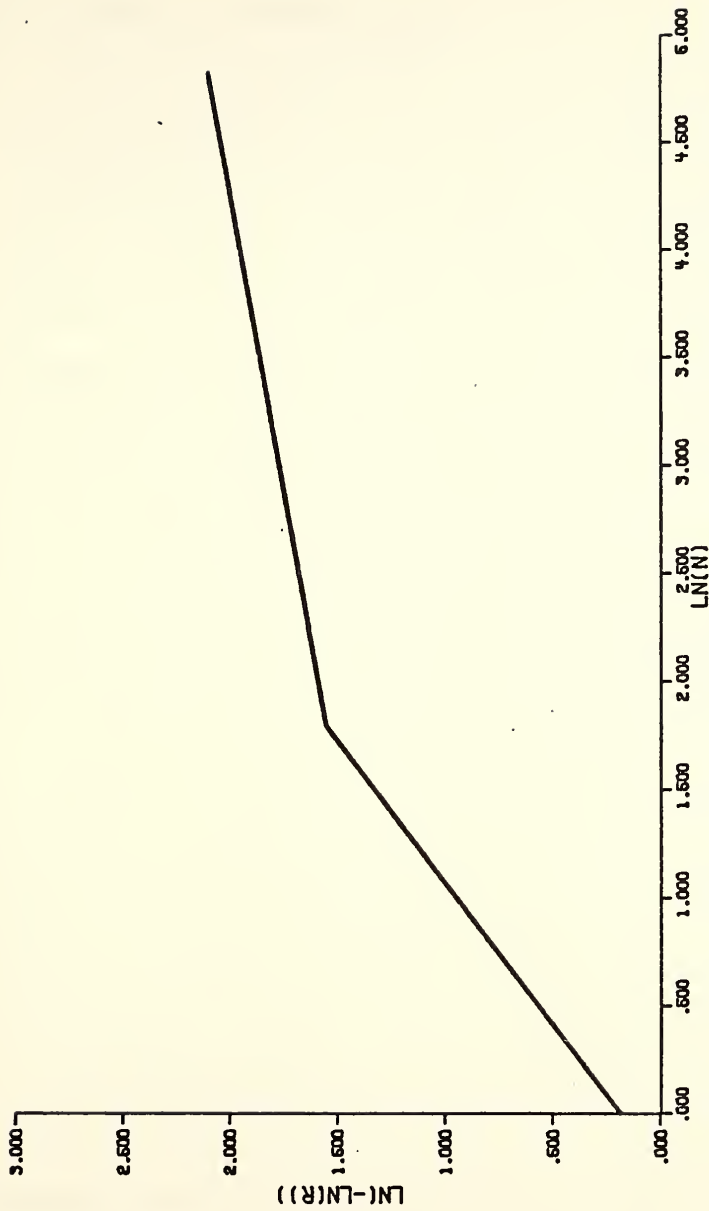


FIGURE 3.4  $LN(-LN(R))$ ,  $LN(N)$  RELATIONSHIP

HYNDOTTE ROAD OVER I-65 IN TIPPECANOE CO.  
 122.6-122.6 FT. SPANS 35 FT. WIDTH  
 EAST BOUND LANE RIGHT WHEEL PATH



FIGURE 3.5 SUGGESTED  $\text{LN}(-\text{LN}(R))$  ,  $\text{LN}(N)$  RELATIONSHIP



### 3.3 Simulation of the Road Roughness

Equations (3.7) and (3.8) give the "average" proportions of the amplitudes (R values) in the cosine expansion in Equation (3.2). Using a random generating function such as "RANF", from the computer library of Purdue University, a series of uniformly distributed random angles between  $-90^\circ$  and  $+90^\circ$  with  $0^\circ$  mean can be generated. Using these angles with calculated R values in Equation (3.2), a simulated bridge roughness can be obtained. The term bridge roughness, as explained previously, refers to surface roughness plus initial grade elevation. This term, "bridge roughness", is the deviation of the bridge surface from a horizontal line drawn through the first support and includes both surface roughness and initial grade elevation. This roughness, which is used in the analytical programs only, should not be confused with the actual bridge surface roughness which is the deviation of the bridge surface from the theoretical grade line.

Figure (3.6) shows a simulated bridge profile with 1" maximum amplitude. Figure (3.7) shows the same profile with 4" maximum amplitude of roughness when plotted on 14" axis. Figures (3.8), (3.9), and (3.10) show the power spectrum, phase angle and  $\text{Ln}(-\text{Ln}(R))$  versus  $\text{Ln}(n)$  of the simulated bridge profile, respectively.

### 3.4. Theoretical Comparison of Actual and Simulated Bridge Profiles

It was stated earlier that road roughness had to be included in the analytical study. If the road roughness is not included, the calculated dynamic response of the bridge is very low. The theoretical dynamic response of the two span bridge (KCSG-A-1) was determined for rough deck using a simulated profile. Using a simulated road roughness



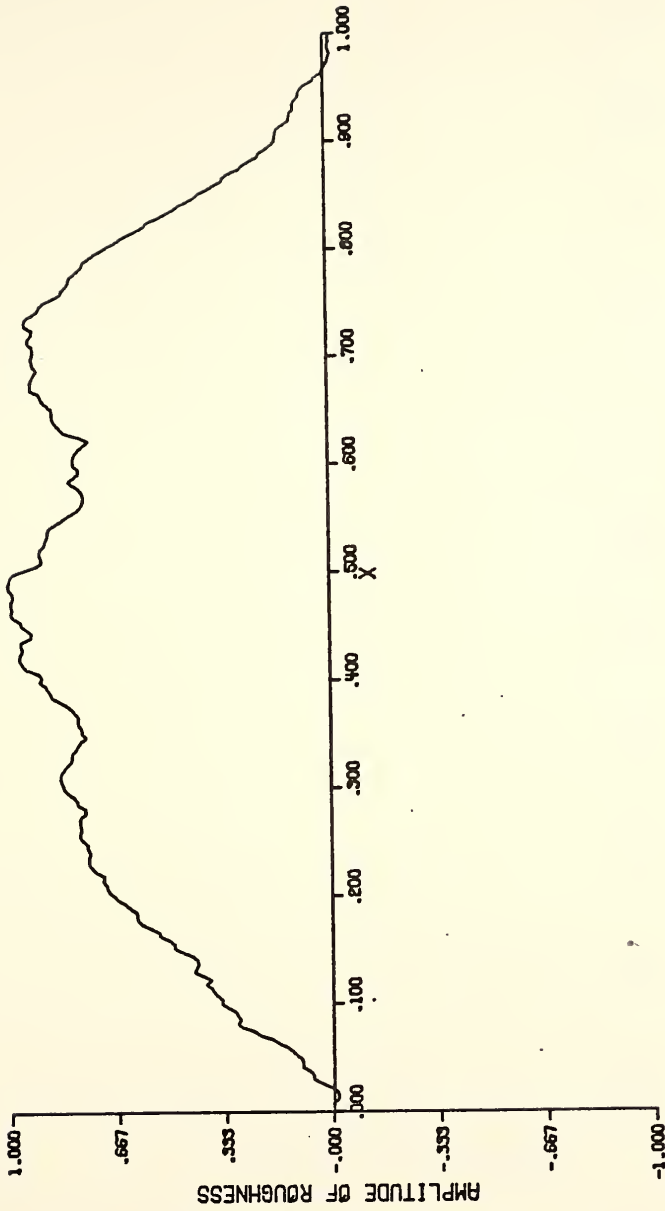


FIGURE 3.6 SIMULATED ROAD ROUGHNESS





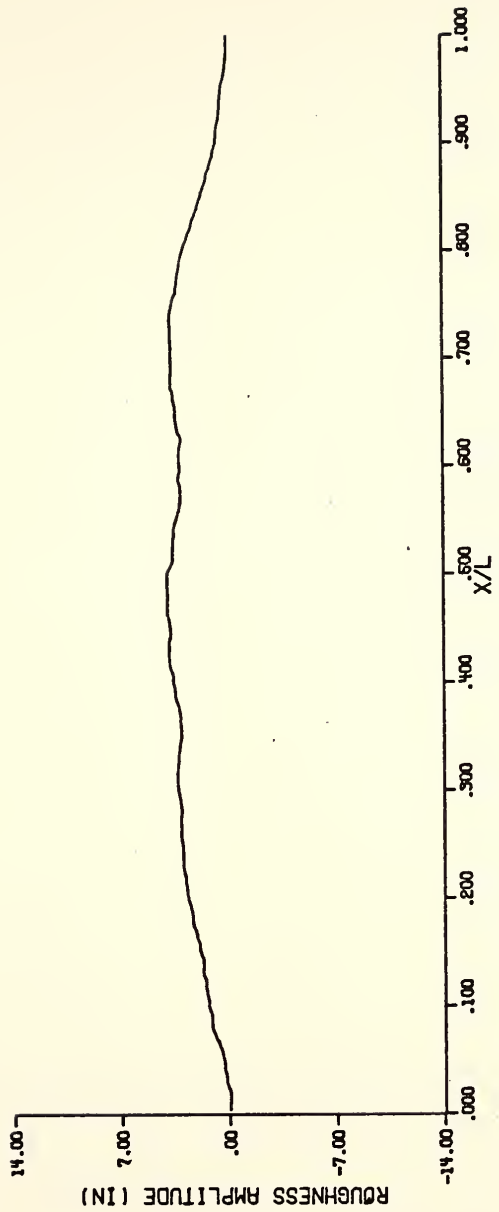


FIGURE 3.7 BRIDGE ROUGHNESS PROFILE  
SIMULATED BRIDGE ROUGHNESS



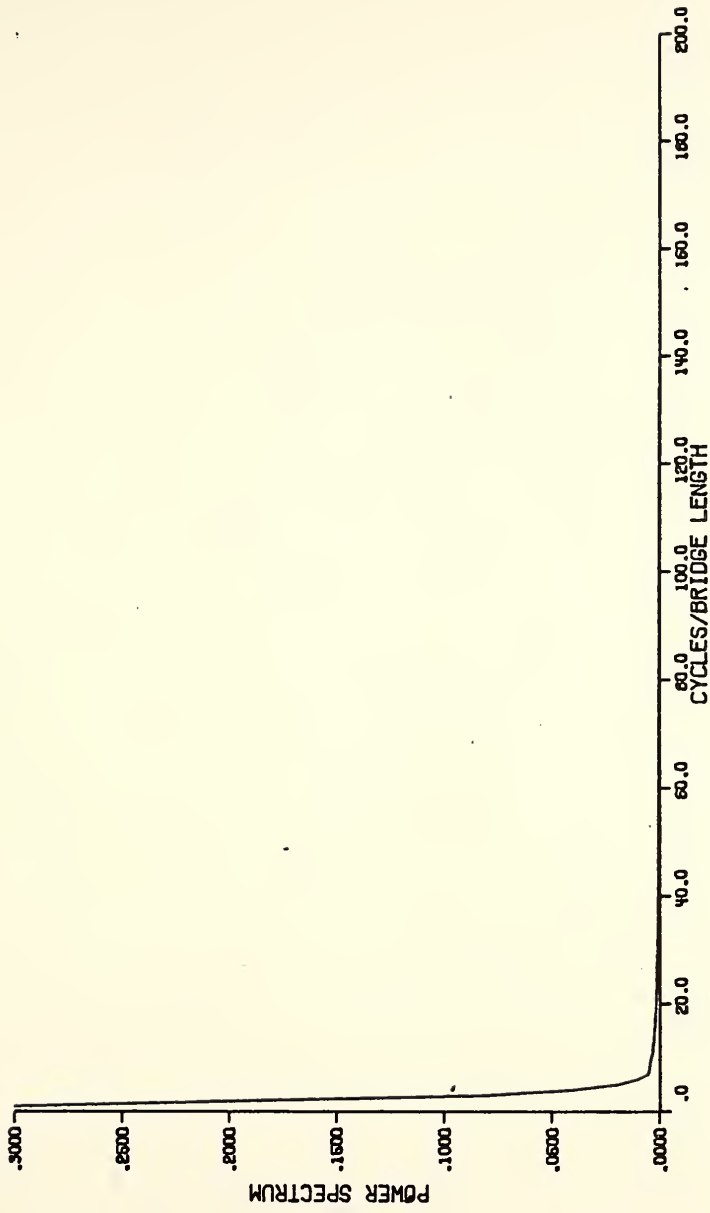


FIGURE 3.8 POWER SPECTRUM

SIMULATED BRIDGE ROUGHNESS



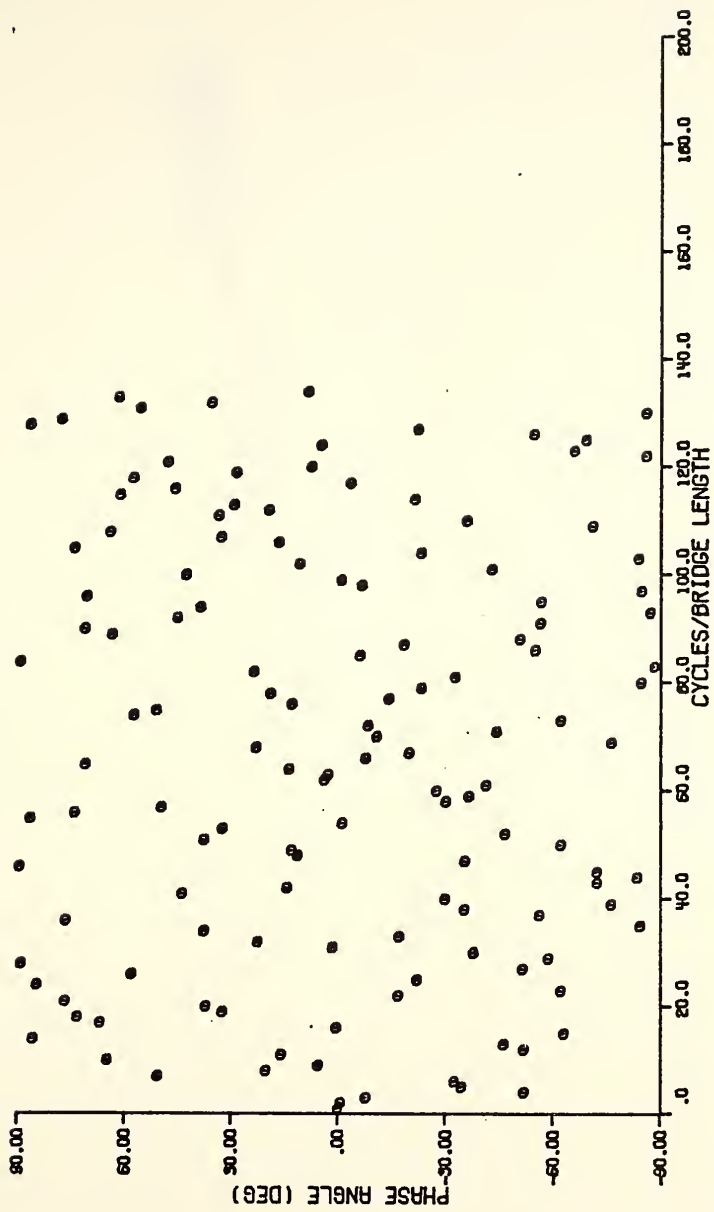


FIGURE 3.9 PHASE ANGLE

SIMULATED BRIDGE ROUGHNESS



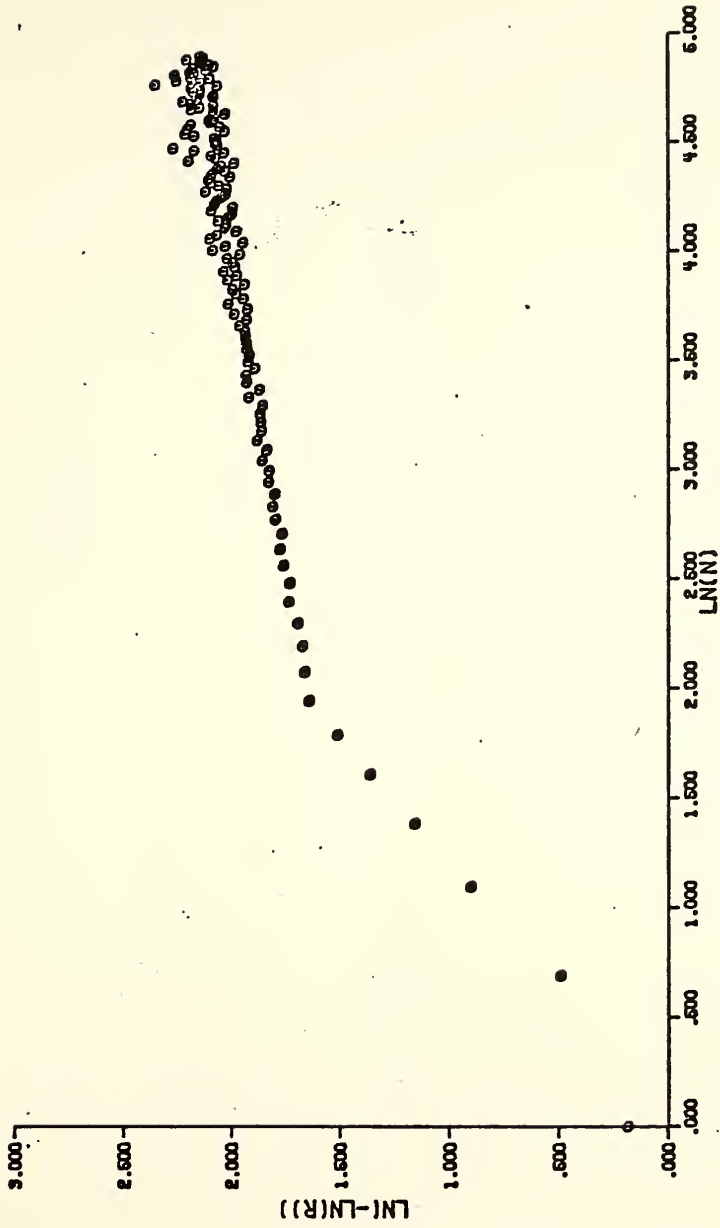


FIGURE 3.10  $LN(-LN(R))$  ,  $LN(N)$  RELATIONSHIP  
SIMULATED BRIDGE ROUGHNESS





VELOCITY 65 MPH  
 2-AXLE 21.3-KIP VEHICLE  
 SMOOTH DECK

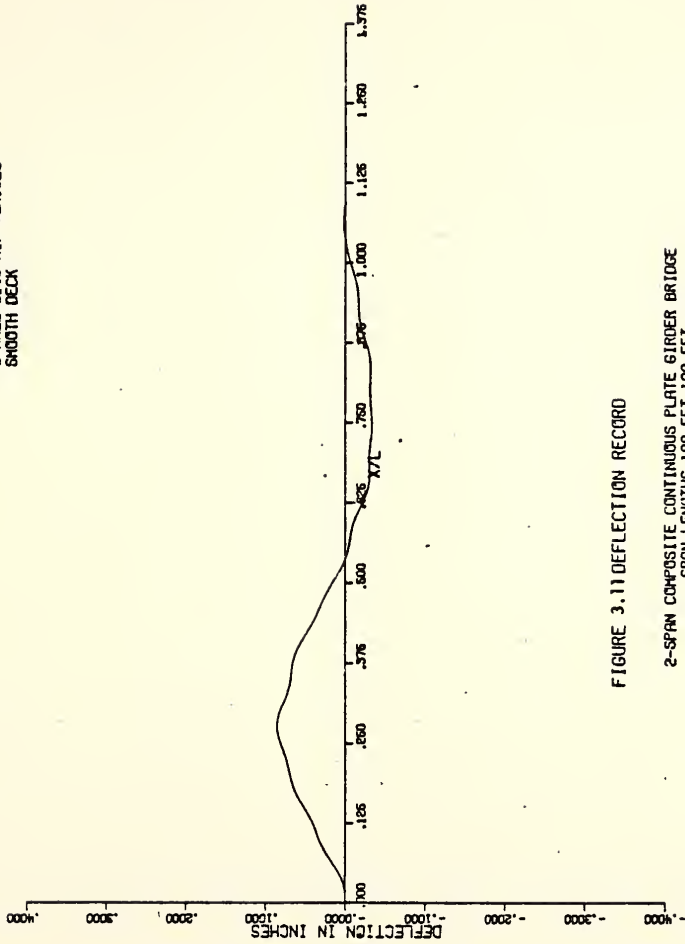


FIGURE 3.11 DEFLECTION RECORD

2-SPAN COMPOSITE CONTINUOUS PLATE GIRDER BRIDGE  
 SPAN LENGTHS 122.5FT, 122.5FT  
 WIDTH - 32.0FT  
 WYNDOTTE ROAD OVER I-65 TIPPECANOE COUNTY  
 BRIDGE STUDY NUMBER KCSG-A-1



VELOCITY 65 MPH  
2-AXLE 21.3-KIP VEHICLE  
SMOOTH DECK

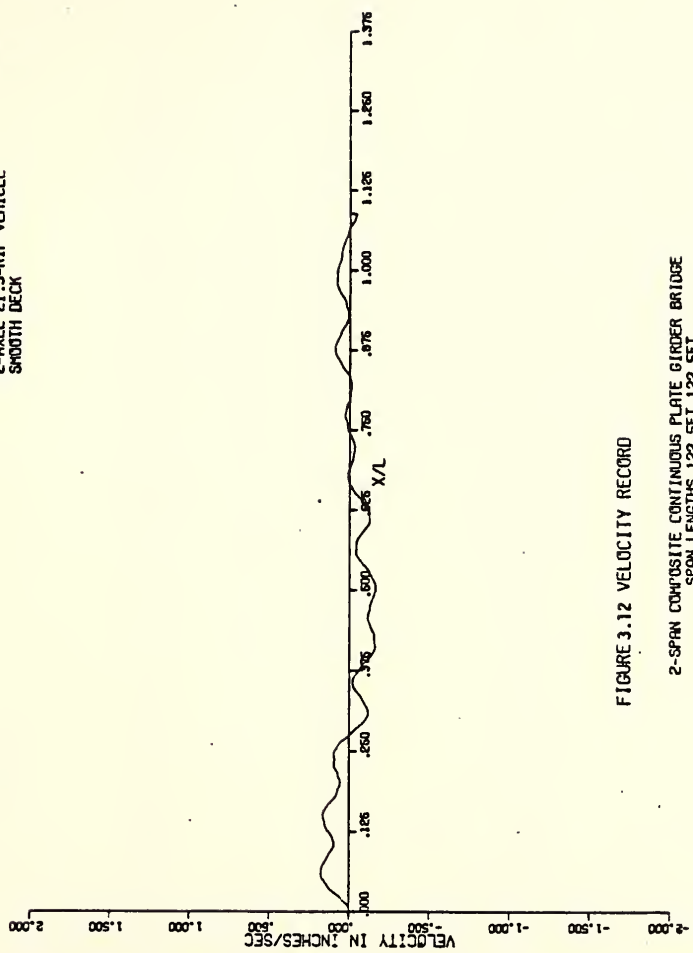


FIGURE 3.12 VELOCITY RECORD

2-SPAN COMPOSITE CONTINUOUS PLATE GIRDER BRIDGE  
SPAN LENGTHS 122.5FT, 122.5FT  
WIDTH - 32.0FT  
WYNDOTTE ROAD OVER I-65 TIPPECANOE COUNTY  
BRIDGE STUDY NUMBER KCS6-A-1



VELOCITY 55 MPH  
2-AXLE 21.3-KIP VEHICLE  
SMOOTH DECK

--- NODE 1  
--- NODE 2  
--- NODE 3

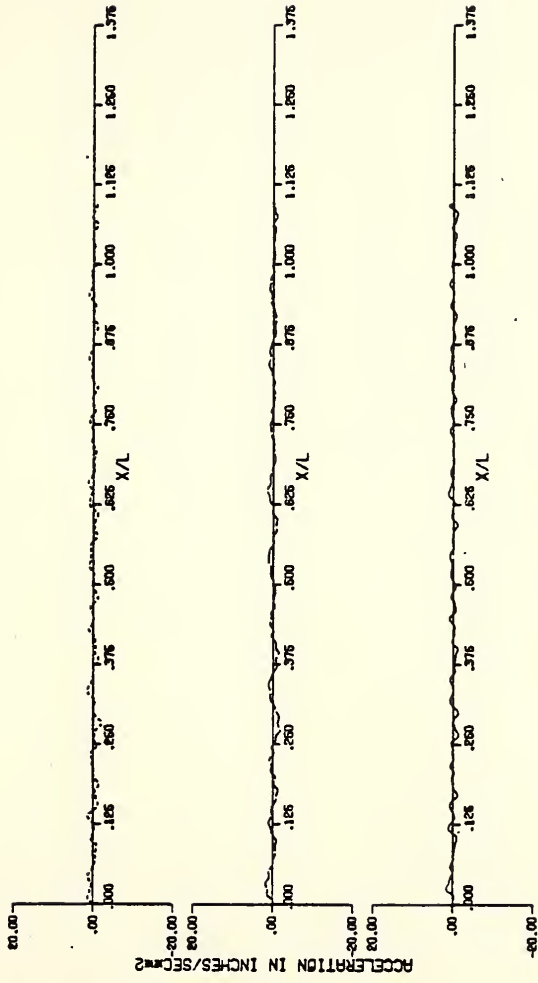


FIGURE 3.13 ACCELERATION RECORDS  
2-SPAN COMPOSITE CONTINUOUS FLAT GIRDER BRIDGE  
SPAN LENGTHS 122.5 FT, 122.5 FT  
WIDTH - 32.0 FT  
WINDOTTE ROAD OVER I-65 TIPPECANOE COUNTY  
BRIDGE STUDY NUMBER KC55-A-1



VELOCITY 55 MPH  
 2-AXLE 21.3-KIP VEHICLE  
 SMOOTH DECK

..... NODE 1  
 - - - - - NODE 2  
 \_\_\_\_\_ NODE 3

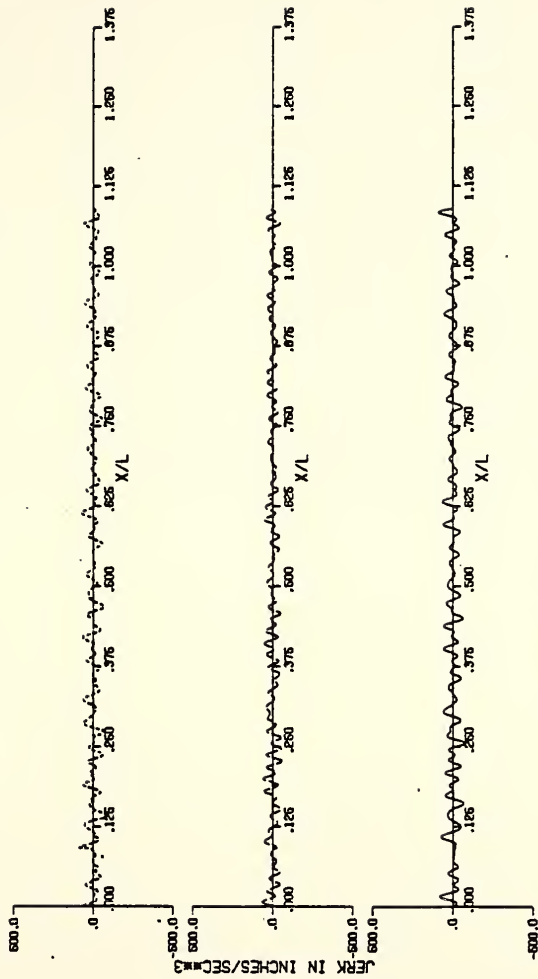


FIGURE 3.14 JERK RECORDS

2-SPAN COMPOSITE CONTINUOUS PLATE GIRDER BRIDGE  
 SPAN LENGTHS 122.5 FT; 122.5 FT  
 WIDTH - 32.0 FT  
 HYNDOTTE ROAD OVER I-65 TIPPECANOE COUNTY  
 BRIDGE STUDY NUMBER KCSG-A-1





with a 4" maximum amplitude yielded results similar to the theoretical response of the bridge with the actual road roughness. Figures (3.11) through (3.14) show the theoretical response of the bridge (KCSG-A-1) with a smooth deck. The first two figures show the dynamic response of the center node of the first span, which corresponds to the mid point of the first span. The other two figures show the dynamic response of all three nodes in the first span. Nodes 1 and 3 are at the quarter points and node 2 is at the mid point of the first span.

Figures (3.15), (3.16), (3.17), and (3.18) show the theoretical dynamic response of the (KCSG-A-1) bridge with the actual road roughness. The actual profile used was the right wheel path of the east bound traffic lane. This profile is shown in Figure (3.1). Figures (3.19), (3.20), (3.21), and (3.22) contain dynamic responses of the same bridge with the simulated road roughness shown in Figure (3.7).



VELOCITY 55 MPH  
2-AXLE 21.3-KIP VEHICLE  
ACTUAL BRIDGE ROUGHNESS

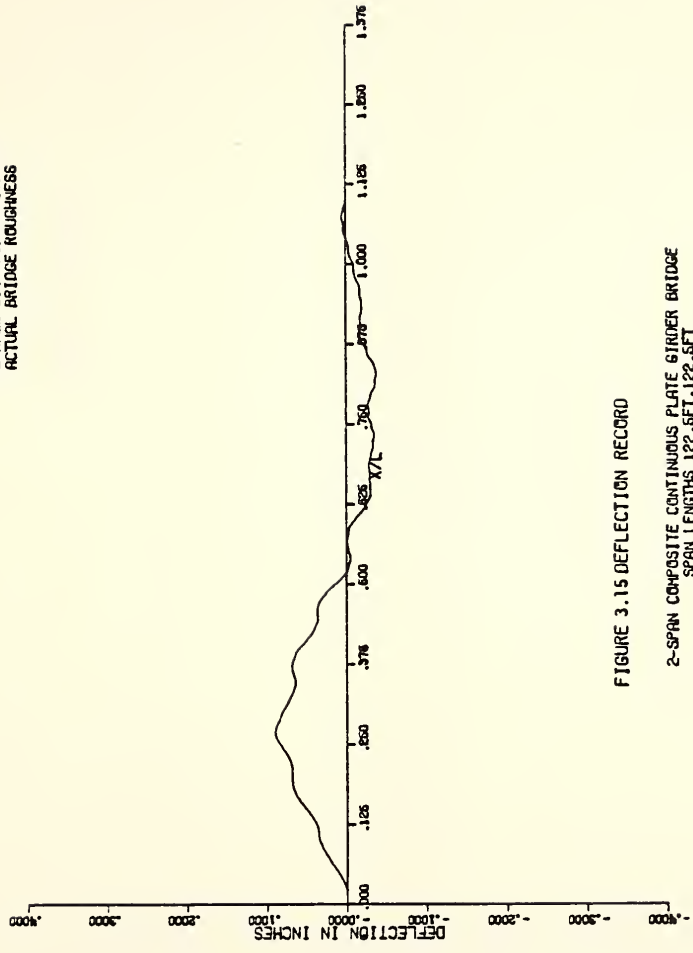


FIGURE 3.15 DEFLECTION RECORD

2-SPAN COMPOSITE CONTINUOUS PLATE GIRDER BRIDGE  
SPAN LENGTHS 122.5FT, 122.5FT  
WIDTH - 32.0FT  
WYNDOTTE ROAD OVER I-65 TIPPECANOE COUNTY  
BRIDGE STUDY NUMBER KCSG-8-1



VELOCITY 55 MPH  
2-AXLE 21.3-KIP VEHICLE  
ACTUAL BRIDGE ROUGHNESS

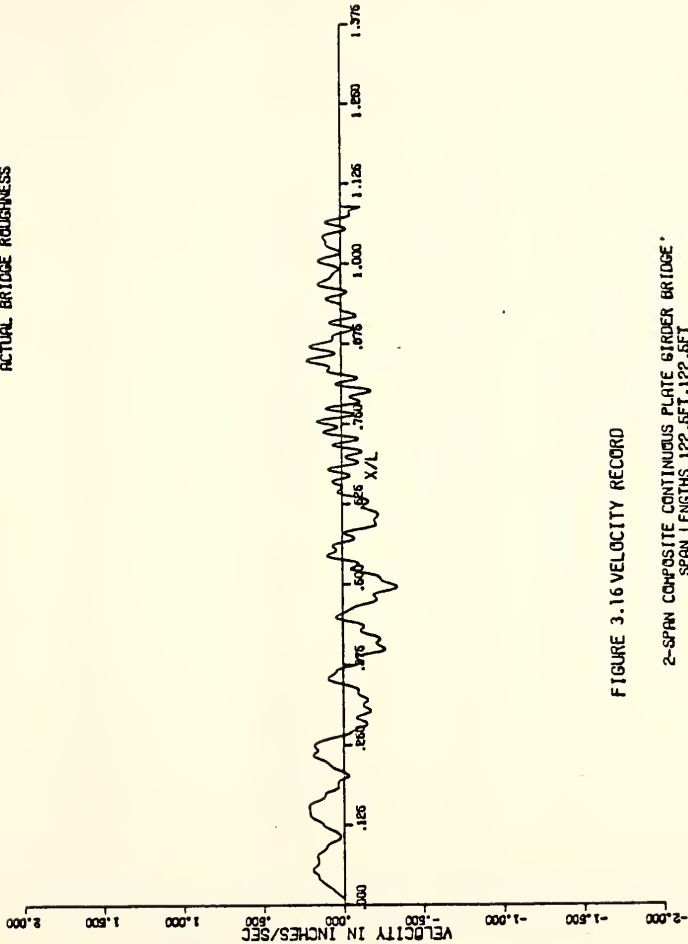


FIGURE 3.16 VELOCITY RECORD

2-SPAN COMPOSITE CONTINUOUS PLATE GIRDER BRIDGE  
SPAN LENGTHS 122.5FT, 122.5FT  
WIDTH - 32.0FT  
BROGO OVER I-65, TIPPECANOE COUNTY  
BRIDGE STUDY NUMBER KCS6-A-1



VELOCITY 65 MPH  
2-AXLE 21.3-KIP VEHICLE  
ACTUAL BRIDGE ROUGHNESS

..... NODE 1  
- - - - - NODE 2  
\_\_\_\_\_ NODE 3

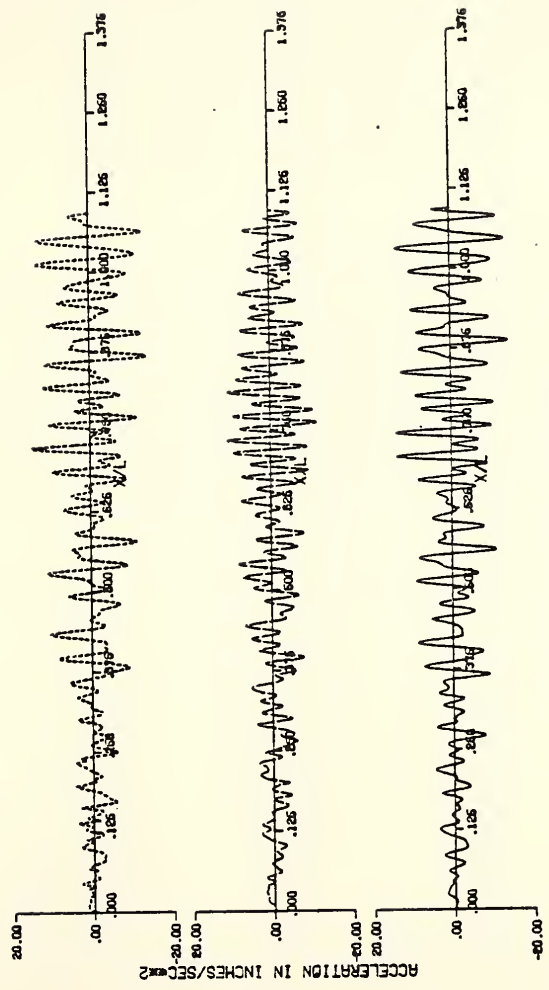


FIGURE 3.17 ACCELERATION RECORDS  
2-SPAN COMPOSITE CONTINUOUS PLATE GIRDER BRIDGE  
SPAN LENGTHS 122.5 FT, 122.5 FT  
WIDTH - 32.0 FT  
WYDOTTE ROAD OVER I-65 TIFPEACRAGE COUNTY  
BRIDGE STUDY NUMBER KCSG-A-1





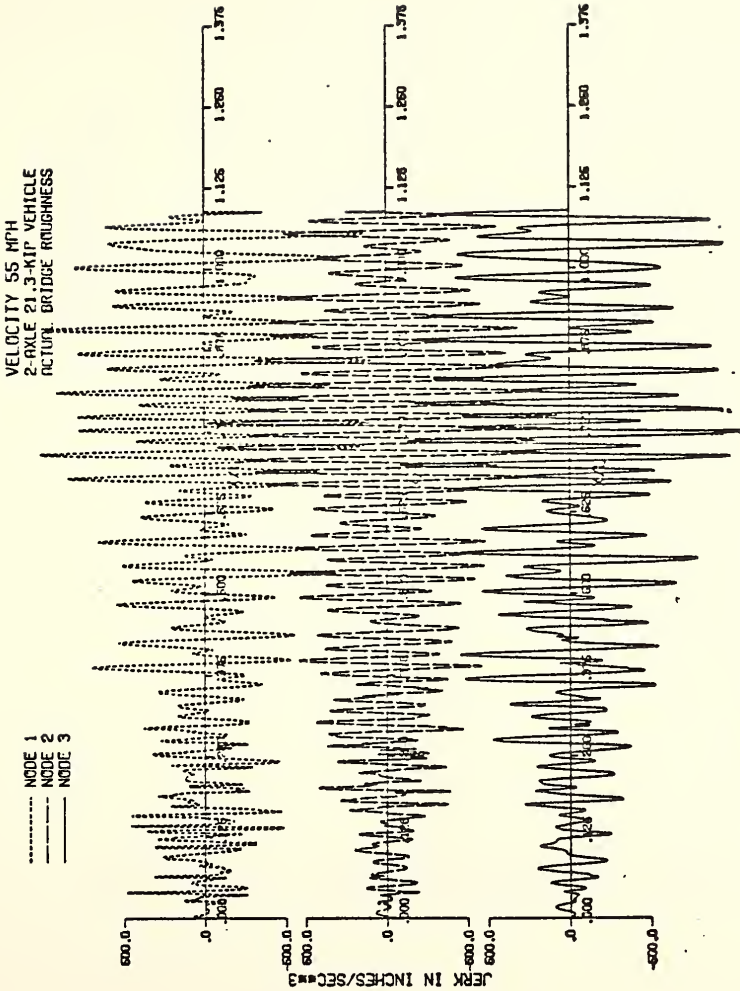


FIGURE 3.18 JERK RECORDS

2-SPAN COMPOSITE CONTINUOUS PLATE GIRDER BRIDGE  
SPAN LENGTHS 122.5 FT, 122.6 FT  
WIDTH - 32.0 FT  
HYNDOTTE ROAD OVER I-65 TIPPECANOE COUNTY  
BRIDGE STUDY NUMBER KCSG-R-1



VELOCITY 55 MPH  
2-AXLE 21.3-KIP VEHICLE  
SIMULATED BRIDGE ROUGHNESS

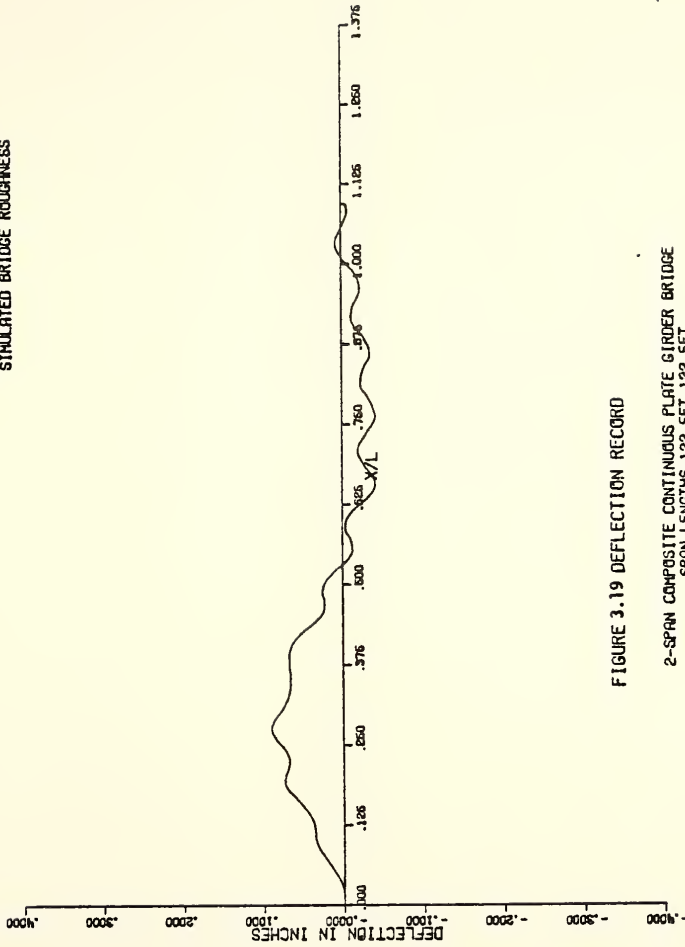


FIGURE 3.19 DEFLECTION RECORD

2-SPAN COMPOSITE CONTINUOUS PLATE GIRDER BRIDGE  
SPAN LENGTHS 122.5FT, 122.5FT  
WIDTH - 32.0FT  
HYNDOTTE ROAD OVER I-66 TIPPECANOE COUNTY  
BRIDGE STUDY NUMBER KCSG-A-1



VELOCITY 65 MPH  
2-AXLE 21.3-KIP VEHICLE  
SIMULATED BRIDGE ROUGHNESS

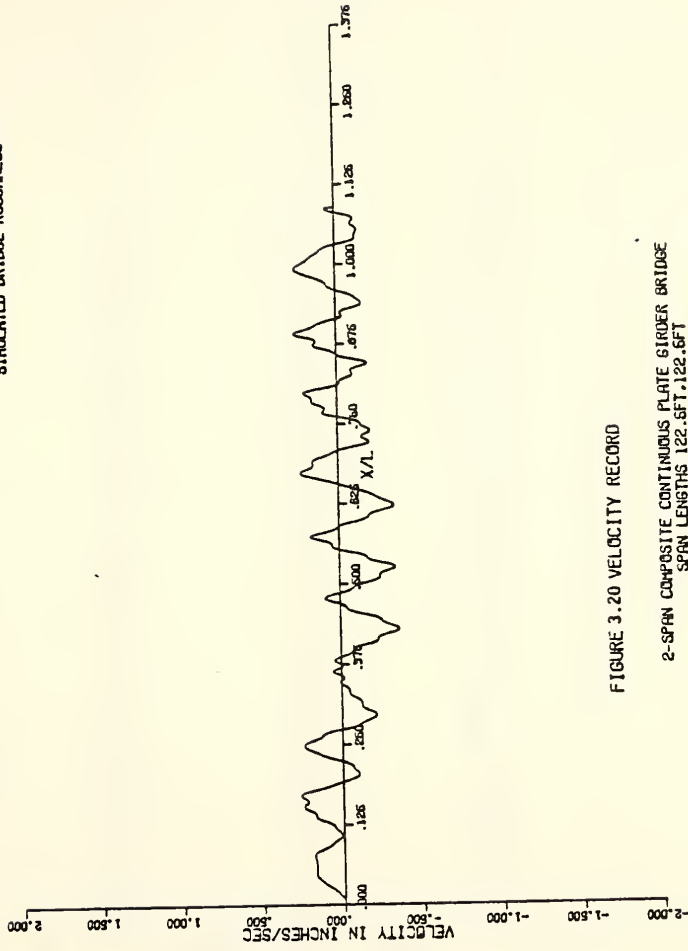


FIGURE 3.20 VELOCITY RECORD

2-SPAN COMPOSITE CONTINUOUS PLATE GIRDER BRIDGE  
SPAN LENGTHS 122.6FT-122.6FT  
WIDTH = 32' OF  
WYDOTTE ROAD OVER I-65 TIPPECANOE COUNTY  
BRIDGE STUDY NUMBER KCS6-9-1



VELOCITY 55 MPH  
 2-RXLE 21.3-KIP VEHICLE  
 SIMULATED BRIDGE ROUGHNESS

..... NODE 1  
 - - - - - NODE 2  
 \_\_\_\_\_ NODE 3

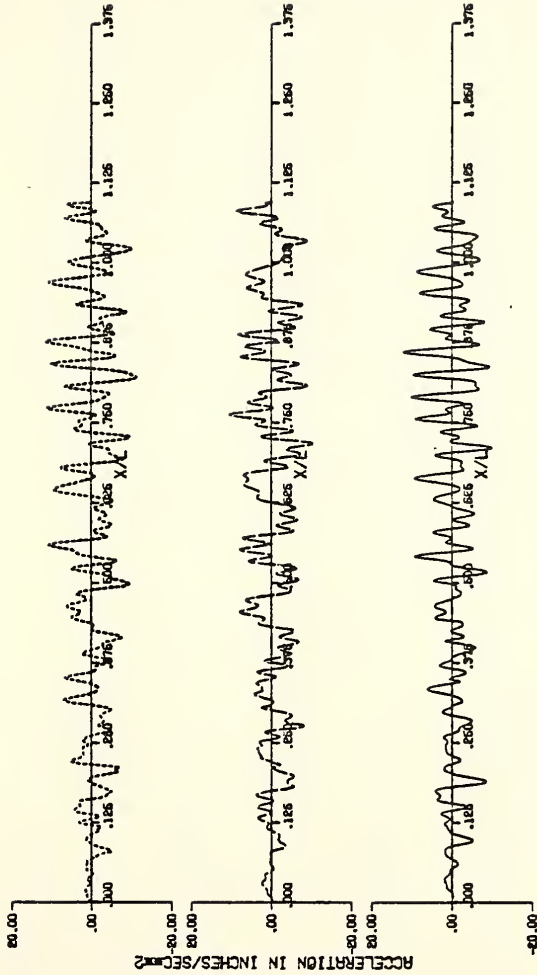


FIGURE 3.21 ACCELERATION RECORDS

2-SPAN COMPOSITE CONTINUOUS PLATE GIRDER BRIDGE  
 SPAN LENGTHS 122.5FT, 122.5FT  
 WIDTH - 32.0FT  
 HINDOTTIE ROAD OVER I-55 TIPPECANOE COUNTY  
 BRIDGE STUDY NUMBER KCS9-A-1





VELOCITY 55 MPH  
 2-AXLE 21.3-KIP VEHICLE  
 SIMULATED BRIDGE ROUGHNESS

--- NODE 1  
 --- NODE 2  
 --- NODE 3

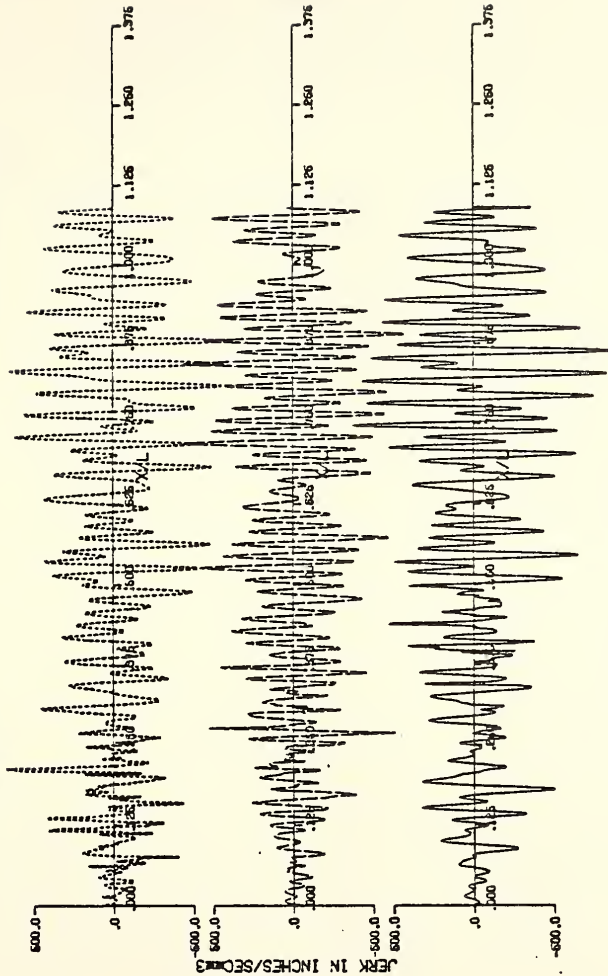


FIGURE 3.22 JERK RECORDS  
 2-SPAN COMPOSITE CONTINUOUS PLATE GIRDER BRIDGE  
 SPAN LENGTHS 122.5FT, 122.5FT  
 WIDTH - 32.0FT  
 WYDOTTE ROAD OVER I-65 TIPPECANOE COUNTY  
 BRIDGE STUDY NUMBER KCS9-4-1



## CHAPTER IV

### LOAD DISTRIBUTION ON HIGHWAY BRIDGES

#### 4.1. General

In the studies done on the dynamic response of two span and three span bridges the assumption has usually been made that all girders participate equally in carrying the load. Based on this assumption two span and three span bridges have been modeled as continuous single beams thereby neglecting torsional effects. In Chapter II it was found that the torsional mode of vibration is significant and should not be neglected, especially when the vehicle is not traveling down the middle of the bridge.

In this chapter, the effects of parameters such as transverse position of the vehicle, speed of the vehicle, weight of the vehicle and bridge related parameters, such as slab thickness and girder stiffness, on distribution of load are studied. The bridge used for this part of the study is (SB-C-1). A complete description of the properties of this bridge may be found in Appendix D. This bridge has nine steel girders which are equally spaced. Due to limitations of the simple span program, which cannot handle more than eight girders, the moment of inertia of one girder has been equally distributed on the other eight beams. Therefore, this model has the same dimensions and total cross sectional moment of inertia as the actual bridge but it has one less girder.



Since the modeled bridge uses a flat slab with no reinforcement, the thickness of the bridge in the study has been increased such that the plain slab would have the same uncracked transverse stiffness as the uncracked reinforced slab.

#### 4.2. Effect of Transverse Position of the Vehicle on Load Distribution

Keeping in mind that the load carried by each girder is proportional to the deflection of that girder, the percentage of the load carried by each girder of the bridge can easily be determined from its dynamic deflection. The term "dynamic deflection" refers to the deflection under moving load. Due to vibrations, bridges show slightly more or less deflection under moving loads than they do under stationary loads. Figure (4.1) shows different wheel positions that are used for this study. For each of these wheel positions, the dynamic deflection at the middle of each girder is calculated. Table (4.1) shows the dynamic deflection at the middle of each beam for different load positions.

Table (4.2) contains the percentage of the dynamic load picked up by each beam for each of these load positions. Calculations in Table (4.2) are based on the assumption that the slab is not carrying any load and 100% of the load is carried by the girders. These results are shown graphically in Figure (4.2). Except for the first two cases, where the vehicle is either on the curb or about 3 feet from the curb, no beam carries more than 25% of the load.



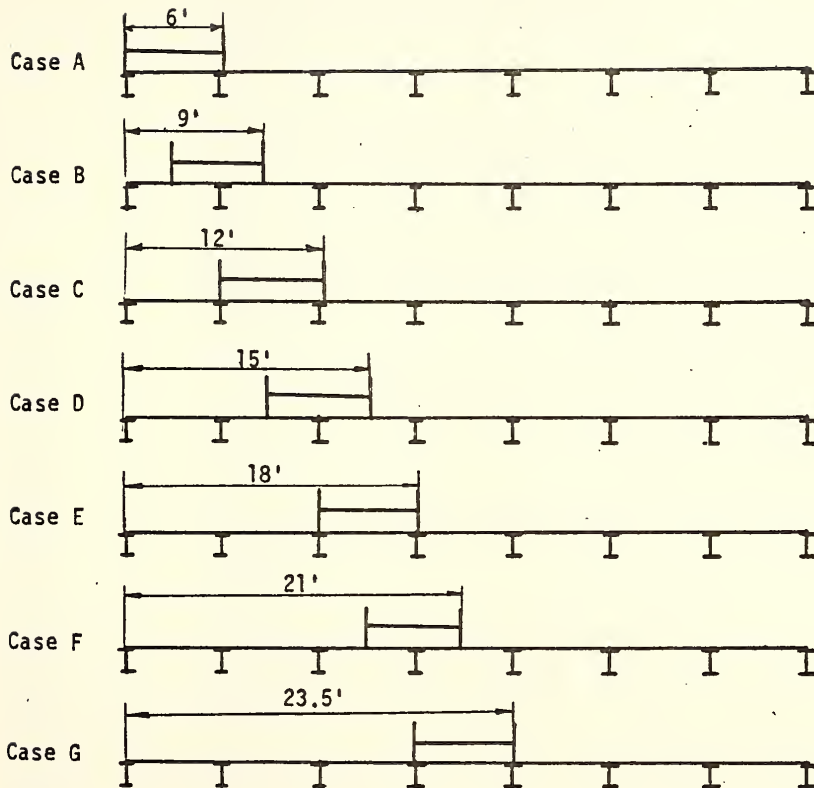


Figure 4.1. Transverse Position of Vehicle on Bridge





Table 4.1. Effect of Load Position on Dynamic Deflection

Loading Case	Deflection (in.)							
	Beam 1	Beam 2	Beam 3	Beam 4	Beam 5	Beam 6	Beam 7	Beam 8
A	.2088	.1443	.0775	.0295	.0031	-.0080	-.0107	-.0100
B	.1457	.1380	.1009	.0529	.0186	-.0008	-.0104	-.0155
C	.0948	.1229	.1165	.0760	.0357	.0089	-.0068	-.0171
D	.0549	.0994	.1211	.1001	.0583	.0246	.0022	-.0135
E	.0234	.07302	.1140	.1173	.0824	.0429	.0130	-.0097
F	.00572	.05141	.0973	.1221	.1039	.0620	.0239	-.0080
G	-.0033	.0362	.0797	.1169	.1169	.0797	.0362	-.0033



Table 4.2. Effect of Load Positions on Percentage of Load on Each Beam

Loading Case	Percentage of Load on Each Beam							
	Beam 1	Beam 2	Beam 3	Beam 4	Beam 5	Beam 6	Beam 7	Beam 8
A	42.4	29.3	15.7	6.0	.6	1.6	2.1	2.0
B	30.2	28.6	20.9	10.9	3.8	.1	2.1	3.1
C	19.0	24.7	23.4	15.2	7.2	7.2	1.8	1.4
D	11.6	20.9	25.5	21.0	12.3	5.2	.4	2.8
E	4.9	15.3	23.9	24.6	17.3	9.0	2.7	2.0
F	1.2	10.8	20.5	25.7	21.9	13.0	5.0	1.7
G	.7	7.6	16.9	24.7	24.7	16.9	7.6	.7



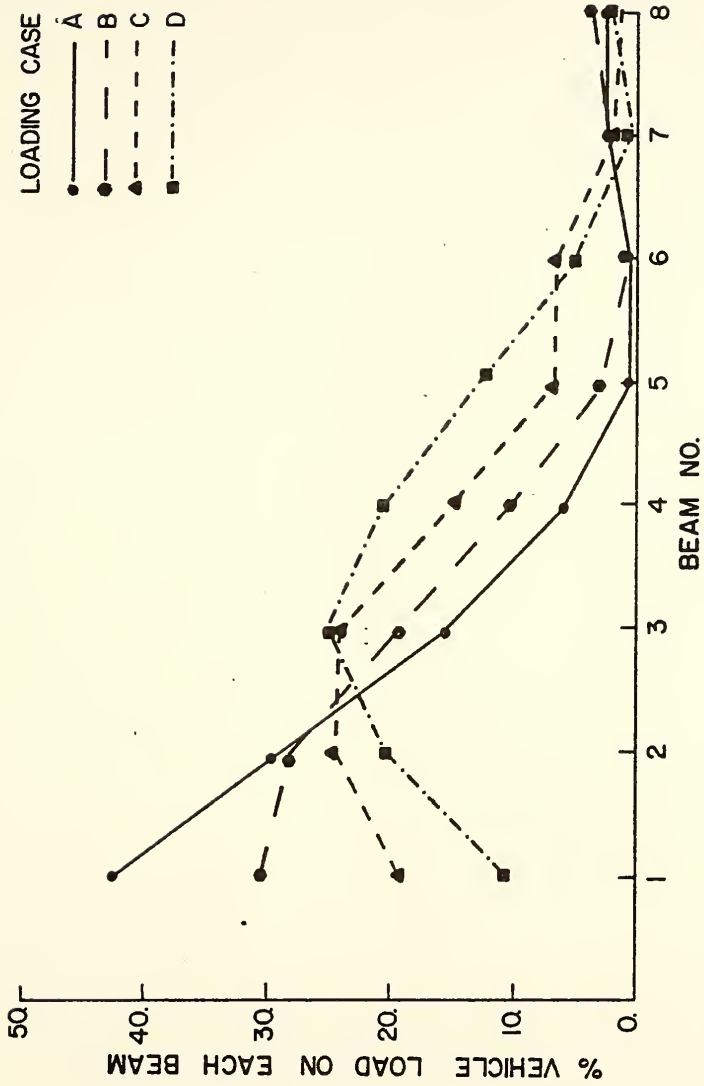


Figure 4.2. Effect of Load Position on Percentage of Load on Each Beam



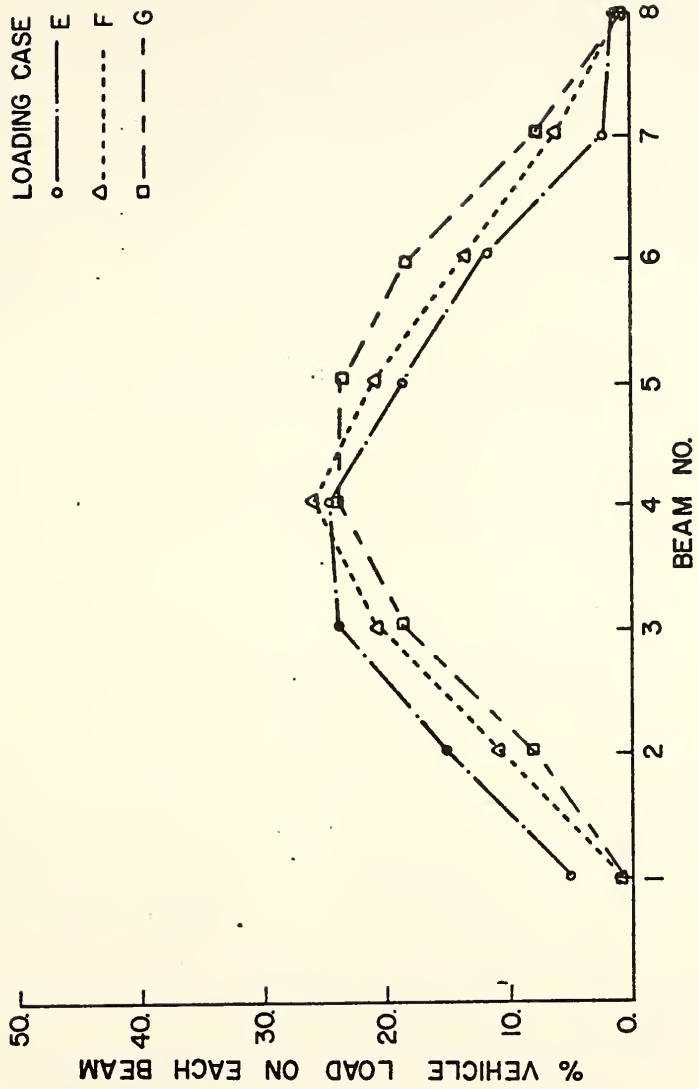


Figure 4.2. Continued





#### 4.3. Effect of Speed on Dynamic Deflection of the Beams

The effect of speed has been studied only for the most likely position of the vehicle on the bridge, case C, which corresponds to the vehicle in the travel lane. Table (4.3) displays the dynamic deflection of the beams for various speeds of the vehicle. Table (4.4) shows corresponding changes in the percentage of the dynamic load on each beam. Results indicate that speed of the vehicle has almost no effect on the girder loads for a smooth deck.

#### 4.4. Effect of the Weight of the Vehicle on Dynamic Deflection

Tables (4.5) and (4.6) show the effect of vehicle weight on dynamic deflection of the girders. Although dynamic deflection increases as the vehicle weight increases, the percentage of the load on each beam stays the same.

#### 4.5. Effect of Slab Thickness on Dynamic Deflection

In this part of the study, effect of slab thickness on distribution of dynamic deflection is studied. The bridge under the study (SB-C-1) has a slab thickness of 6.0 inches. The slab thickness used in the program is 6.2". The .2 inch decrease in thickness increases the gross moment of inertia of the plain concrete slab so it is the same as uncracked moment of inertia of the reinforced slab.

Table (4.7) shows dynamic deflections at the middle of the girders for various slab thicknesses. Table (4.8) shows effect of slab thickness on percentage of the load picked up by each beam. Figure (4.3) displays the results in Table (4.8). It can be seen that these large variations in the bending stiffness of the slab do not cause a very significant redistribution of the loads to the girders.



Table 4.3. Effect of Speed on Dynamic Deflection

Speed (mph)	Deflection (in.)							
	Beam 1	Beam 2	Beam 3	Beam 4	Beam 5	Beam 6	Beam 7	Beam 8
20	.0880	.1171	.1122	.0733	.0348	.0098	.0036	-.0114
30	.0889	.1169	.1116	.0733	.0354	.0107	-.0024	-.0100
40	.0911	.1195	.1146	.0762	.0376	.0122	-.0017	-.0102
50	.0948	.1229	.1165	.0760	.0357	.0089	-.0068	-.0171
60	.0945	.1250	.1211	.0824	.0423	.0151	-.0010	-.0117



Table 4.4. Effect of Speed of the Vehicle on Percentage of the Dynamic Load on Each Beam

Speed (mph)	Percentage of Load on Each Beam							
	Beam 1	Beam 2	Beam 3	Beam 4	Beam 5	Beam 6	Beam 7	Beam 8
20	19.5	26.0	24.9	16.2	7.7	2.1	.8	2.5
30	19.7	26.0	24.8	16.3	7.8	2.4	.5	2.2
40	19.6	25.8	24.7	16.4	8.1	2.5	.4	2.2
50	19.0	24.7	23.4	15.2	7.2	7.2	1.8	1.4
60	19.1	25.3	24.5	16.7	8.6	3.0	.2	2.4



TABLE 4.5. EFFECT OF VEHICLE WEIGHT ON DYNAMIC DEFLECTION

Weight (kips)	Deflection (in.)							
	Beam 1	Beam 2	Beam 3	Beam 4	Beam 5	Beam 6	Beam 7	Beam 8
10.	.0444	.0576	.0546	.0357	.0169	.0044	-.0030	-.0079
21.3	.0948	.1229	.1165	.0760	.0357	.0089	-.0068	-.0171
30.	.1352	.1754	.1664	.1088	.0515	.0134	.0089	-.0235
40.	.1816	.2356	.2237	.1466	.0699	.0189	-.01097	-.0304





Table 4.6. Effect of Vehicle Weight on Percentage of the Load on Each Beam

Vehicle Weight (kips)	Percentage of Load on Each Beam							
	Beam 1	Beam 2	Beam 3	Beam 4	Beam 5	Beam 6	Beam 7	Beam 8
10.	19.7	25.6	24.3	15.9	7.5	1.9	1.3	3.5
21.3	19.0	24.7	23.4	15.2	7.2	7.2	1.8	1.4
30.	19.8	25.6	24.3	15.9	7.5	1.9	1.3	3.4
40.	19.8	25.6	24.4	15.9	7.6	2.0	1.2	3.3



Table 4.7. Effect of Slab Thickness on Dynamic Deflection of Each Beam

Slab Thickness (in.)	Deflection (in.)							
	Beam 1	Beam 2	Beam 3	Beam 4	Beam 5	Beam 6	Beam 7	Beam 8
5.0	.0795	.1329	.1319	.0789	.0300	.0031	-.0086	-.0142
6.2	.0948	.1229	.1165	.0760	.0357	.0089	-.0068	-.0171
7.0	.1012	.1182	.1091	.0734	.0366	.0100	-.0064	-.0174
8.0	.1058	.1149	.1058	.0779	.0479	.0243	.0073	-.0062



Table 4.8. Effect of Slab Thickness on Percentage of Load on Each Beam

Slab Thickness (in.)	Percentage of Load on Each Beam							
	Beam 1	Beam 2	Beam 3	Beam 4	Beam 5	Beam 6	Beam 7	Beam 8
5.0	16.5	27.7	27.5	16.4	6.2	.6	1.7	2.9
6.2	19.0	24.7	23.4	15.2	7.2	7.2	1.8	1.4
7.0	21.4	25.0	23.0	15.5	7.7	2.1	1.4	3.7
8.0	21.6	23.4	21.6	15.9	9.7	4.9	1.5	1.2



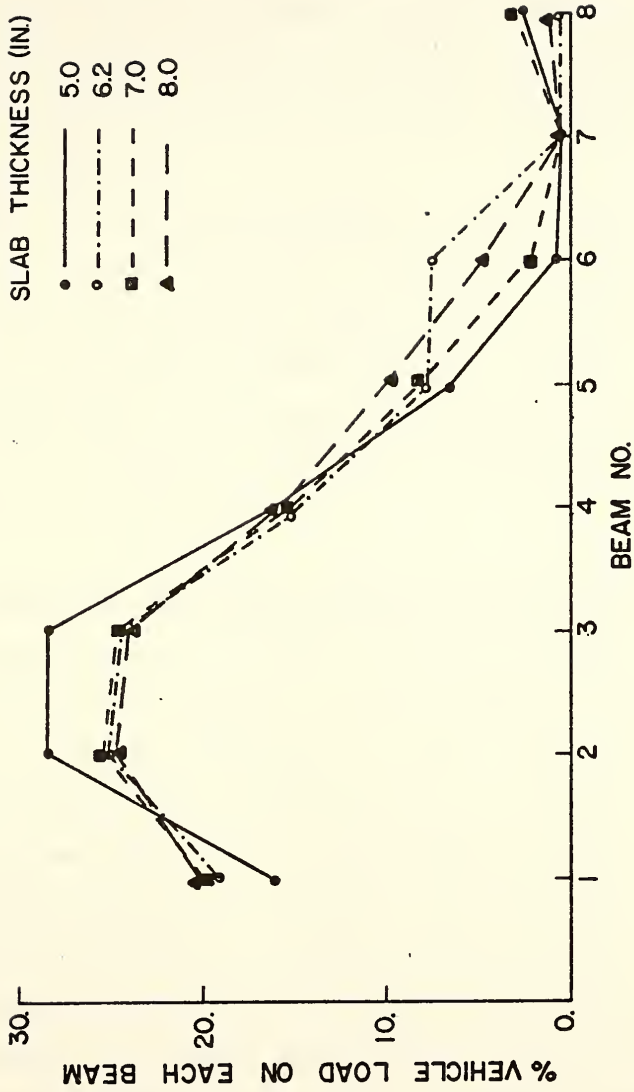


Figure 4.3. Effect of Slab Thickness on Percentage of Load on Each Beam





#### 4.6. Effect of Girder Flexibility on Dynamic Deflection

In this part of the study the effect of reduction of girder stiffness on dynamic deflection and redistribution of traffic load to girders is considered. The use of high strength steel (50 ksi) instead of normal grade (36 ksi) could reduce the moment of inertia of the girders as much as 30%.

Results of 10, 20 and 30% reductions in girder stiffness on dynamic deflections are shown in Table (4.9). The results in this table are for 50 MPH speed and case C loading. Table (4.10) shows the percentage of the load on each girder as the girder stiffness is reduced. These two tables indicate that as the stiffness of the girders is reduced, the deflection of the girders increases but the relative magnitude of the deflections stays the same.

#### 4.7. Comparison of Measured and Theoretical Values of Dynamic Deflections

Dynamic deflections at midspan on the traffic side curb were measured for different speeds and transverse wheel positions on the bridge. The vehicle was driven down the center line of the bridge, in the normal traffic lane, and close to the curb. The vehicle used for these tests was the Research and Training Center Bus (more information is available in the paper by Kropp [30]). Results of tests on the single span bridge (SB-C-1) are shown in Table (4.11) and the results of the same tests on the two span bridge (KCSG-A-1) and the three span bridge (CSB-C-1) are shown in Tables (4.12) and (4.13), respectively. Comparison of Table (4.11) and Table (4.1) shows that the measured values are in the range of values given in Table (4.1). Results in



Table 4.9. Effect of Reduction of Moment of Inertia of Girders on Dynamic Deflection

Percentage of Reduction in I	Deflection (in.)							
	Beam 1	Beam 2	Beam 3	Beam 4	Beam 5	Beam 6	Beam 7	Beam 8
0	.0948	.1229	.1165	.0760	.0357	.0089	-.0068	-.0171
10	.1070	.1335	.1254	.0827	.0393	.0093	-.0086	-.0202
20	.1201	.1485	.1419	.0994	.0542	.0220	.0020	-.0117
30	.1471	.1743	.1642	.1159	.0650	.0274	.0022	-.0164



Table 4.10. Effect of Reduction in Moment of Inertia on Percentage of Load on Each Beam

Percentage of Reduction in I	Percentage of Load on Each Beam							
	Beam 1	Beam 2	Beam 3	Beam 4	Beam 5	Beam 6	Beam 7	Beam 8
0	19.0	24.7	23.4	15.3	7.2	7.2	1.8	1.4
10	20.3	25.3	23.8	15.7	7.4	1.7	1.6	3.8
20	20.0	24.7	23.6	16.5	9.0	3.6	.34	1.9
30	20.6	24.4	23.0	16.2	9.1	3.8	.31	2.3



Table 4.11. Maximum Measured Dynamic Deflections of Single Span Bridge(SB-C-1) for Various Speeds and Transverse Vehicle Positions

Vehicle Position	Deflection (in.)			
	20 mph	30 mph	40 mph	50 mph
Center line	-.010	-.006	-.004	.005
Travel lane	-.031	-.030	-.030	-.025
Curb lane	-.052	-.046	-.044	-.043





Table 4.12. Maximum Measured Dynamic Deflections of Two-Span Bridge (KCSG-A-1) for Various Speeds and Transverse Vehicle Positions

Vehicle Position	Deflection (in.)		
	30 mph	40 mph	50 mph
Center line	-.09	-.09	-.08
Travel lane	-.13	-.12	-.12
Curb lane	-.15	-.15	-.15



Table 4.13. Maximum Measured Dynamic Deflections of Three-Span Bridge (CSB-C-1) for Various Speeds and Transverse Vehicle Positions

Vehicle Position	Deflection (in.)		
	20 mph	30 mph	40 mph
Center line	-.018	.017	.020
Travel lane	-.038	-.039	-.041
Curb lane	-.062	-.067	-.060



Tables (4.11), (4.12) and (4.13) show that position of the vehicle on the bridge has a significant effect on dynamic deflections but speed of the vehicle has essentially no effect on dynamic deflections. The same conclusions were reached in the analytical study. The percentage increase in dynamic deflection as the vehicle gets closer to the curb is considerably more for single span than for two or three span bridges.



## CHAPTER V

### JERK STUDY

#### 5.1. General

In the literature review on human response to vibration, it was found that for the low frequency range human sensitivity to vibration may be approximated by different jerk levels. Results of the frequency study on highway bridges by Kropp [33] show that, generally, the dominant frequencies are relatively low. Based on these findings it was thought to be of some value to do a parametric study on the effects of girder flexibility, slab flexibility, transverse load position and road roughness on jerk. Due to limitations of the available programs, the effects of girder flexibility, slab flexibility, and transverse load position on jerk are studied using the single span program. The effect of road roughness on jerk is studied using the two span program and the simulated road roughness developed in Chapter III.

The vehicle model used with the simple span program to study the effects of girder flexibility, slab flexibility and transverse load position on jerk is a single axle two wheel vehicle. This vehicle model weighs 21.3 kips and crosses the bridge at a speed of 50 mph. The vehicle model used with the two span program to study the effect of road roughness on jerk is a two axle 21.3 kip vehicle with a 23 ft. axle spacing (the Research and Training Center bus). The speed of this vehicle is 50 mph also.





Theoretical jerk values are obtained from the first time derivative of the acceleration function. The derivative routine used for this purpose is explained in Appendix E.

### 5.2. Effect of Transverse Position of Load on Jerk

Theoretical maximum jerk values of bridge (SB-C-1) for various transverse load cases A through G, shown in Figure 4.1, have been determined. Table 5.1 shows maximum jerk values at the middle of each beam for different load positions. Table 5.2 shows the jerk values at the middle of each beam for various load positions at the instant that the maximum of all jerk values occurs. Since absolute maximums in each loading case occurred in the edge beam, beam 1, the first columns of Table 5.1 and 5.2 are the same. It is of interest to note that maximum jerk values in different beams do not occur at the same time.

Results in Tables 5.1 and 5.2 are graphically shown in Figures 5.1 and 5.2. Since only the magnitude of the jerk is of importance, absolute values are plotted in Figures 5.1 and 5.2. Results show as the vehicle gets closer to the curb, the bridge shows higher values of response in jerk. Comparison of case C and case G shows an increase of more than 45% in jerk for case C, where the vehicle is in the travel lane, than case G, where vehicle is on the middle of the bridge. This increase is considerably less than the increase in dynamic deflection which was observed in field tests and the analytical study.

### 5.3. Effect of Slab Stiffness on Jerk

The effect of slab stiffness on jerk is studied by varying the slab thickness. The study has been done for case C loading only. It



Table 5.1. Effect of Load Position on Maximum Jerk in Each Beam

Loading Case	(IN/SEC**3)							
	Beam 1	Beam 2	Beam 3	Beam 4	Beam 5	Beam 6	Beam 7	Beam 8
A	989.	-459.	-499.	-428.	-424.	-441.	-501.	-874.
B	749.	-615.	342.	493.	-396.	423.	-499.	-714.
C	766.	535.	484.	497.	-401.	534.	-521.	-678.
D	-755.	-355.	533.	385.	398.	499.	472.	-613.
E	-718.	489.	460.	523.	-466.	438.	466.	690.
F	680.	518.	369.	563.	-511.	399.	-470.	676.
G	589.	-422.	339.	481.	481.	339.	-422.	589.



Table 5.2. Effect of Load Position on Jerk in Each Beam at the Instant That Maximum Jerk Value Occurs

Loading Case	Jerk (IN/SEC**3)							
	Beam 1	Beam 2	Beam 3	Beam 4	Beam 5	Beam 6	Beam 7	Beam 8
A	989.	432.	75.	-27.	-2.	8.	-6.	4.
B	749.	58.	36.	81.	-231.	-373.	-227.	-200.
C	766.	-42.	-136	59.	-34.	-245.	-320.	-351.
D	-755.	-188.	-21.	-169.	-277.	-192.	-6.	183.
E	-718.	-161.	-119.	-137	-33.	-200.	-280.	268.
F	680.	9.	-23.	153.	85.	49.	200.	328.
G	589.	103.	32.	213.	213.	32.	103.	589.



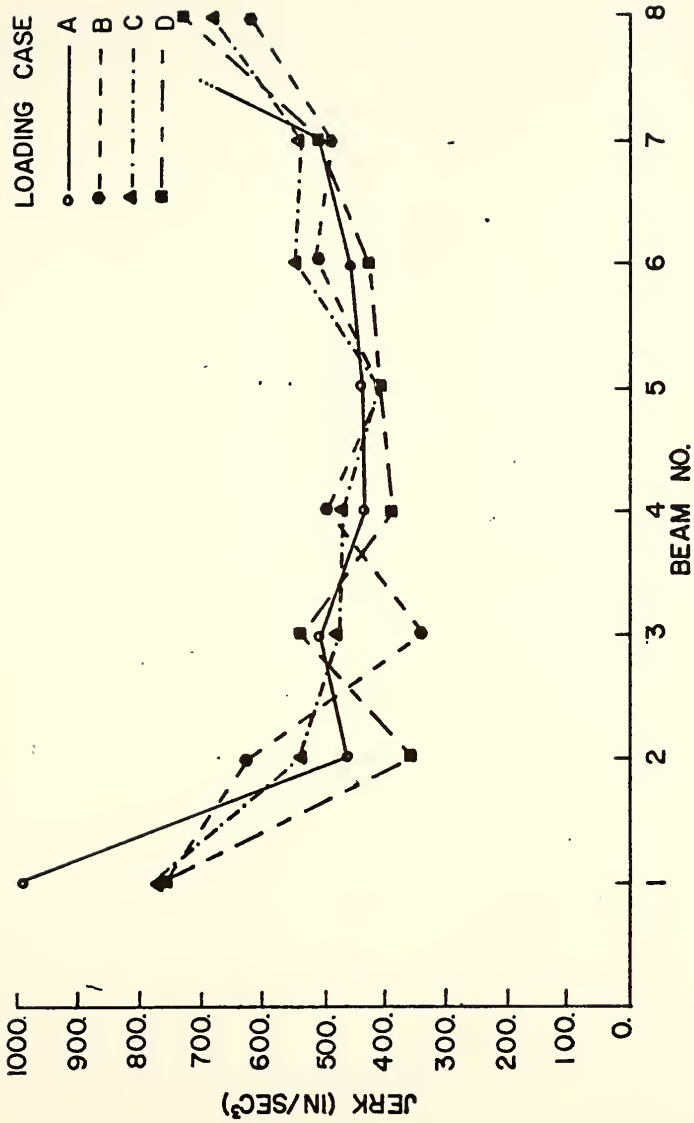


Figure 5.1. Effect of Load Position on Maximum Jerk in Each Beam





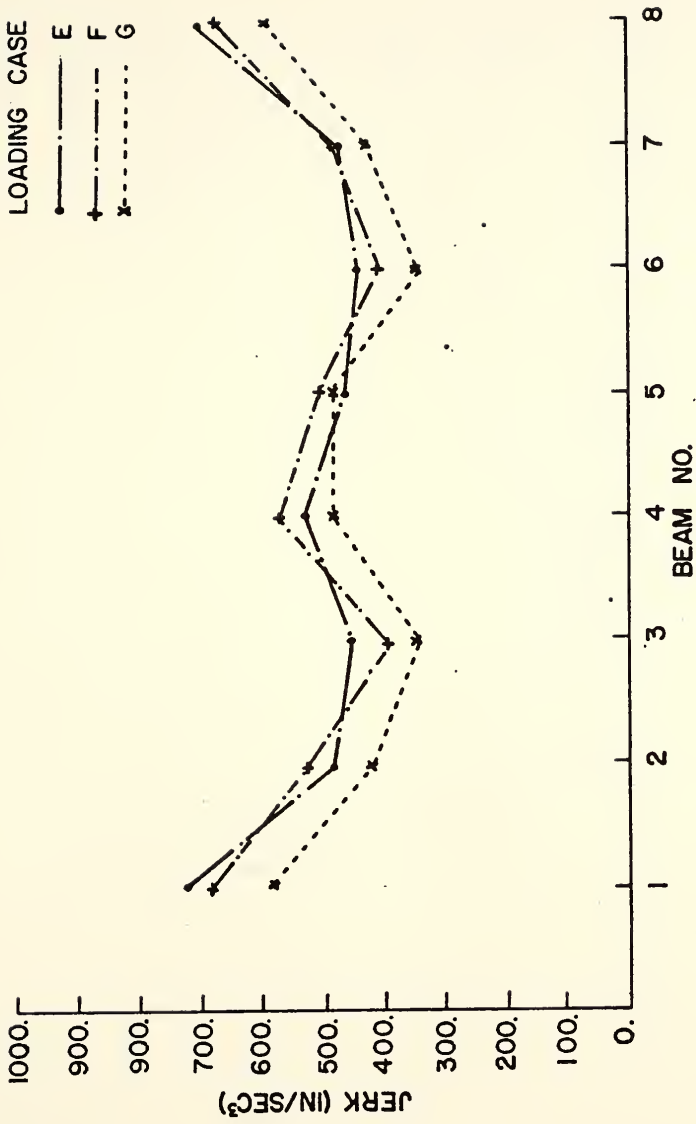


Figure 5.1. Continued



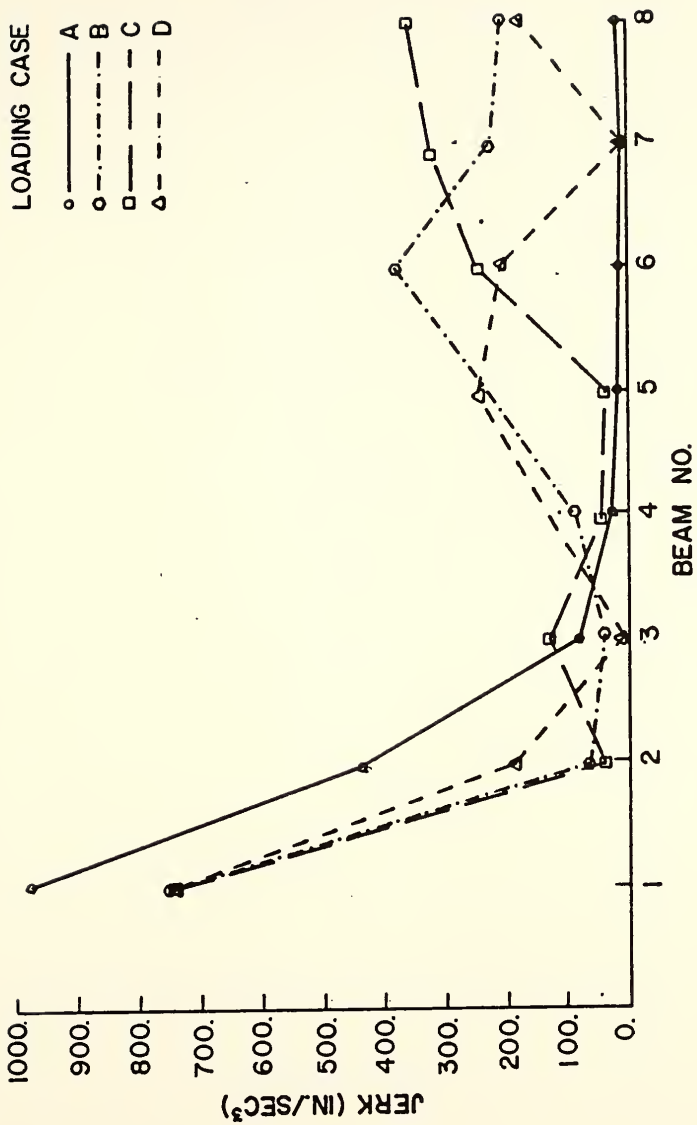


Figure 5.2. Effect of Load Position on Jerk in Each Beam at the Instant that the Maximum Jerk Value Occurs



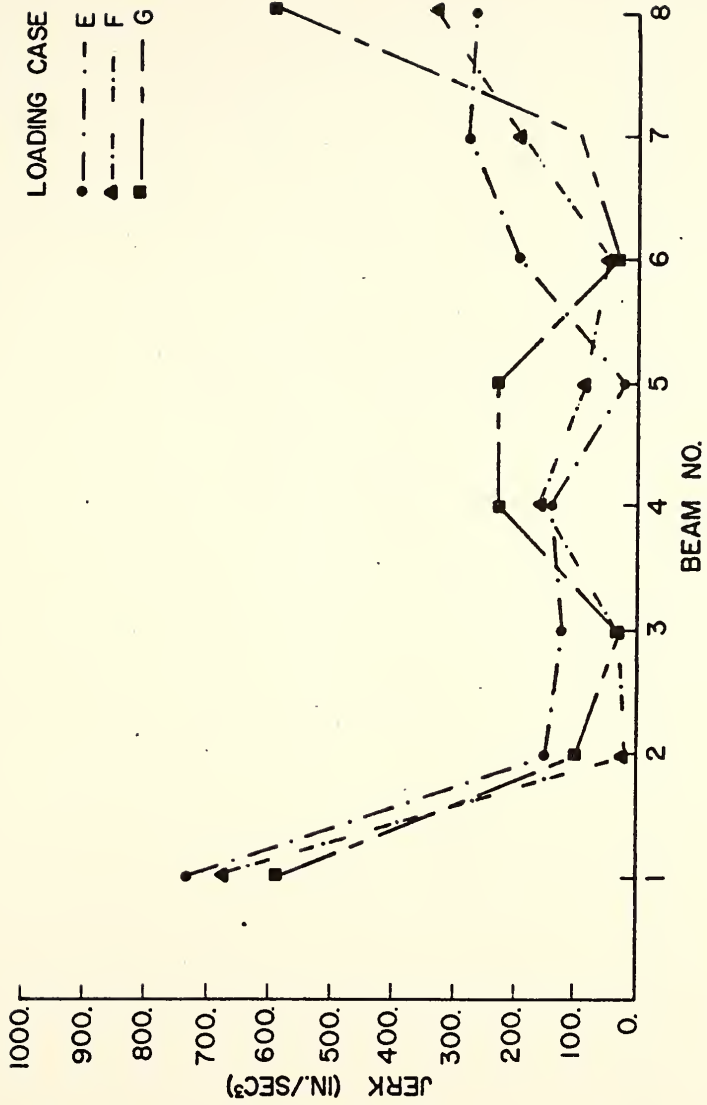


Figure 5.2. Continued



is believed that this case represents the most likely position of the vehicle on the bridge. Table 5.3 shows maximum jerk values in each beam for 5, 6.2, 7, and 8 inch slab thicknesses. Results in Table 5.3 indicate that a 200% increase in slab stiffness, which results from an increase in slab thickness of 6.2" to 8", has less than a 10% effect on maximum jerk values. A decrease of 50% in slab stiffness, due to thickness change of 6.2 to 5", increases maximum jerk values by not more than 10%. Figure 5.3 graphically shows the results in Table 5.3.

#### 5.4. Effect of Reduction in Moment of Inertia of Girders on Jerk

Use of high strength steel results in a reduction of moment of inertia of girders. The effect of this reduction, which could be up to 30% of the comparable design with normal grade steel, on jerk has also been studied. Table 5.4 shows maximum jerk values for 10, 20 and 30% reduction in the moment of inertia of the girders. The same results are presented in graphical form in Figure 5.4. Based on these results it may be concluded that girder stiffness has a very small effect on jerk, at least for this range of reduction in moment of inertia.

#### 5.5. Effect of Road Roughness on Acceleration and Jerk of Highway Bridges

The effect of sinusoidal road roughness on the dynamic response of highway bridges has been investigated in previous studies. Since uniform and equally spaced sine waves are not likely to result from normal surface wear, a simulation method was developed in Chapter III, which was based on several actual road profiles. Using the procedure in Chapter III one can generate road profiles which represent an "average" roughness. The theoretical response of the two span bridge (KCSG-A-1)





Table 5.3. Effect of Slab Thickness on Maximum Jerk in Each Beam

Thickness (in.)	Jerk (IN/SEC**3)							
	Beam 1	Beam 2	Beam 3	Beam 4	Beam 5	Beam 6	Beam 7	Beam 8
5.0	841.	635.	562.	-590.	469.	603.	620.	916.
6.2	766.	535.	484.	497.	-401.	534.	-521.	678.
7.0	728.	479.	442.	386.	400.	436.	-462.	-747.
8.0	690.	420.	-453	352.	350.	-442.	474.	670



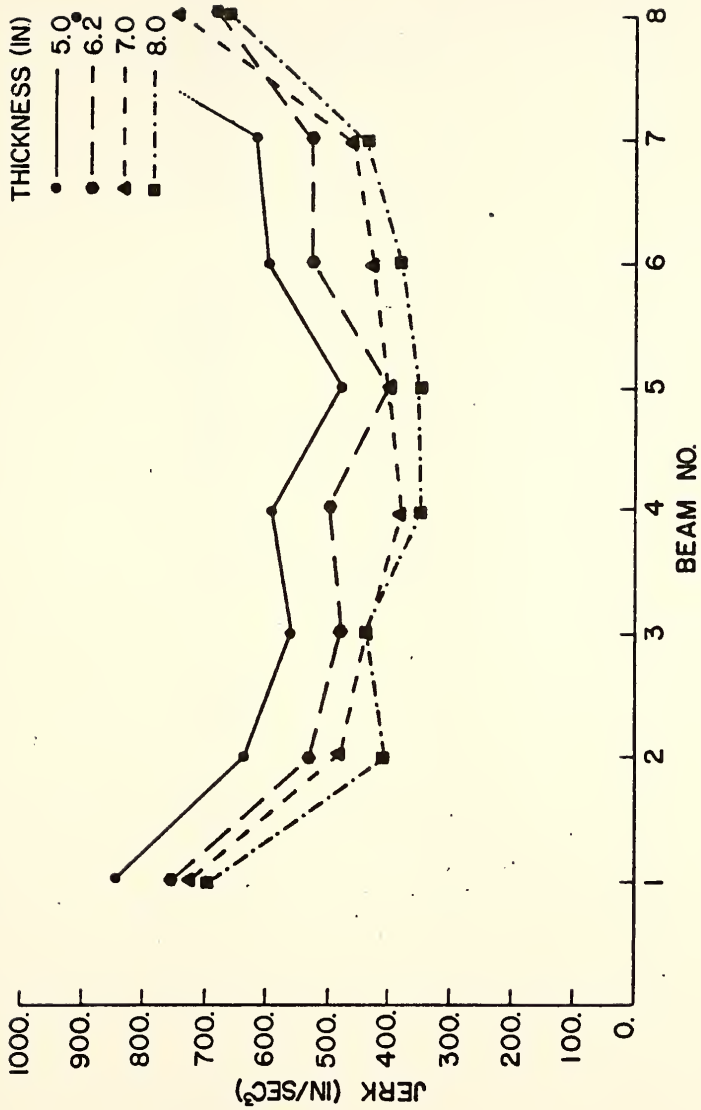


Figure 5.3. Effect of Slab Thickness on Maximum Jerk in Each Beam



Table 5.4. Effect of Reduction in Moment of Inertia on Maximum Jerk in Each Beam

Percent Reduction	Jerk (IN/SEC**3)							
	Beam 1	Beam 2	Beam 3	Beam 4	Beam 5	Beam 6	Beam 7	Beam 8
0	766.	535.	484.	497.	-401.	534.	-521.	678.
10	-738.	535.	485.	504.	368.	501.	-484.	699.
20	-752	536.	486.	485.	402.	-520.	-546.	766.
30	-787.	536.	486.	439.	427.	-475.	-476.	-705.



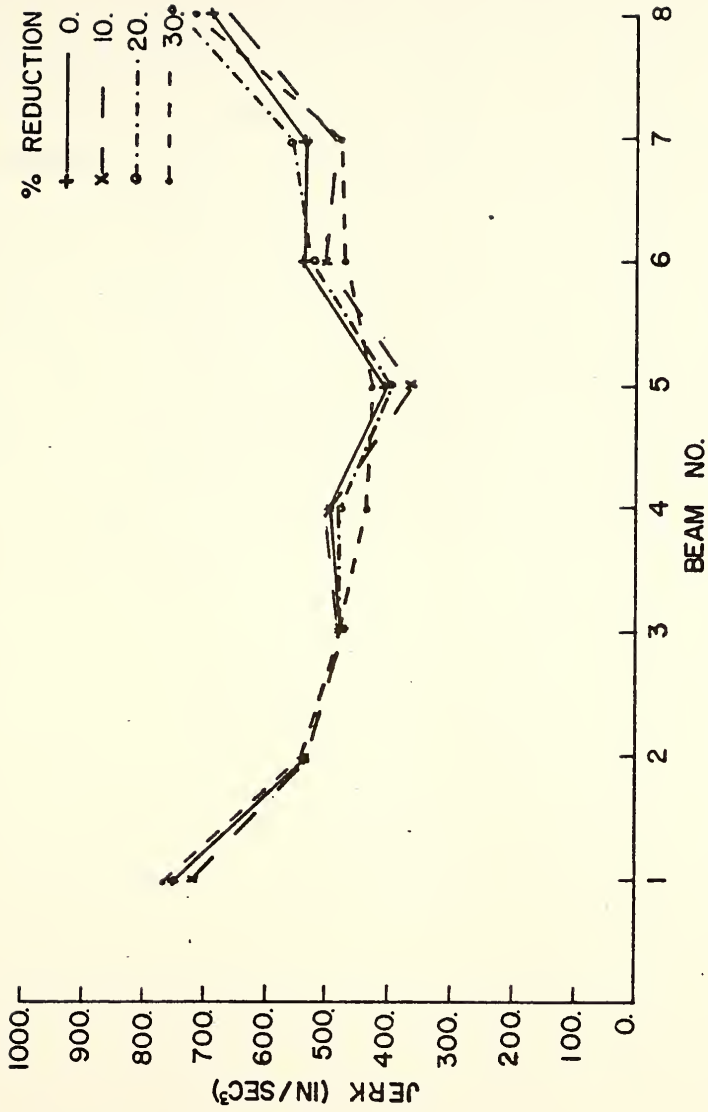


Figure 5.4. Effect of Reduction in Moment of Inertia on Maximum Jerk in Each Beam





to a number of these profiles was determined. It was found that as long as the roughness amplitudes were the same, regardless of which simulated profile was used, dynamic responses of the bridge were in the same order of magnitude. Dynamic responses of the bridge did increase as the amplitude of roughness was increased. Tables 5.5 and 5.6 show how maximum acceleration and maximum jerk of the three nodes of the first span vary with maximum amplitude of roughness. Results in Table 5.5 and 5.6 are plotted in Figure 5.5 and 5.6. Using this type of simulated road roughness, the resonance phenomena, which was observed by using half sine waves in study by Aramraks [31], did not occur. As explained previously, amplitude of roughness is referred to the total deviation of the bridge surface from a horizontal line drawn through the first support. This deviation is equal to the surface roughness plus a vertical curve.



Table 5.5. Effect of Maximum Amplitude of Simulated Road Roughness on Acceleration

Amplitude (in.)	Acceleration (IN/SEC**2)		
	Node 1	Node 2	Node 3
0	2.3	2.0	2.2
.5	4.1	3.9	3.7
1.0	5.7	4.2	5.6
2.0	9.7	8.0	10.9
4.0	11.7	10.5	12.4
8.0	15.3	14.8	16.1



Table 5.6. Effect of Maximum Amplitude of Simulated Road Roughness on Jerk

Amplitude (in.)	Jerk (IN/SEC**3)		
	Node 1	Node 2	Node 3
0.	87.	65.	88.
.5	241.	220.	265.
1.0	339.	312.	334.
2.0	641.	583.	761.
4.0	739.	694.	872.
8.0	1342.	1216.	1390.



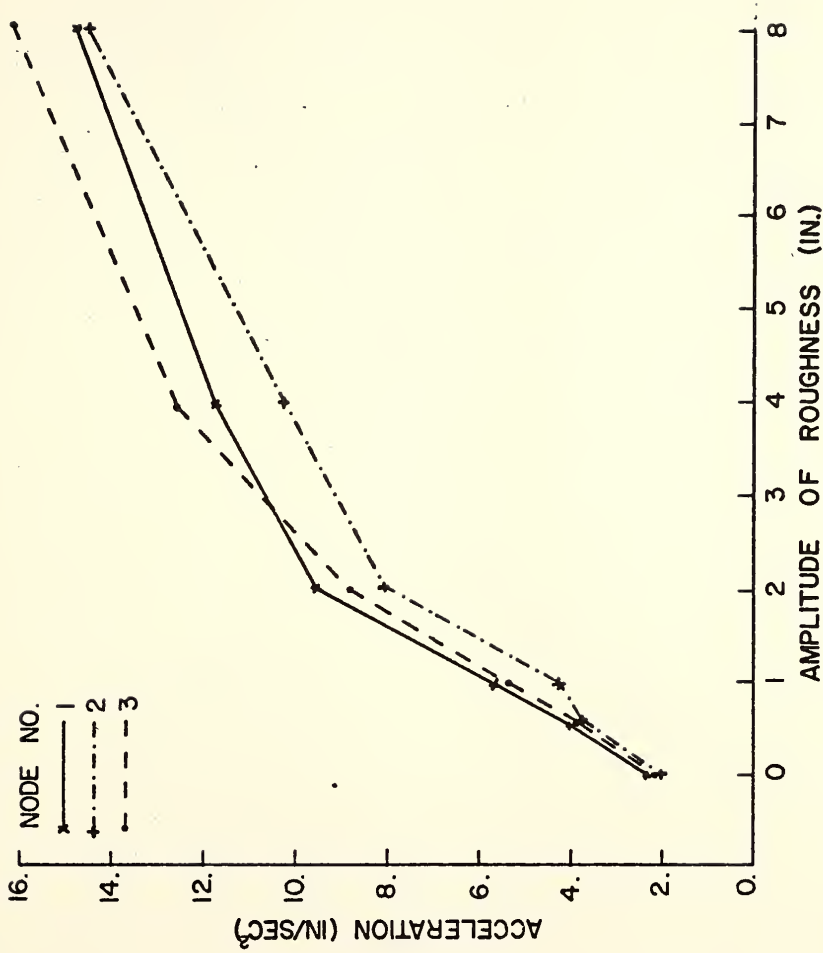


Figure 5.5. Effect of Maximum Amplitude of Simulated Road Roughness on Acceleration





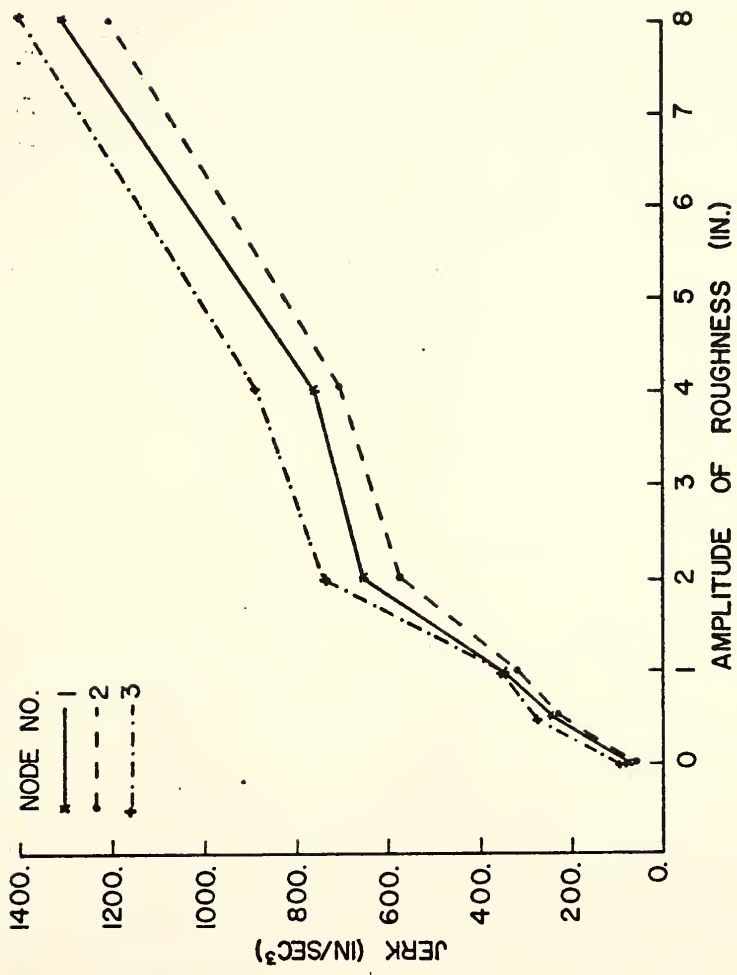


Figure 5.6. Effect of Maximum Amplitude of Simulated Road Roughness on Jerk



## CHAPTER VI

### COMPARISON OF ACTUAL AND THEORETICAL DYNAMIC RESPONSES

#### 6.1. General

In previous chapters, factors affecting dynamic responses of highway bridges were studied. In this chapter, actual field measurements are compared to theoretical results. Before making these comparisons the reader should be reminded of the limitations and capabilities of the available programs used for the analysis. The single span program analyzes a bridge as a flat slab with constant thickness resting on equally spaced girders. There is no composite action between the slab and the girders. The effect of composite action can be included by increasing the girder stiffness. The maximum number of girders that can be handled by the program is 8. The vehicle model is a spring-mass system with one axle and one or two wheels as shown in Figure 6.1. There is no damping either in the bridge or in the vehicle model. Only sinusoidal roadway roughness can be considered.

The model used for two and three span bridges is a single continuous beam with lumped masses. Damping is considered in the form of a series of dash pots under the lumped masses as shown in Figure 6.2. The vehicle model used is much more sophisticated than the one used for the single span program. This vehicle model takes into account the weight of the vehicle, tire and spring stiffnesses, axle spacing, and the damping effect of shock absorbers. The vehicle model can be used



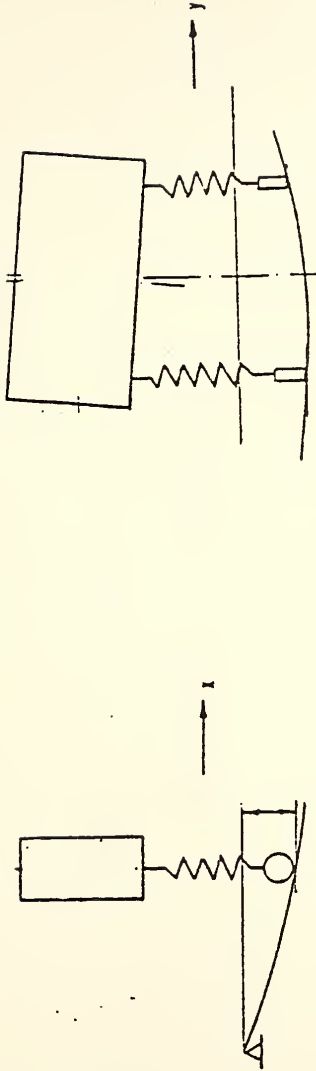
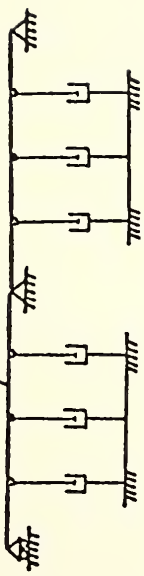


Figure 6.1. Vehicle Models for Single Span Bridge



Flexible beam with lumped masses



Flexible beam with lumped masses

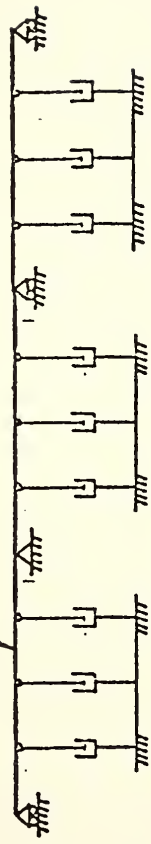


Figure 6.2. Bridge Model for Two and Three Span Bridges





with one, two or three axles. Figure 6.3 shows three different vehicle models that can be used by this program. For more description of the vehicle model the reader is referred to reference [31].

Two and three span programs are capable of determining the response of a given bridge using its actual surface roughness. The only disadvantage of the two and the three span program is that it does not take into account the rotational effect of either the vehicle or the bridge along its longitudinal axis because the bridge model used is a single beam.

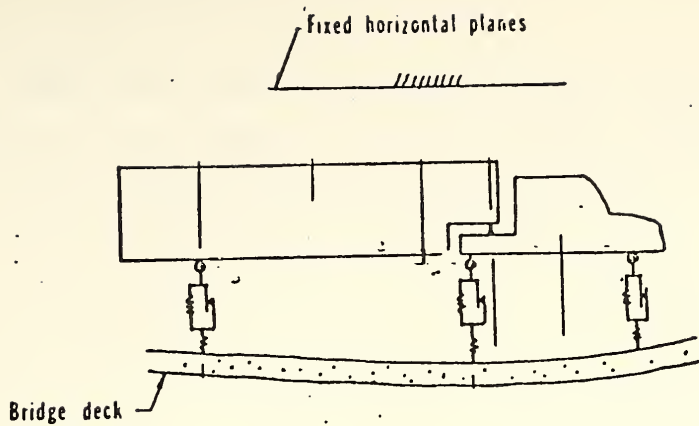
In this study and previous studies several different parameters were found to be of great interest when considering the dynamic response of bridges, especially acceleration and jerk. In the comparison of measured and theoretical values, the extent of the influence of these parameters is discussed.

## 6.2. Comparison of Dynamic Deflections

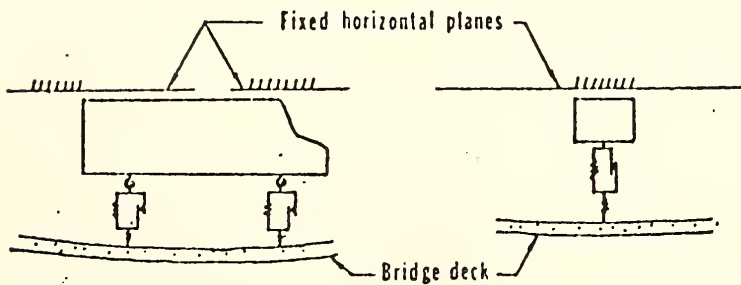
The parameter that had the most effect on dynamic deflection was found to be the transverse location of the vehicle on the bridge. This is due to the fact that beams closer to the wheels of the vehicle carry more load than the beams farther away from the wheels. This unequal distribution of load to the beams is more pronounced for wider bridges and less so for narrower bridges.

Comparison of Tables 4.1 and 4.11 shows that the theoretical values bound the measured values. This means that the single span program can be used to determine dynamic deflections of a single span bridge produced by a moving vehicle if the exact transverse location of the vehicle and the proper moment of inertia of the girders are used.





(a) Model for Three Axle Vehicle



(b) Model for Two Axle Vehicle

(c) Model for Single Axle Load

Figure 6.3. Vehicle Models for Two and Three Span Bridge



Effect of the transverse load position on dynamic deflections of the two span bridge (KCSG-A-1) could not be determined analytically but field measurements indicated that deflections increased by more than 60% when the vehicle was close to the curb (Table 4.12).

Figure 6.4 shows a deflection record for the two span bridge under study. Comparison of this figure and Figure 3.15 shows that the dynamic component of the deflection of the actual bridge is considerably greater. The reason is that in computing the theoretical response the moments of inertia of all girders were lumped together, based on the assumption that all the girders participate equally in carrying the load. It has been found that this assumption is not valid and, in order to get a reasonable comparison, a fraction of the total cross sectional moment of inertia should be used. This fraction was found to be about 70% for the (KCSG-A-1) bridge. Similar results were obtained for the three span bridge (CSB-C-1).

### 6.3. Comparison of Measured and Theoretical Accelerations

Since the vehicle model used in the single span program is a single axle vehicle, it is necessary to know how the number of axles affects acceleration. The study done by Aramraks [31] showed that the theoretical acceleration of the midpoints of a two span bridge was essentially the same for two and three axle vehicles but it increased considerably for a single axle vehicle. The percentage increase was found to be about 80%. It is believed that this percentage increase may be even more for the single span program because there is no damping in either the bridge or the vehicle model. It was found in Chapter III that road roughness did not have much effect on magnitude



FILE 903  
VELOCITY 19 MPH

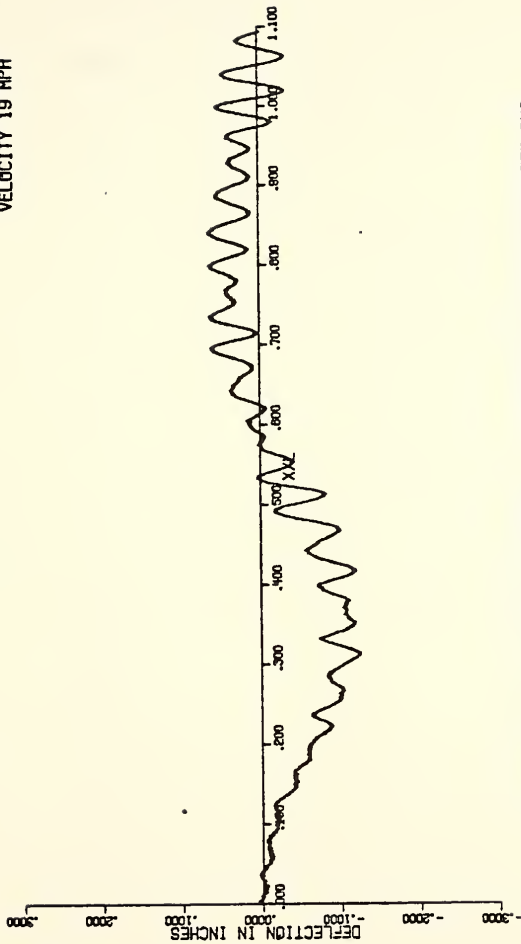


FIGURE 6.4. DEFLECTION RECORD , RESEARCH AND TRAINING CENTER BUS  
DEFLECTION GAGE LOCATED AT .50L IN FIRST SPAN  
2-SPAN COMPOSITE CONTINUOUS PLATE GIRDER BRIDGE  
SPAN LENGTHS 122.5FT,122.5FT  
WIDTH 32-0FT  
WYDOTTE ROAD OVER I-65-TIPPECANOE COUNTY  
BRIDGE STUDY NUMBER KCS6-A-1





of deflection but it had a pronounced effect on acceleration. Based on these ideas it would be expected that the theoretical results using the single span program for one axle vehicle and no road roughness on one hand would be higher than actual values because of single axle effect and on the other hand would be less than actual values because of the road roughness effect. The net result is that the theoretical acceleration values obtained from the single span program are close to the actual measured accelerations.

Using actual or simulated road roughness, two span and three span programs give theoretical results which were found to be, in most cases, in the same order of magnitude as the measured values. It was found that the maximum accelerations from the two span and three span programs should be increased if the vehicle is traveling close to the curb. These higher accelerations are due to the excitation of torsional modes of vibration which cannot be considered by the two and three span programs.

Tables 6.1, 6.2 and 6.3 contain results of the measured and calculated values of dynamic responses of the bridges (SB-C-1), (KCSG-A-1), and (CSB-C-1).



Table 6.1. Comparison of Measured and Calculated Dynamic Responses of the Single Span Bridge (SB-C-1)

Vehicle Position	Measured+			Calculated+++		
	Deflection IN	Velocity IN/SEC	Acceleration IN/SEC**2 Jerk**3 IN/SEC**3	Deflection IN	Velocity IN/SEC	Acceleration IN/SEC**2 Jerk IN/SEC**3
Center line	.005	.25	11.2 403	.003	.30	12.5 589.
Travel lane	.025	.43	16.8 485	.023	.40	14.1 718
Curb lane	.0436	.57	18.6 554	.054	.48	15.2 755

+Measured values for 50 MPH.

++Estimates using 3rd degree polynomial and 6 points.

+++These values are for Case G, E, D vehicle position.



Table 6.2. Comparison of Measured on Calculated Dynamic Responses of the Two Span Bridge (KCSG-A-1)

Vehicle Position	Measured+			Calculated+++			
	Deflection IN	Velocity IN/SEC	Acceleration IN/SEC**2	Deflection IN	Velocity IN/SEC	Acceleration IN/SEC**2	Jerk IN/SEC**3
Center line	.09	.48	13.9				1095
Travel lane	.12	.65	14.2	.09	.41	11.4	1100
Curb lane	.15	.70	15.7				1402

+Measured values for 50 MPH.

++Estimates using 3rd degree polynomial and 6 points.

+++These values are for Case G, E, D vehicle position



Table 6.3. Comparison of Measured and Calculated Dynamic Responses for the Three Span Bridge (CSB-C-1)

Vehicle Position	Measured+			Calculated+++				
	Deflection IN	Velocity IN/SEC	Acceleration IN/SEC**2	Jerk IN/SEC**3	Deflection IN	Velocity IN/SEC	Acceleration IN/SEC**2	Jerk IN/SEC**3
Center Line	.022	.38	12.3	933				
Travel Lane	.045	.51	15.1	963	.027	.22	12.1	1540
Curb Lane	.065	.58	16.8	1109				

+Measured values for 50 MPH.

++Estimates using 3rd degree polynomial and 6 points.

+++ These values are for Case G, E, D vehicle position.





CHAPTER VII  
SIMPLIFIED METHOD OF DETERMINING MAXIMUM DYNAMIC  
RESPONSES OF HIGHWAY BRIDGES

7.1. General

Due to the numerous variables which influence the dynamic response of bridges under moving vehicles, calculation of the exact dynamic response has not been possible. It has been determined that the analytical programs do give results in the same order of magnitude as the actual measured values if the proper values of vehicle weight, vehicle position, and moment of inertia of girders are used.

Since the design engineer is concerned primarily with the maximum values of dynamic response, an empirical formula is suggested in this chapter which enables designers to estimate the maximum dynamic response of a given bridge. This method can also be used to determine dynamic responses of existing bridges. As a check to this simplified method, accelerations of the bridges in the field study have been calculated and compared to the actual measured values.

7.2. Description and Usage of the Simplified Method

This simplified approach is based on the assumption that a bridge vibrates in its fundamental mode only. Since contributions of the higher modes are likely to have a damping effect rather than a magnifying effect, the results obtained from this method would likely be higher than actual values, so they could be used as upper bounds.



Consider the bridge vibrating in its fundamental mode to be a lightly damped single degree-of-freedom system whose maximum displacement is  $D$ . Corresponding maximum velocity, acceleration, and jerk are  $2\pi fD$ ,  $(2\pi f)^2D$ , and  $(2\pi f)^3D$ , respectively, where  $f$  is the natural frequency of the system. In earthquake engineering these quantities are known as pseudovelocity, pseudoacceleration, and pseudojerk [37]. A reasonable estimate for the maximum acceleration of a beam bridge is then  $(2\pi f)^2D$  where  $f$  is either the fundamental bending frequency or the fundamental torsional frequency, depending on the transverse position of the vehicle on the bridge.

In the field study dynamic deflection and acceleration were directly measured using transducers whereas velocity and jerk had to be calculated from deflection and acceleration. In calculation of jerk it was observed that there was a rather wide range of answers, varying by as much as 15 to 30 times depending on how acceleration values were differentiated. Because of this wide range of jerk values, only acceleration values from field results are compared to the ones obtained from the simplified method.

Table 7.1, which is obtained from Tables 4.2 and 4.8 of the thesis by Kröpp [33], shows the measured values of maximum deflection, maximum acceleration and fundamental frequencies for the 37 bridges in the field study. Fundamental frequencies were obtained from the frequency spectrum of the free vibration of the bridge, whereas the maximum acceleration and the deflection values occurred while the vehicle was on the bridge.



Table 7.2 shows the calculated acceleration values for all the bridges in Table 7.1 using both fundamental frequencies. For ease of comparison actual measured values from Table 7.1 are also shown in Table 7.2. The results in Table 7.2 are shown graphically in Figure 7.1. The results indicate that, with the exception of one series of three span bridges, (CSB-B), the simplified method gives results which are reasonable upper bounds on acceleration. Theoretically, for cases in which the vehicle is not close to the curb, using the fundamental bending frequency in the simplified equations should be sufficient. If the vehicle gets close to the curb then it would excite the torsional mode which results in a higher dynamic response. In such cases the torsional frequency should be used in the simplified equation. This approach gives reasonable upper bounds on acceleration as long as the bridge has "average" surface roughness. For cases where the bridge has a very rough surface, this method is not recommended. If dynamic deflection and fundamental frequencies cannot be measured then they can be calculated with reasonable accuracy.

### 7.3. Procedure for Estimating Dynamic Deflection and Fundamental Frequencies

The fundamental bending frequency for simple span and two span beam bridges can be calculated by Eq. B.1. Using the full composite moment of inertia of the cross section, Kropp [33] obtained good agreement with measured values of fundamental frequency. Bending frequency for three span bridges can be calculated by Eq. F.1. Based on the results of the analysis in Chapter II, a reasonable upper bound estimate



for the fundamental torsional frequency of typical beam bridges is 1.3 times the fundamental bending frequency.

The maximum dynamic deflection for a given bridge under a moving vehicle can be estimated by the maximum static deflection produced by the vehicle. A reasonable estimate of the static deflection can be obtained by assuming the bridge to be a single beam with the total moment of inertia of the bridge cross section and by replacing the vehicle weight by a single concentrated load.

It is suggested that for design purposes a more detailed dynamic analysis would be necessary only if the maximum dynamic response estimated by this simplified approach exceeds the HRV comfort limit.





Table 7.1. Measured Fundamental Frequencies and Maximum Measured Accelerations and Deflections for the Bridges in the Study

Bridge Type	Fundamental Frequency (Hz)		Deflection (IN)	Acceleration (IN/SEC**2)
	Bending	Torsion		
Single Span				
SB-A-1 thru SB-A-5	7.62	8.40	.060	89.
SB-B-1 thru SB-B-3	6.77	7.88	.047	57.
SB-C-1	4.88	5.27	.058	50.
Two Span				
KCSB-A-1 and KCSB-A-2	2.73	3.32	.277	34.
KCSB-B-1	2.15	2.73	.124	33.
KCPG-P-1 and KCPG-B-2	2.25	2.83	.154	36.
KCSB-C-1 thru KCSB-C-4	3.81	4.10	.228	133.
KCSB-D-1 and KCSB-D-2	2.83	3.03	.123	42.
KCSG-A-1 and KCSG-A-2	2.34	2.83	.131	30.
KCSG-B-1 and KCSG-B-2	2.22	2.90	.117	23.
KCPG-A-1 thru KCPG-A-3	2.44	3.12	.112	27.
Three Span				
CSB-A-1 thru CSB-A-4	7.54	8.96	.049	105.
CSB-B-1 thru CSB-B-4	5.27	5.96	.075	124.
CSB-C-1	3.91	4.49	.137	83.



Table 7.2. Comparison of the Maximum Measured Accelerations with the Accelerations Obtained from the Simplified Method

Bridge Type	Acceleration (IN/SEC**2)		
	Measured	Calculated Using	Fundamental Frequency
		Bending	Torsion
Single Span			
SB-A-1 thru SB-A-5	89.0	137.0	167.0
SB-B-1 thru SB-B-3	57.0	85.0	115.0
SB-C-1	50.0	54.0	63.0
Two Span			
KCSG-A-1 and KCSG-A-2	34.0	81.0	120.0
KCSB-B-1	33.0	22.0	36.0
KCPG-B-1 and KCPG-B-2	36.0	32.0	50.0
KCSB-C-1 thru KCSB-C-4	133.0	130.0	151.0
KCSB-D-1 and KCSB-D-2	42.0	38.0	44.0
KCSG-A-1 and KCSG-A-2	30.0	28.0	41.0
KCSG-B-1 and KCSG-B-2	23.0	22.0	39.0
KCPG-A-1 thru KCPG-A-3	27.0	26.0	43.0
Three Span			
CSB-A-1 thru CSB-A-4	105.0	109.0	155.0
CSB-B-1 thru CSB-B-4	124.0	82.0	105.0
CSB-C-1	83.0	82.0	109.0



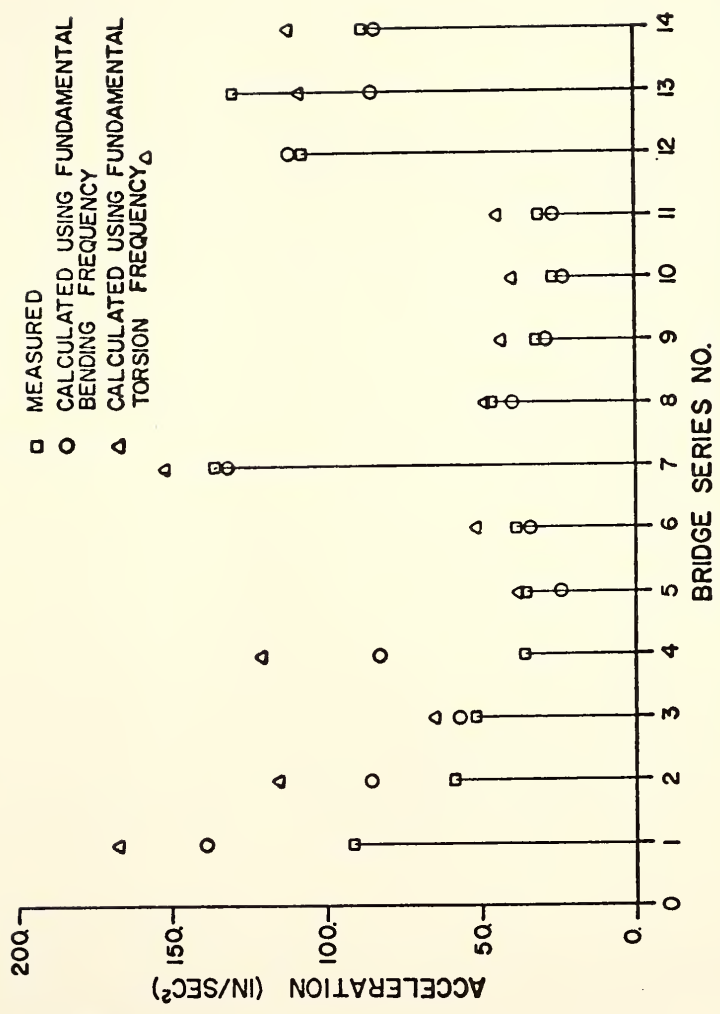


Figure 7.1. Comparison of the Maximum Measured Accelerations with the Accelerations Obtained from the Simplified Method



## CHAPTER VIII

## CONCLUSIONS AND RECOMMENDATIONS

8.1. Conclusions

## 8.1.1. Human Response to Vibration

Based on the literature review on HRV, the controlling factors for the HRV were found to be jerk for the low frequency range (1-6 CPS) and acceleration for the medium frequency range (6-20 CPS). Maximum comfort limits on acceleration and jerk were found to be  $120 \text{ in/sec}^2$  and  $3600 \text{ in/sec}^3$ , respectively. On the basis of these limits none of the bridges in the field study, except one, was found to have excessive vibrations. The acceleration of the bridge in the CSB-C series, which exceeded the comfort limits, was  $133 \text{ in/sec}^2$ . Accelerations of this magnitude are not intolerable but rather they are unpleasant to an average person.

As a result of this study it has been concluded that the vibration of the highway bridges due to the moving vehicles did not cause any physiological disturbance to the bridge users. It was suspected that the discomfort of some of the bridge users might have had a psychological basis. Bridge users experience vibrations where they are not expecting any movements at all.

## 8.1.2. Torsional Frequency

The frequency study showed that the contributions of the torsional modes to the dynamic response of a bridge could be significant.





Contributions of the torsional modes were determined to be highly dependent on the transverse location of the vehicle on the bridge. The torsional modes were excited more than the bending modes as the vehicle moved closer to the curb and less than the bending modes as it moved away from the curb and closer to the center line of the bridge. It was determined, analytically, that the jerk for the mid-point of the edge beams was increased by as much as 60% when torsional modes were excited.

### 8.1.3. Dynamic Load Distribution

Distribution of the vehicle load to the girders of a bridge is not uniform and depends on the transverse position of the vehicle on the bridge. In the analytical study of the single span bridge (SB-C-1) it was determined that except in case A, where one of the wheels of the vehicle was on the curb, no girder carried more than 30% of the vehicle load. In case A 42% of the vehicle load was carried by the edge beam.

### 8.1.4. Jerk

Jerk, which is a significant factor in human discomfort, was not sensitive to an increase in the girder flexibility. Reduction of 30% in the girder stiffness resulted in about 11% increase in the jerk. Therefore, use of high strength steel, which can reduce the girder stiffness up to 30% when compared to a similar design using normal grade steel, will not cause an appreciable increase in jerk.

## 8.2. Recommendations

### 8.2.1. Analytical Computer Programs

The available analytical computer programs can be used to determine the dynamic response of a given beam bridge to a moving vehicle. When



using the multi-span computer program, it is necessary to include the surface roughness in the analysis. If no surface roughness is available, a simulated road roughness such as one obtained by the method explained in Chapter III should be used.

Although there are limitations on the type of bridges that the analytical programs can handle, a majority of the highway bridges built nowadays can be analyzed using these programs.

### 8.2.2. Simplified Method

For a quick analysis of the dynamic response of a highway bridge to a moving vehicle, the simplified method outlined in Chapter VII can be used. Since this simplified method, in general, overestimates the dynamic response of a bridge, it can be used as an upper bound on the maximum dynamic response of a bridge. It is suggested that if the response obtained using the simplified method is less than the recommended limit for human comfort, no further dynamic analysis is necessary.

A field study on the dynamic response of a very flexible bridge is recommended for future studies. It is also recommended that more sophisticated computer programs be developed that can handle torsional modes of vibration of highway bridges as well as their bending modes.



## BIBLIOGRAPHY



## BIBLIOGRAPHY

1. Janeway, R. N., "Passenger Vibration Limits", Society of Automotive Engineers Journal, V. 55, 1947.
2. McFarland, R. A., Human Factors in Air Transportation, Occupational Health and Safety, McGraw-Hill, New York, 1953.
3. Getline, G. L., "Vibration Tolerance Levels in Military Aircraft", Supplement to Shock and Vibration Bulletin, n 22, p. 24, US Department of Defense, Research and Development, Washington, 1955.
4. Mallock, H. R. A., "Vibrations Produced by the Working of Traffic on the Central London Railway", Board of Trade Report, Command Papers, n 951, 1902.
5. Parmelee, R. A. and Wiss, J. F., "Human Perception of Transient Vibrations", Journal of the Structural Division, ASCE, April 1974.
6. Pradko, F., Orr, T. R., and Lee, R. A., "Human Vibration Analysis", Society of Automotive Engineers, Inc., Report 650426, New York, N.Y., 1965.
7. C. M. Harris and C. E. Crede, Shock and Vibration Handbook, Second Edition, McGraw-Hill Book Company.
8. Dieckmann, D., "Study of the Influence of Vibration on Man", Ergonomics, Vol. 1, 1958, pp. 345-355.
9. Goldmann, D. E., "A Review of Subjective Response to Vibratory Motion of the Human Body in the Frequency Range 1 to 70 cycles per second", Naval Medical Research Institute, Report No. 1, Project MM004001, 16 March 1948.
10. Gorrill, R. B. and F. W. Snyder, "Preliminary Study of Aircrew Tolerance to Low Frequency Vertical Vibration", Boeing Airplane Co., Doc. No. D3-1189, 3 July 1957 (AD155462).
11. Janeway, R. N., "Vertical Vibration Limits to Fit the Passenger", Journal of Automotive Engineers, v 56, n 8, 1948.
12. Reiher, H. and Meister, J. J., "The Effect of Vibration on People", (in German), Forschung auf dem Gebite des Ingenieurwesens, v 2, II, p. 381, 1931. (Translation: Report No. F-TS-616-RE H.Q. Air Material Command, Wright Field Ohio. 1946.)





13. Jacklin, H. M. and G. J. Liddle, "Riding Comfort Analysis", Engineering Bulletin, Purdue University, Vol. XVII, No. 3, May 1933.
14. Hirschfield, R. J., "Effects of Whole-Body Vibration in Three Directions Upon Human Performance", J. Eng. Psychol. Vol. 1 No. 3, 1962, pp. 93-101.
15. Digby, W. P. and Sankey, H. R., "Some Preliminary Notes on a Study as to Human Susceptibility to Vibration", The Electrician, Vol. 67, N. 23, p. 888, 1911.
16. Zeller, W., "Proposal for a Measure on Strength of Vibration (in German)", Ziet, V.D.I., v 77, n 12, p. 323, 1933.
17. Koch, H. W., "Determination of the Effect of Vibrations on Buildings", (in German), Ziet V.D.I., v 95, n 21, p. 733, 1953. (Translation Building Research Station DSIR, L.C. 597, 1954).
18. Lenzen, K. H., "Vibration of Steel Joist-Concrete Slab Floors", Engineering Journal, AISC, Vol. 3, No. 3, July 1966, pp. 133-136.
19. Jacobson, L. S. and Ayre, R. S., Engineering Vibrations, McGraw-Hill Book Co., New York, 1958, p. 201.
20. International Organization for Standardization Technical Committee 108, "Guide for the Evaluation of Human Exposure to Whole-body Vibration", ISO/TC 108/WG7, Dec. 1968.
21. Bolt, Beranek, and Newman, Inc., The MBTA South Shore Project, "Passenger Noise and Vibration Criteria", BBN Rep. No. 1428, Job No. 138127, 25 August 1966.
22. United States Navy: Buchmann, E., "Criteria for Human Reaction to Environmental Vibration on Naval Ships", Report 1635, June 1962 (AD404-834).
23. Spërling, E. and C. Betzhold, "Beitrag zur Beurteilung des Fahrkomforts in Schienenfahr", Glaser's Annalen, October 1956, pp. 314-317.
24. Association of American Railroads, Joint Committee on Relation Between Track and Equipment, "Effect of Wheel Unbalance, Eccentricity, Tread Contour and Track Gauge on Riding Quality of Railway Passenger Cars", AAR, Operations and Maintenance Dept., Chicago, Ill., April 4, 1950.
25. Batchelor, G. H., "Determination of Vehicle Riding Properties-Part II", The Railway Gazette, 28 July 1962, pp. 97-100.



26. Matsubara, K., "Track for New Tokaido Line", Permanent Way Society Bulletin, Vol. 7, No. 2-3, Dec. 1964, pp. 1-69.
27. Nieto Ramirez, J. A., A. S. Velotos, "Response of Three Span Continuous Highway Bridges to Moving Vehicle", Civil Engineering Studies, Structural Research Series No. 276, University of Illinois, Urbana, Illinois, 1964.
28. Huang, T., "Dynamic Response of Three Span Continuous Highway Bridges", Ph.D. Thesis, University of Illinois, Urbana, Illinois, 1960.
29. Eberhardt, A. C., "A Finite Element Approach to the Dynamic Analysis of Continuous Highway Bridges", Ph.D. Thesis, University of Illinois, Urbana, Illinois, 1972.
30. "Torsion Analysis of Rolled Steel Sections", Handbook 1963-C, Bethlehem Steel Corporation, Bethlehem, Pennsylvania.
31. Aramraks, T., "Highway Bridge Vibration Studies", Joint Highway Research Project, Engineering Experiment Station, Purdue University.
32. Subroutine "FORIT", Computer Library of Purdue University, method used is described in A. Ralston, H. Wilf, Mathematical Methods for Digital Computers, Chap. 24, John Wiley and Sons, New York, 1960.
33. Kropp, P. K., "Experimental Study of the Dynamic Response of Highway Bridges", Joint Highway Research Project, Engineering Experiment Station, Purdue University, May 1977.
34. Subroutine "SMOOTH" Computer Library of Purdue University.
35. Oran, C. and Veletsos, A. S., "Analysis of Static and Dynamic Response of Simple-Span, Multigirder Highway Bridges", Civil Engineering Studies, Structural Research Series No. 221, University of Illinois, Urbana, Illinois, July 1961.
36. Veletsos, A. S. and Huang, T., "Analysis of Dynamic Response of Highway Bridges", Journal of the Engineering Mechanics Division, ASCE, Vol. 96, No. EM5, October 1970.
37. Newmark, N. M. and Rosenblueth, E., Fundamentals of Earthquake Engineering, Prentice-Hall, Inc., Englewood Cliffs, New Jersey, 1971.
38. Hanès, R. M., "Human Sensitivity to Whole-Body Vibration in Urban Transportation Systems", Johns Hopkins University, May 1970.
39. Wright, D. T. and Green, R., "Human Sensitivity to Vibrations", Report No. 7, Queen's University, February 1959.



## APPENDICES



APPENDIX A  
HUMAN RESPONSE TO VIBRATION CURVES

Results of the human response to vibration studies are mostly presented in form of a series of curves. These curves are usually plotted on acceleration-frequency coordinates. Each curve represents a certain level of human sensitivity to vibration for various frequencies and accelerations. Figures A.1 thru A.7, show the results of some of the experiments done on human response to vertical vibration. Human sensitivity corresponding to each curve is explained on or above each figure. The vertical bars in Figure A.5 show one standard deviation of the response plotted about the mean value.

The following abbreviations have been used in Chapter I.

IOS	International Organization of Standardization [20]
B,B,&N	Bolt, Beranek, and Newman [21]
U.S.N.	United States Navy [22]
S&B	Sperling and Betzhold [23]
AAR	American Association of Railroads [24]





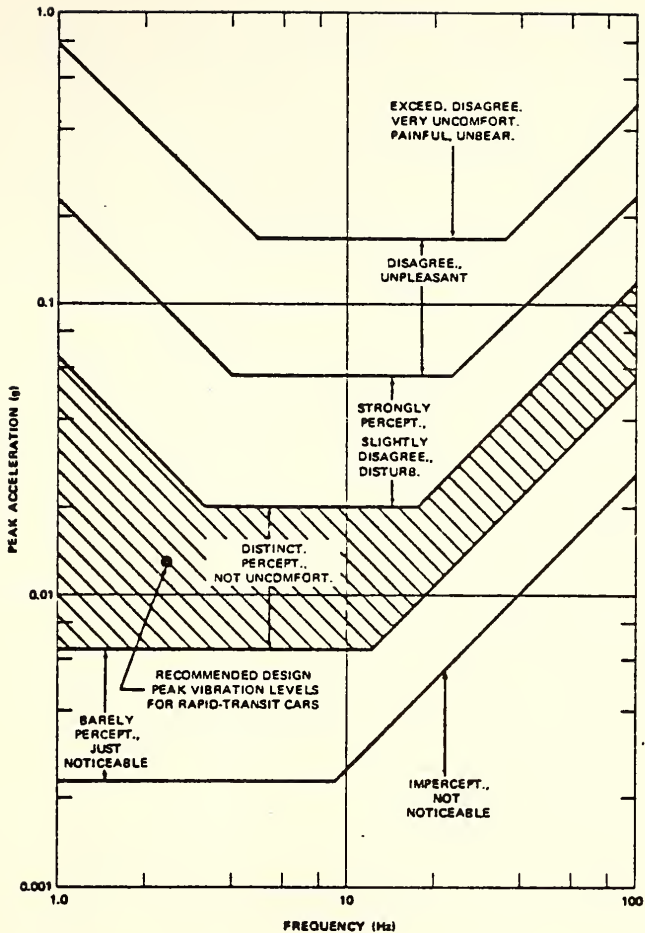


Figure A.1. Human Response to Vibration as Reported by Bolt, Beranek, and Newman



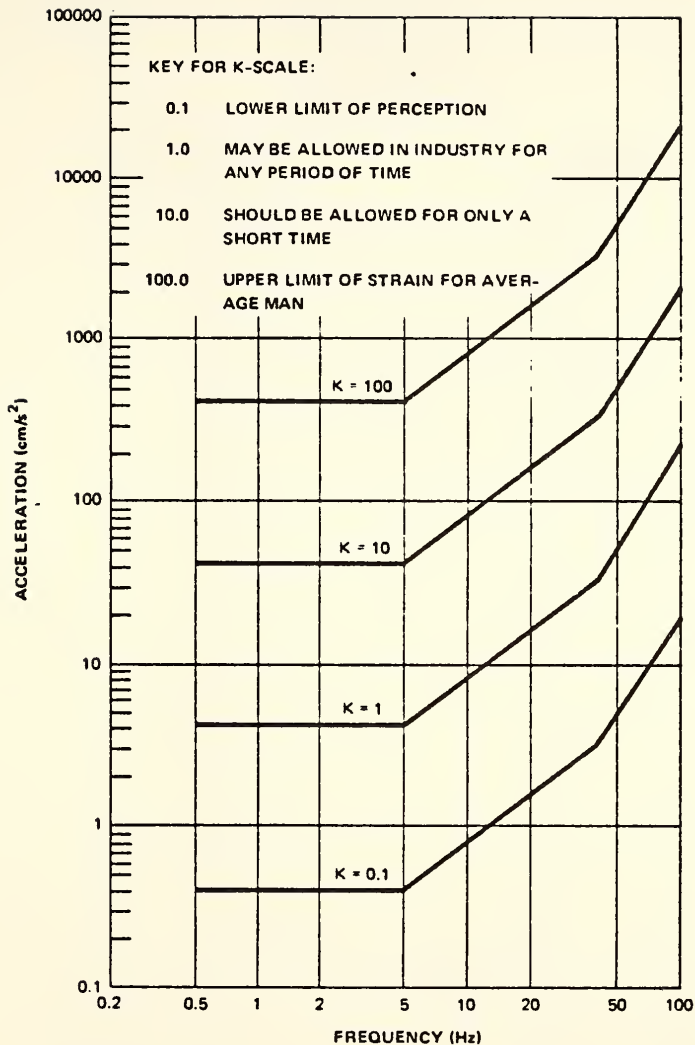


Figure A.2. Dieckmann's Scale of Strain for Vertical Vibrations



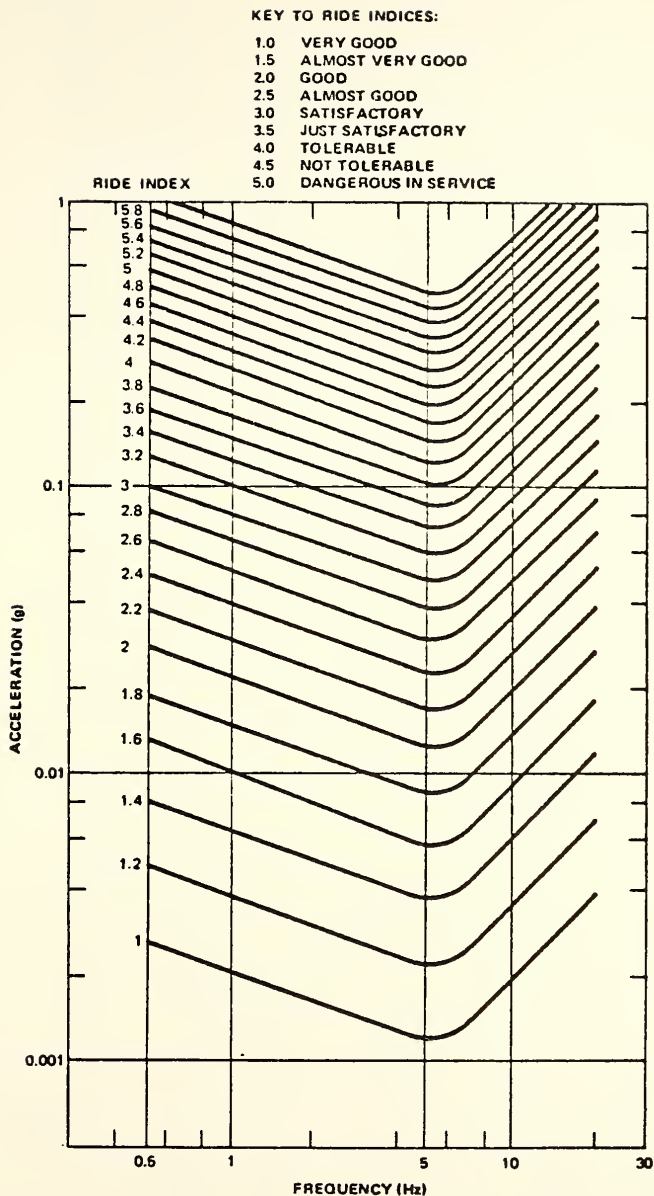


Figure A.3. Ride Indices for Vertical Accelerations as Reported by Batchelor [25]



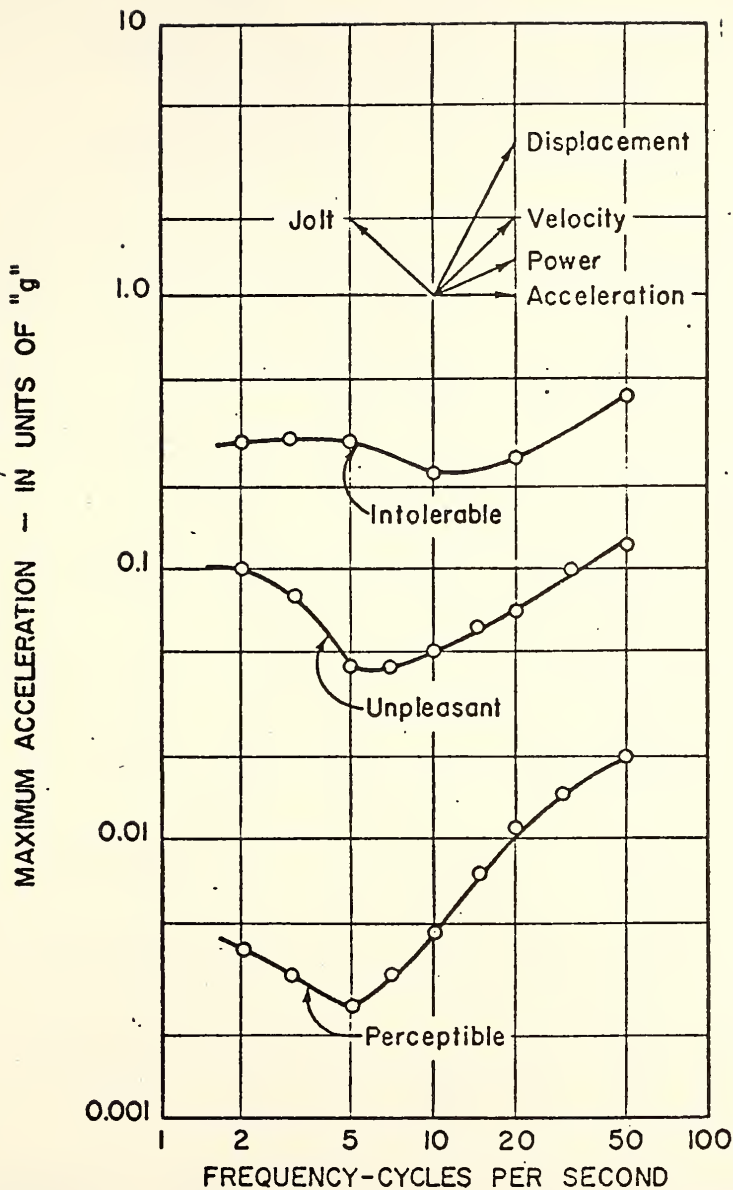


Figure A.4. Subjective Responses of the Human Body to Vibratory Motion, After Goldman





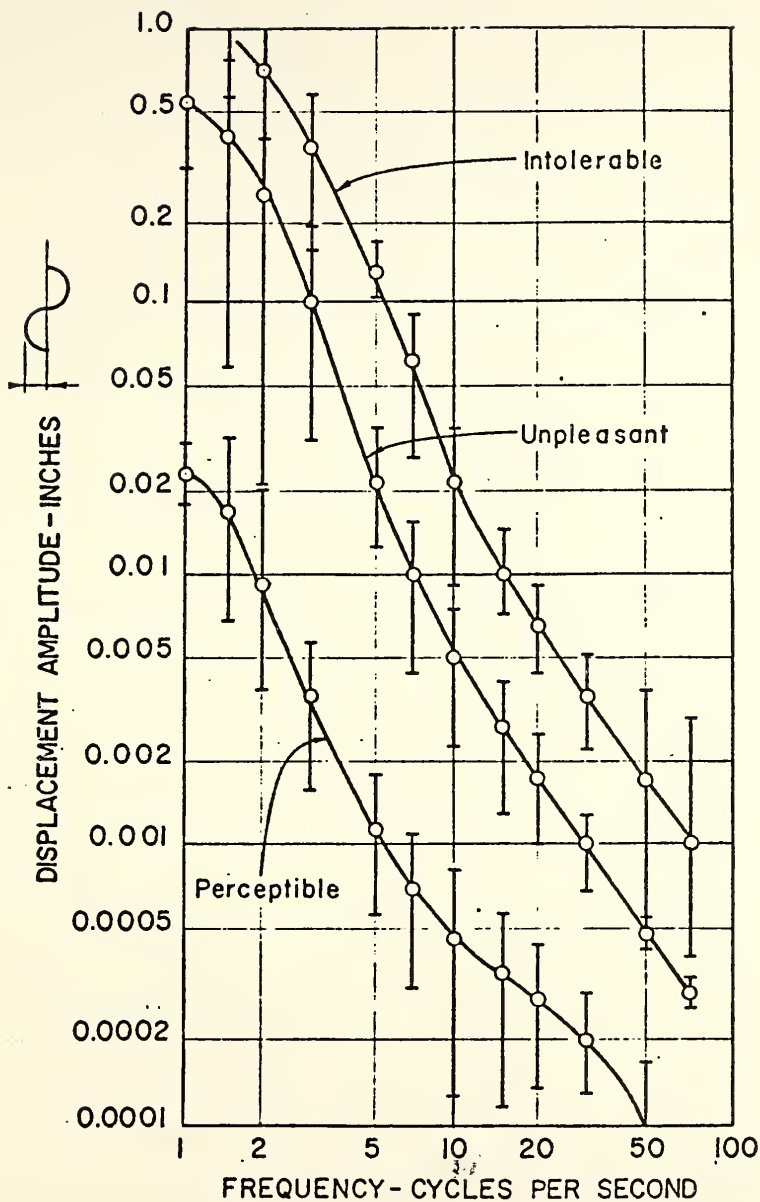


Figure A.5. Subjective Responses of the Human Body to Vibratory Motion, After Goldman



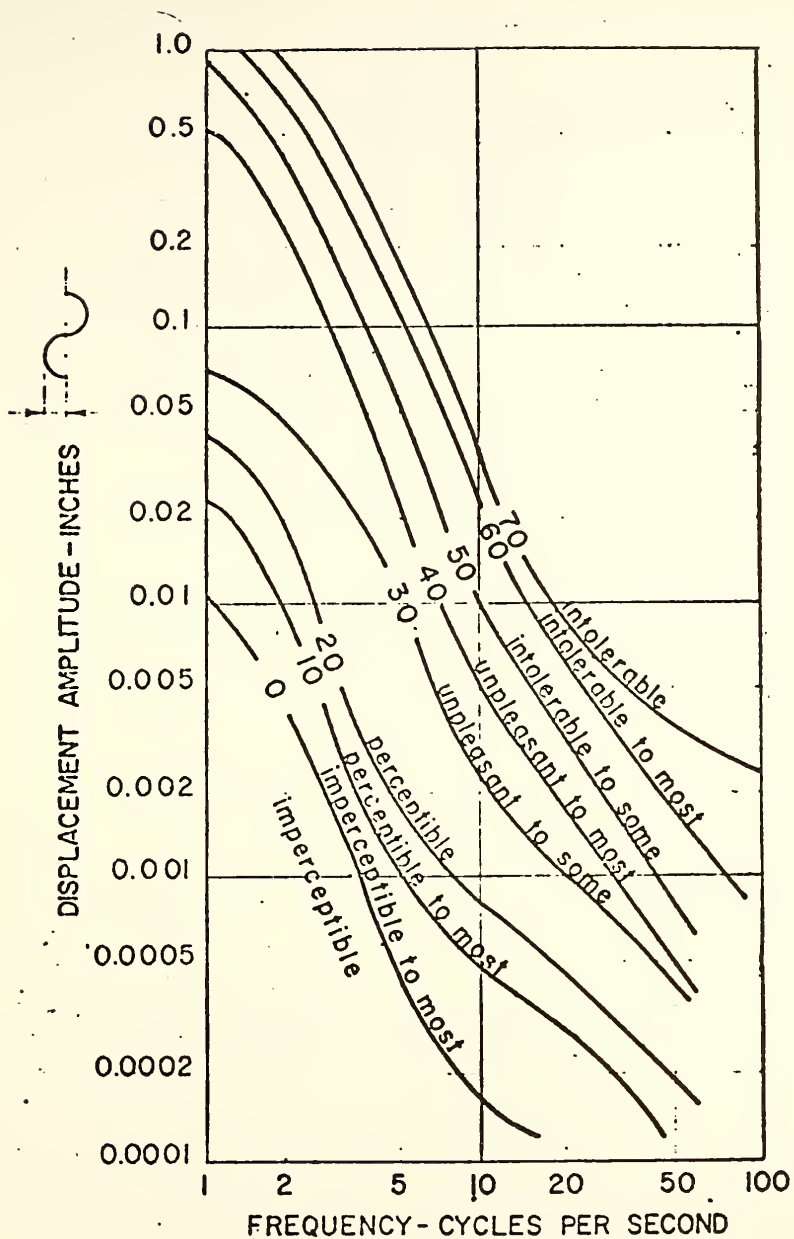


Figure A.6. Contours of Equal Sensitivity to Vibration, After Goldman



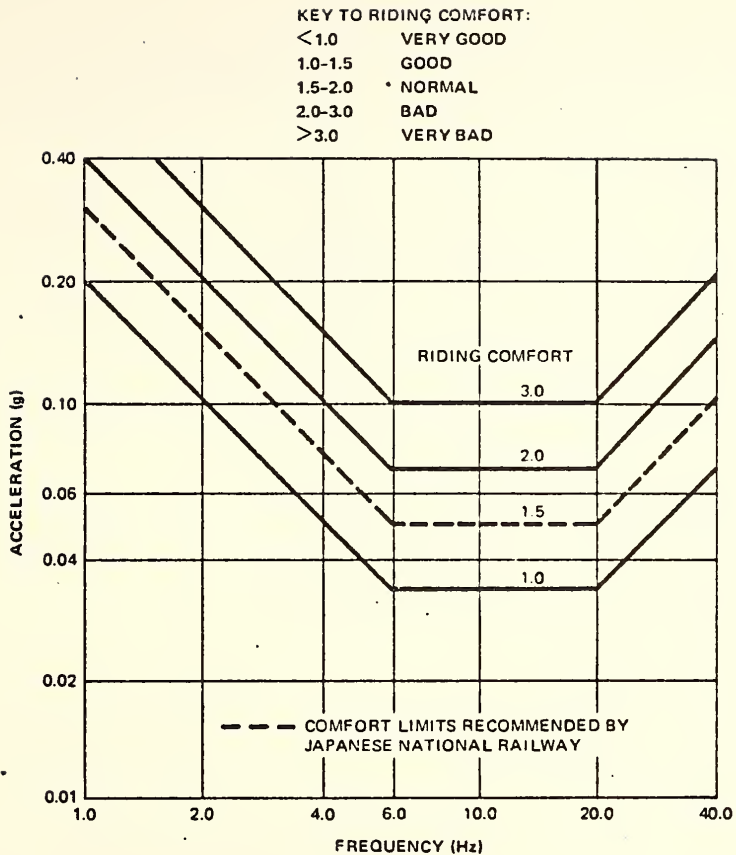


Figure A.7. Riding Comfort Indices for Vertical Vibration, After Matsubara [26]



## NOTICE

The following Appendices, listed in the Table of Contents of this Report, have not been included in this copy of the Report.

	<u>Title</u>	<u>Pages</u>
Appendix B	Simplified Methods for Determining Fundamental Frequencies	154-176
Appendix C	Road Roughness Analysis Curves	177-213
Appendix D	Description of the Single Span Bridge (SB-C-1)	214
Appendix E	Time Derivative of Discrete Functions	215-228
Appendix F	Fundamental Bending Frequency of Three Span Bridges	229-230

A recipient of the Report may secure a copy of any Appendix desired upon request to:

Joint Highway Research Project  
Civil Engineering Building  
Purdue University  
West Lafayette, Indiana 47907







COVER DESIGN BY ALDO GIORGINI